PRODUCTION AND CHARACTERIZATION OF ERYTHROPOIETIC PROTOPORPHYRIC HETERODIMERIC FERROCHELATASES

by

WIDED NAJAHI-MISSAOUI

(Under the Direction of Harry A. Dailey)

ABSTRACT

Erythropoietic protoporphyria (EPP) is caused by mutations in the gene coding for ferrochelatase, the enzyme that catalyzes the last step in the heme biosynthesis pathway. In this study, we suggest a molecular explanation for the decrease in ferrochelatase activity for a number of EPP missense mutations. We constructed homodimeric and heterodimeric mutant ferrochelatases; we measured their activities and examined their physical properties to see if the loss of activity is additive or greater than expected. The results showed that heterodimers with the mutation in the dimer interface were not isolated suggesting that they were unstable. Mutations in the active site resulted in loss of activity that differed between homodimers and heterodimers. Mutations in the C-terminal extension resulted in loss of the [2Fe-2S] cluster and of enzyme activity for both homodimeric and heterodimeric mutants. Western blot and dynamic light scattering (DLS) results suggest that human ferrochelatase may form a dimer with one or no cluster but it needs both clusters to maintain its stability and activity. Our data also suggest a possible different entry path of the iron substrate of ferrochelatase to the active site pocket than previously reported.

INDEX WORDS: Ferrochelatase, EPP, erythropoietic protoporphyria, missense mutations, homodimers, heterodimers.

PRODUCTION AND CHARACTERIZATION OF ERYTHROPOIETIC PROTOPORPHYRIC HETERODIMERIC FERROCHELATASES

by

WIDED NAJAHI-MISSAOUI

BS, Faculte de Pharmacie Monastir, Tunisia, 1999

A Thesis Submitted to the Graduate Faculty of The University of Georgia in Partial Fulfillment of the Requirements for the Degree

MASTER OF SCIENCE

ATHENS, GEORGIA

2003

PRODUCTION AND CHARACTERIZATION OF ERYTHROPOIETIC PROTOPORPHYRIC HETERODIMERIC FERROCHELATASES

by

WIDED NAJAHI-MISSAOUI

Major Professor: Harry A. Dailey

Committee: Debra Mohnen
Walter K. Schmidt

Electronic Version Approved:

Maureen Grasso
Dean of the Graduate School
The University of Georgia
December 2003

ACKNOWLEDGEMENTS

I wish to express my sincere gratitude to Dr. Harry A. Dailey who has provided me with support throughout this work.

I am grateful to the members who served on my committee and took the time to review this document including Dr. Debra Mohnen and Dr. Walter K. Schmidt. I also express my deep appreciation to Kai-Fen Wang who has helped during the first phase of this project.

Finally, I am deeply indebted to my family and especially my husband Ali for their constant support, encouragement and love. Their inspiration remains my main support throughout all my endeavors.

TABLE OF CONTENTS

CHAPTER 1

LITERATURE REVIEW

Ferrochelatase

Heme is essential for many aspects of the cell function and is required in many oxygen-binding and electron-transfer proteins such as hemoglobin, cytochromes and catalases. These proteins have a large range of functions including electron transport, nitrogen oxide synthesis, and drug metabolism.

Ferrochelatase (also called protoheme ferro-lyase, EC 4.99.1.1) is the enzyme involved in the last step in the pathway of heme synthesis (Fig.1). It catalyzes the insertion of ferrous iron into the tetrapyrrolic macrocycle protoporphyrin IX to form protoheme (Fig. 2) (see Dailey et al, 2000). In bacteria, ferrochelatase is found in the cytoplasm or associated with the cytoplasmic membrane (Dailey, 1990; Dailey and Dailey, 2003). In eukaryotes, ferrochelatase is associated with the inner mitochondrial membrane and its active site is on the mitochondrial matrix side of the membrane (Harbin and Dailey, 1985). It is synthesized in the cytosol as high molecular weight precursor and is proteolytically processed during its translocation into the mitochondria to form the mature protein (Karr and Dailey, 1988). The human enzyme exists as a homodimer with a molecular weight of 86 kDa (Burden et al, 1999).

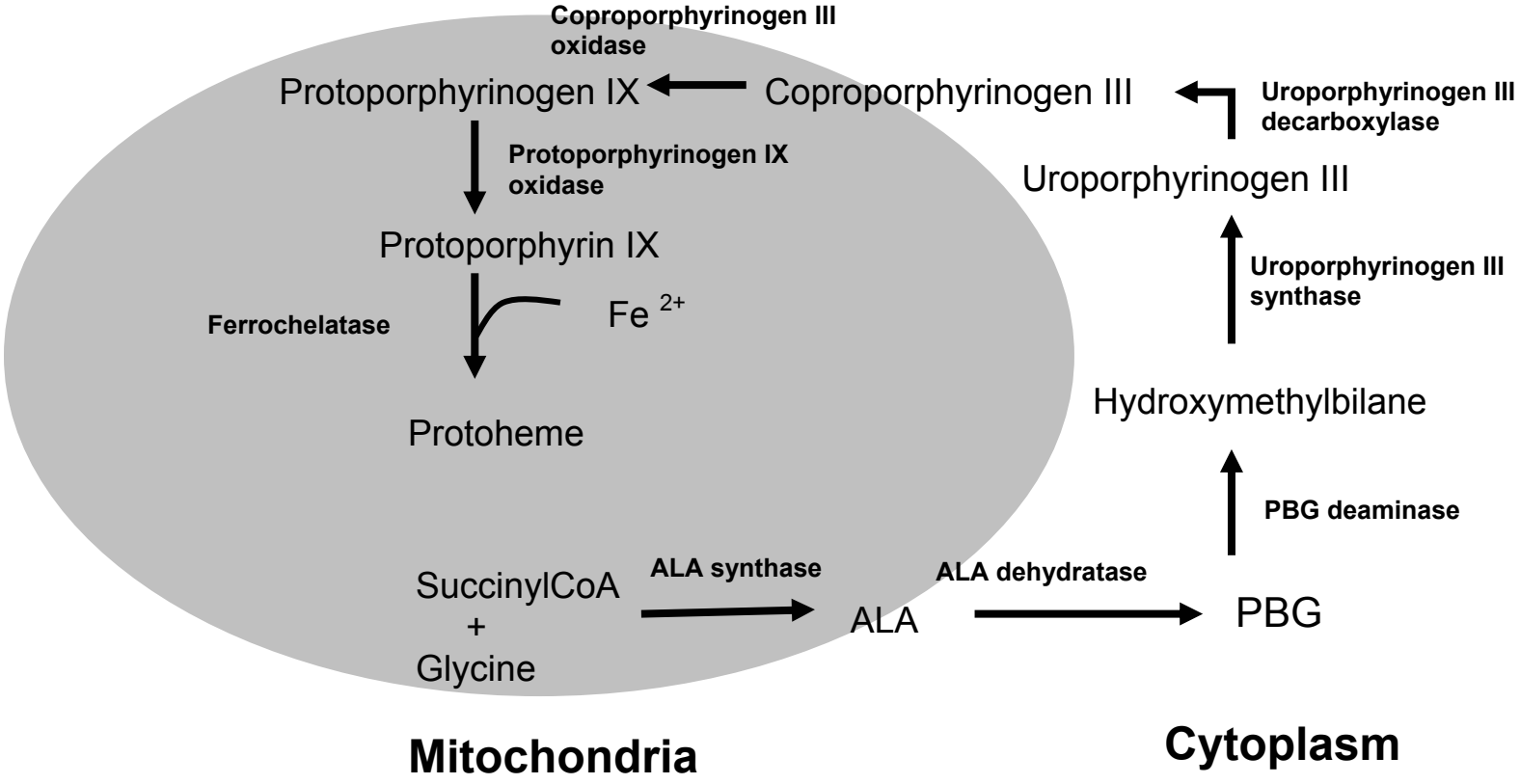

Figure 1. The pathway of Heme biosynthesis. ALA: aminolevulinic acid, PBG: porphobilinogen.

Protoporphyrin IX

Protoheme

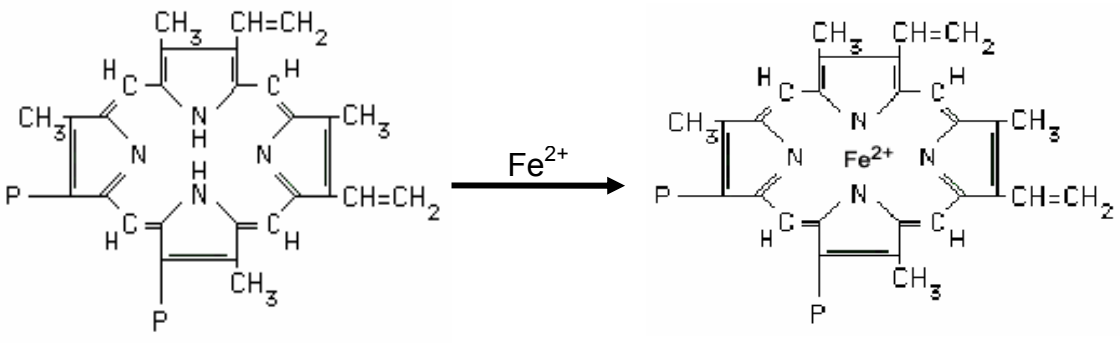

P: $-CH_2CH_2COOH$

Figure 2. Reaction catalyzed by ferrochelatase.

History

Studies of the heme biosynthesis pathway started in the early 1950s. Ferrochelatase was first identified in avian erythrocytes in 1956 and was named "protoheme ferrolyase" (Goldberg et al, 1956). Ferrochelatase has since been identified in a wide range of organisms including bacteria and eukaryotes. The purification of ferrochelatase from non-recombinant sources is complicated by its association with the membrane and its low level in the cell. In 1981, Taketani and associates succeeded in purifying ferrochelatase from rat liver mitochondria. This was followed by enzyme purification from diverse sources such as bovine liver (Dailey and Fleming, 1983; Taketani and Tokunaga, 1982) and yeast (Camadro and Labbe, 1988). Even though ferrochelatase was successfully purified, the amounts obtained were not sufficient to allow detailed biochemical studies. This problem was overcome by the cloning of the gene for the enzyme from different sources like *Saccharomyces cerevisiae* (Labbe-Bois, 1990), mouse (Brenner and Frasier, 1991; Taketani et al, 1990) and human (Taketani et al, 1992). Since then, high expression of recombinant ferrochelatase has been obtained using baculovirus or *Escherichia coli* systems (Eldridge and Dailey, 1992; Dailey et al, 1994a).

Isolation and enzyme assays

The ferrochelatase gene has been sequenced and the protein purified from both eukaryotic and prokaryotic sources, including *Bacillus subtilis (*Hansson and Hederstedt, 1992), *E. coli* (Miyamoto et al, 1991), *S. cerevisia* (Labbe-Bois, 1990; Camadro and Labbe, 1988), *Arabidopsis thaliana* (Smith et al, 1994), barley (Miyamoto et al, 1994), *Xenopus laevis* (Day et al, 1998), *Gallus gallus* (Day et al, 1998), *Drosophila melanogaster* (Sellers et al, 1998), mouse (Brenner and Frasier, 1991; Taketani et al, 1990), human (Nakahashi et al, 1990),

Bradyrhizobium japonicum (Frustaci and O'Brian, 1992), bovine (Dailey and Fleming, 1983, Taketani and Tokunaga, 1982), the bacterium *Rhodopseudomonas sphaeroides* **(**Dailey, 1982), and rat **(**Taketani and Tokunaga, 1981). The gene encoding human ferrochelatase was assigned to chromosome 18 at the region q21.3 (Whitcombe et al, 1991; Brenner et al, 1992). The gene is comprised of 11 exons spanning a region approximately 45 Kb in size (Taketani et al, 1992).

Ferrochelatase has been shown to be a membrane-associated protein in many systems. In bacteria, it is associated to the cytoplasmic membrane (Dailey, 1982), except in gram-positive bacteria where it appears to be soluble, rather than membrane-associated. It is bound to the inner mitochondrial membrane in eukaryotes (Jones and Jones, 1969). Plants have two isoforms of ferrochelatase encoded by two different genes. Using import experiments with isolated chloroplasts and mitochondria, Chow et al. (1998) found that one form of ferrochelatase is targeted specifically to the chloroplast whereas the second form is targeted to both the chloroplast and mitochondria.

A variety of approaches was used to study the kinetics of ferrochelatase. One of these is based on the quantitation of the pyridine hemochromogen using physiological substrates (Porra and Lascelles, 1968; Porra et al, 1967). Another technique is the dual-wavelength assay, which is based on the spectral shift that occurs after metal insertion into the protoporphyrin substrate (Porra et al, 1967). This second method allows monitoring the substrate disappearance and the product formation during reaction time. In the past, some of the problems encountered in studying ferrochelatase were the insolubility of the protein because of its association with the membrane and difficulty in purifying sufficient amounts of the enzyme for biochemical characterization. This problem was solved by molecular recombinant DNA techniques, which have allowed significant amounts of the protein to be readily purified (Dailey et al, 1994a).

Most biochemical studies of ferrochelatase activity are usually conducted *in vitro*. *In vitro* assays may have several limitations, including the use of non-physiological substrates (mesoporphyrin or deuteroporphyrin and zinc) whose chemical properties may be different from those of the physiological substrates (Dailey et al, 2000). There is also the problems of the insolubility of porphyrin, the rapid oxidation of ferrous iron to ferric iron in the presence of oxygen (Punekar and Gokhale, 1991), and the photosensitivity of heme in the presence of thiol-containing compounds (Porra et al, 1967).

Enzyme activity

Ferrochelatase utilizes only dicarboxylate porphyrins of the IX isomer (Dailey and Smith, 1984; Honeybourne et al, 1979; Dailey and Fleming, 1986). Ferrochelatase can use proto-, meso-, deutero-, and hematoporphyrin as substrates (Dailey and Smith, 1984). Porphyrins that are not substrates may be competitive inhibitors of ferrochelatase. Metalloporphyrins with iron, cobalt, zinc, and tin are also inhibitors (Dailey et al, 1989). N-alkylprotoporphyrins are strong inhibitors of ferrochelatase both *in vivo* and *in vitro* (De Matteis et al, 1985). When studied kinetically, N-alkylprotoporphyrins have been shown to be tightly bound to the enzyme. An example is N-methylprotoporphyrin, which was found to be a competitive inhibitor of ferrochelatase with respect to porphyrin (Dailey and Fleming, 1983).

Ferrochelatase utilizes ferrous iron but not ferric iron (Dailey, 1990). Ferrous iron is easily oxidized to ferric iron, but it has been suggested that the intracellular environment is reducing enough to keep iron in its reduced form (Porra and Jones, 1963). Ferrochelatase catalyzes the insertion of a variety of divalent cations like ferrous iron, cobalt, and zinc, but not monovalent or trivalent metals (Dailey, 1990, Dailey, 1996). Ferric iron is neither a substrate

nor an inhibitor of the enzyme. Many divalent cations like manganese, cadmium, lead, and mercury are competitive inhibitors of ferrochelatases (Dailey, 1987).

When purified from rat liver, ferrochelatase was reported to be associated with fatty acids (Taketani and Tokunaga, 1981), and it has been suggested that enzyme activity can be stimulated by their addition. Phospholipids slightly stimulate the activity of some ferrochelatases (Taketani and Tokunaga, 1981, Camadro and Labbe, 1988). The role of phospholipids or fatty acids in ferrochelatase activity has been suggested to be either through changing the structure of the enzyme or by helping the substrates reach the active site (Labbe-Bois, 1990).

Genetics and biological aspects

Sequence alignment of known ferrochelatases revealed that they have only 5% identity among their 330 core residues (Dailey et al, 2000) and less than 10% highly conserved residues (Olsson et al, 2002). The two best-characterized ferrochelatases are from human and *B. subtilis*. These ferrochelatases have only 7% identity (Dailey et al, 2000) and it is believed that these few conserved residues are most likely involved in enzyme function (Olsson et al, 2002).

As mentioned above, ferrochelatase is synthesized in a precursor form and then translocated to the matrix side of the inner mitochondrial membrane. The effect of the enzyme localization to this site has been investigated since the product heme is utilized in the cytoplasmic compartment by microsomal cytochrome b_5 and P450 and on the cytoplasmic side of the inner mitochondrial membrane by respiratory cytochromes. In addition, the enzyme that catalyzes the preceding step (oxidation of protoporphyrinogen IX into protoporphyrin IX) in the heme biosynthesis pathway (protoporphyrinogen oxidase) (Poulson and Polglase, 1975) is

localized on the opposite side of the mitochondrial membrane from ferrochelatase (Deybach et al, 1985, Ferreira et al, 1988).

Using a full-length ferrochelatase and a truncated form that lacked the mitochondrial targeting sequence, Prasad and Dailey (1995) found that the targeting sequence of ferrochelatase is necessary for proper localization of the enzyme. The improperly localized enzyme is able to catalyze iron insertion into the protoporphyrin IX to form heme, but this *in situ* form of ferrochelatase has a reduced intracellular activity compared to the properly distributed enzyme.

Kinetic studies of the two terminal enzymes of heme biosynthesis pathway suggested that substrate channeling occurred between these two enzymes and that they may form a complex in the mitochondrial membrane (Ferreira et al, 1988). The stability of this complex is unknown. Through channeling, the cell could avoid the accumulation of free protoporphyrinogen IX. Ferreira et al. (1988) proposed a possibility of protein-protein interactions between these two enzymes. The possibility of the existence of an intermediate carrier seems appealing but there is no evidence for this. In later studies, Proulx et al. (1993) undertook substrate dilution experiments with radiolabeled porphyrins and porphyrinogens and measured intermediate and product accumulation. Their data suggested that an obligatory intermediate channeling complex between the three terminal enzymes in the heme biosynthesis pathway does not exist. However, the idea that these terminal enzymes function in such a way that the cell avoids significant accumulation of intermediates cannot be dismissed.

Using the target size analysis, which determines the mass of macromolecules, Straka and co-workers (1991) studied the functional size of ferrochelatase localized in the mitochondrial membrane and found that the total mass of the functional protein in intact mitochondria is about 82 kDa. They suggested that the membrane bound ferrochelatase functions as a dimer in two

possible ways: (i) the protein could be a homodimer or (ii) it could complex with another protein of a similar size to form a heterodimer. They also suggested that one peptide may function to stabilize the dimer and that the catalytic activity may reside in only one monomer, in case of a heterodimer, or in both subunits if it is a homodimer.

One of the differences between eukaryotic and prokaryotic ferrochelatases is the presence of a carboxyl-terminal extension of 30 or more residues in all eukaryotes. In animals, this carboxyl-terminal extension contains three of the four residues responsible for the iron-sulfur cluster binding (Crouse et al, 1996, Sellers et al, 1998a, Dailey et al, 2000). Plant ferrochelatases do not have a cluster (Dailey and Dailey, 2003). Originally, it was thought that all bacteria lack the carboxyl-terminal region and therefore the [2Fe-2S] cluster, but recently Dailey and Dailey (2002) showed that the [2Fe-2S] cluster exists in some microbial organisms. The role of the [2Fe-2S] cluster is not known.

Crystal structure

At present the crystal structure for *B. subtilis* (Al-Karadaghi et al, 1997), human (Wu et al, 2001), and *S. cerevisiae* (Karlberg et al, 2002) ferrochelatases have been solved. The crystal structure of *B. subtilis* ferrochelatase demonstrated that it is a monomeric enzyme (Al-Karadaghi et al, 1997; Lecerof et al, 2000). In contrast, the human ferrochelatase is a homodimer and the x-ray crystallographic structure (Wu et al, 2001) along with examination of enzyme mutations (Dailey et al, 1994a; Sellers et al, 1998b) showed that the dimerization is mediated by the 30 carboxyl-terminal residues that are lacking in the monomeric *B. subtilis* ferrochelatase. The removal of this carboxyl-terminal extension in eukaryotic ferrochelatases results in loss of

enzyme activity. Ferrochelatase from the yeast *S. cerevisiae* is also dimeric (Grzybowska et al, 2002).

The structure of the human ferrochelatase has been solved at 2.0 Å resolution showing that it is a homodimer with a molecular weight of 86 kDa, with two [2Fe-2S] clusters (one in each subunit) (Wu et al, 2001). The structure of the monomer contains approximately 48% α-helices and 14% β-sheets. Each monomer is comprised of two similar domains, each with a four-stranded parallel β-sheet flanked by an α-helix in a β-α-β motif.

Active site pocket

One of the important features of the ferrochelatase enzyme is its active site pocket. The opening of the active site has two hydrophobic lips, believed to be involved in membrane association (Wu et al, 2001; Dailey and Dailey, 2003) and serving as an access route to the active site surface by allowing the poorly soluble porphyrin substrate and heme product to enter and leave via the mitochondrial membrane (Wu et al, 2001). In contrast to the surface of the active site, the interior is relatively hydrophilic with several highly conserved residues. These conserved residues form the path for the porphyrin substrate emerging from the protein's surface to the center of the active site specified by the histidine residue (His 263) (Sellers et al, 2001). This residue was suggested to be involved in proton abstraction from the porphyrin substrate during catalysis (Sellers et al, 2001). Based on the recently resolved structure of the human ferrochelatase, the active site pockets of the two monomers are localized on a common surface (Wu et al, 2001). In 1986, Dailey and Fleming proposed that the ferrochelatase active site is relatively protected and they suggested the existence of a porphyrin-binding pocket in the active

site of the enzyme (Dailey and Fleming, 1986). The recently resolved crystal structure of ferrochelatase is consistent with these suggestions.

The iron-sulfur [2Fe-2S] cluster

One of the most interesting features of ferrochelatase is the presence of a single [2Fe-2S] cluster in each monomer (Dailey et al, 1994a; Dailey et al, 1994b; Ferreira et al, 1994). Both clusters are located near the interphase between the two monomers (Dailey et al, 2000). The cluster is bound by only four cystein residues (C403, C 406, C411 and C196), three of which are located in the 30 carboxyl-terminal extension and the fourth ligand in the interior of the protein in a NH_2-Cys-X_{206}-Cys-X_2-Cys-X_4-cys-COOH arrangement (Crouse et al, 1996; Sellers et al, 1998a). These cysteines are absent in yeast and plant proteins.

Initial studies using spectroscopic characterization and metal analysis of recombinant human and mouse ferrochelatases led to the discovery of an [2Fe-2S] cluster in mammalian systems (Dailey et al, 1994b; Ferreira et al, 1994). Crouse et al. (1996) used site-directed mutagenesis and spectroscopic studies in an attempt to identify the residues involved in the [2Fe-2S] cluster binding. They conducted point mutations on the five cysteines (C403D, C403H, C406D, C406H, C406S, C411H, C411S, C360S and C395S) closest to the carboxyl terminus of human ferrochelatase. They found that the mutation of only the three cysteines (C403, C406, and C411) resulted in inactive protein that lacked its [2Fe-2S] cluster, suggesting that these conserved cysteines are involved in iron-sulfur cluster association. Several studies showed that the [2Fe-2S] cluster is labile and gradually disappears within 1-3 days upon storage at 4ºC (Dailey et al. 1994b; Crouse et al. 1996; Ferreira et al. 1994). The finding that only three cysteines in the carboxyl terminal extension are involved in the cluster binding led Crouse et al.

(1996) to conclude that the cluster lability may be attributed to a fourth non-cysteinyl, oxygenic cluster ligand. Sellers et al. (1998a) solved the mystery of the fourth cluster ligand by conducting site-directed mutagenesis on conserved residues that were suspected to be involved in cluster ligation and by finding the cluster in *Drosophila melanogaster* ferrochelatase, which has the four cysteines and possesses the [2Fe-2S] cluster. Their data revealed that C196 is the fourth cysteine ligating the cluster and they associated the cluster lability to its sensitivity to nitric oxide, suggesting that ferrochelatase activity is regulated via cluster degradation as part of the protein immune response system (Sellers et al, 1996; Sellers et al, 1998a).

A direct involvement of [2Fe-2S] cluster in the catalytic activity of ferrochelatase has not been proven, but some studies indicated that the activity of the protein is dependent on the presence of the cluster (Medlock and Dailey, 2000). A notable feature of the enzyme regarding its clusters is that it functions independently of the redox state of the cluster (Dailey, 1997). The role of the cluster in ferrochelatase is still not defined. Studies with chimeric constructs from human and yeast ferrochelatases indicated that the enzyme activity is not strictly dependent upon the presence of the cluster (Medlock and Dailey, 2000). Plant, yeast, and some bacterial ferrochelatases do not have the cluster but they have enzymatic activity suggesting that this cluster may not be directly involved in the catalytic mechanism of the protein (Day et al, 1998; Sellers et al, 1998a). Studies on truncated mutants of ferrochelatase missing the last 30 carboxyl residues showed the absence of the cluster and completely impaired activity (Dailey et al, 1994a). Another feature of the cluster is that its iron ions do not serve as substrates in the catalytic mechanism of the enzyme (Dailey et al, 2000). Many hypotheses have been proposed concerning the function of the [2Fe-2S] cluster ranging from a structural role in maintaining the dimer stability (Wu et al, 2001) to playing a role as a nitric oxide sensor in the immune response

(Sellers et al, 1996). However, the more recent discovery of the cluster in some bacterial ferrochelatases (some of which are monomeric) brings into question these models.

Catalytic mechanism

Ferrochelatases isolated from different organisms have very similar catalytic properties, suggesting that the major features of the catalytic mechanism are conserved (Olsson et al, 2002).

Porphyrin binding

In vivo and *in vitro* studies of *B. subtilis* ferrochelatase suggested that the porphyrin substrate is channeled between the two, and possibly the three, last enzymes of heme synthesis (Olsson et al, 2002; Ferreira et al, 1988). Eventhough, Proulx et al (1993) suggested that an obligatory intermediate channeling complex between the three terminal enzymes in the heme biosynthesis pathway does not exist.

Access to the active site of membrane-associated ferrochelatases of the porphyrin substrate is suggested to be from the membrane-facing surface (Dailey, 1982). Co-crystallization of *B. subtilis* ferrochelatase with a potent inhibitor, N-methylmesoporphyrin, indicated that after porphyrin binding the enzyme induces porphyrin distortion by holding pyrrole rings B, C, and D in a "vice-like grip" and forcing the ring A to tilt 36º (Lecerof et al, 2000). The mechanism of porphyrin distortion is not fully understood, nor are the residues involved in the porphyrin binding. Studies of yeast ferrochelatase showed that this distortion occurs only when mercury, a yeast ferrochelatase inhibitor, was bound to the enzyme (Blackwood et al, 1997), suggesting that an allosteric mechanism may mediate ferrochelatase activity in which metal binding induces a

change in the conformation of the ferrochelatase protein and induces the predicted distortion of the porphyrin macrocycle (Blackwood et al, 1997).

Investigation of the residues involved in porphyrin binding suggested that alteration of arginyl residues in mammalian ferrochelatase leads to inactivation of the enzyme (Dailey and Fleming, 1986). In fact, arginyl residues are frequently found in heme-binding proteins (Perutz, 1979) and it is probable that arginyl residues are involved in the orientation of the tetrapyrrolic macrocycle in the active site. These findings do not exclude the involvement of other ferrochelatase residues in porphyrin binding.

Metal ion binding

Different techniques have been used to investigate the metal binding site. It was proposed that a highly conserved histidine may serve as the metal binding site and site directed mutagenesis of human ferrochelatase suggested that histidine 263 (H263) is involved in iron metal binding (Kohno et al, 1994). However, Sellers et al. (2001) conducted a series of site-directed mutagenesis on the residue H263 of the human ferrochelatase, including the mutation conducted by Kohno et al., and they found that all mutants had no measurable activity. The authors suggested that this residue has a key role in the ferrochelatase catalysis, not as an iron ligand but as an acceptor of the abstracted protons from the porphyrin macrocycle (Sellers et al. 2001). The crystal structure of human and *B. subtilis* ferrochelatases shows that residue H263 (human numbering) and H183 (*B. subtilis* numbering) are located in the porphyrin binding cleft (Lecerof et al, 2000; Wu et al, 2001).

In an attempt to identify the residues involved in the transportation of the metal ion to the active site pocket, Sellers et al. showed that this metal is bound in a site occupied by His 230 and

Asp 383, on the opposite site of His 263 based on crystal structure of human ferrochelatase using Co^{2+}. This suggests that the initial iron binding may occur at the His 230/Asp 383 site on the matrix side of the protein and that the metal is then transported via conserved residues (Trp 301, Trp 227, Tyr 191, Tyr 165, and Arg 164) to the active site and finally to the porphyrin substrate (Sellers et al, 2001; Wu et al, 2001).

Catalytic mechanism

Several models regarding ferrochelatase catalytic mechanism have been suggested, the most appealing model was suggested by Wu et al. (2001). According to this model, the first steps consist of iron binding, porphyrin binding and distortion by conserved residues. The next step involves abstraction of protons, with His 263 being the first acceptor. The last step consists of metal transport to the active site where it is incorporated into the distorted porphyrin substrate. The entry site of the metal ion was suggested to be in the opposite site of His 263 and the active site. Wu et al, (2001) suggested that the last step involving porphyrin metallation is mediated by a series of highly conserved residues including Arg 164 and Tyr 165. Studies of porphyrin metallation suggest that the arriving metal forms a "sitting-atop" complex on the porphyrin macrocycle and inserts into the distorted porphyrin as the pyrrole protons leave from the opposite side (Takeda et al, 1992). Karlberg et al (2002) suggested that the residue histidine 263 (human numbering) is involved in this sitting-a-top complex formation, unlike the suggestion of Wu et al. (2001) that this highly conserved residue is involved in proton abstraction from protoporphyrin IX substrate.

In spite of the differences between the two models, it appears that porphyrin distortion is important for ferrochelatase reaction. This distortion allows iron metal insertion and once the

metal is inserted, the protoporphyrin/heme becomes planar prior to its release as the final product of ferrochelatase reaction (Dailey, 1997). Kinetic analysis of the inhibition of ferrochelatase using different agents, led Dailey and Fleming (1983) to postulate that during the catalytic mechanism of heme production, iron binding occurs prior to porphyrin binding and the release of the heme product precedes the release of the two-abstracted protons. Bain-Ackerman and Lavallee (1979) proposed that the metal ion is inserted into protoporphyrin IX and then it displaces the two-pyrrole protons, suggesting that metal insertion precedes protoporphyrin deprotonation and that the two abstracted protons are released into a different, and possibly an opposite path from the iron entry. Site directed mutagenesis of *S. cerevisiae* ferrochelatase revealed that the iron and protoporphyrin binding sites are not independent of each other. The evidence for this conclusion was that the K_m of both iron and protoporphyrin were affected when mutating only the residues predicted to be involved in metal binding (Gora et al, 1996).

The entry sites for both substrates (iron and protoporphyrin) may not be the same. Porphyrin enters the active site from the ferrochelatase surface that faces the mitochondrial membrane, whereas iron may enter at a different site. It has been suggested that iron binds initially at the surface facing the mitochondrial matrix at the H231/D383 site, and from there, it is transported to the site of metallation via a series of highly conserved residues including W227 and Y191. After protoporphyrin distortion, the metallation occurs via R164 and Y165. H263 is the first acceptor of the two-abstracted protons, which are released via conserved carboxylates including E343, H341 and D340 (Sellers et al, 2001).

Iron transport into mitochondria

Iron is an essential nutrient for almost all organisms and it is not readily available. The poorly soluble ion is usually chelated as ferric iron by various iron-binding proteins to prevent its toxicity if free in the organism (Andrews, 1998). The import of iron into the mitochondria, where ferrochelatase catalyzes its insertion into protoporphyrin IX to form protoheme, is not fully understood. However, this import must be highly regulated to avoid metal ion accumulation (Andrews, 1998). *In vitro* assays tracking the transport of iron into isolated yeast mitochondria showed that iron transport requires a membrane potential across the mitochondrial inner membrane, but it does not require ATP (Heike et al, 1999). The authors suggested that since iron has to be imported into mitochondria and then into ferrochelatase simultaneously with the heme synthesis, ferrochelatase may receive its metal ion substrate directly from the mitochondrial inner membrane in its reduced form, bypassing a need to transiently pass through the mitochondrial matrix. They also suggested that the iron transporter must be highly specific for iron ions and excluded other metal ions like zinc and copper. Based on these results, Heike and co-workers (1999) excluded a role for the known mitochondrial metal transporters Mmt1p and Mmt2p in the transport of iron into ferrochelatase during heme synthesis.

Porphyrin transport into mitochondria

Porphyrin could be imported into ferrochelatase before iron incorporation. Because of its hydrophobicity, porphyrin may be directly provided to ferrochelatase by permeating the mitochondrial membrane (Heike et al, 1999).

Erythropoietic protoporphyria

Porphyrias are a group of disorders caused by deficient activity of one of the enzymes that catalyze the different steps of the heme biosynthesis pathway (Table 1), resulting in overproduction and accumulation of heme precursors (Sassa, 2000). Two major types of porphyrias are known, based on the major site of heme precursor accumulation and the enzyme affected. These are hepatic and erythropoietic porphyrias (Sassa, 2000). Hepatic porphyrias have normal red blood cell porphyrin concentrations and are clinically characterized by neurologic symptoms and abdominal pain. Erythropoietic porphyrias are characterized chemically by an increased concentration of porphyrin within the red blood cells and clinically by cutaneous photosensitivity manifestations.

In humans, a genetic defect in the ferrocheatase (FECH) gene may lead to a reduction in ferrochelatase activity causing the accumulation of the heme precursor, protoporphyrin IX, that is responsible for the development of the disease erythropoietic protoporphyria (EPP). Inheritance of EPP is autosomal dominant with possible association with low expression of the wild-type FECH allele. A decrease in the mRNA levels of the normal ferrochelatase allele combined with an inactivating mutation in the diseased allele has been proposed to be responsible for the decrease of enzyme activity observed in patients with EPP (Gouya et al, 1996). Erythropoietic protoporphyria exists in other mammalian systems. Bovine protoporphyria has a simpler mode of inheritance than the human form. In cattle, this disease is known to be an autosomal recessive disorder with the level of ferrochelatase activity reduced to 40% compared to the normal in the heterozygous asymptomatic carrier, and to only 10% of the normal in homozygous symptomatic ones (Straka et al, 1991; Bloomer et al, 1982). In contrast to the

Table 1. Classification of human porphyrias and heme biosynthesis enzymes involved.

Heme biosynthesis enzymes	Porphyria type	Inheritance	Classification
ALA Dehydratase	ALA Dehydratase Porphyria (ADP) (Doss porphyria)	Autosomal recessive	Acute Hepatic
PBG-Deaminase	Acute intermittent porphyria (AIP)	Autosomal dominant	Acute Hepatic
Uroporphyrinogen III Synthase	Congenital erythropoietic porphyria (CEP)/ Gunther disease	Autosomal recessive	Non-acute Erythropoietic
Uroporphyrinogen III decarboxylase	Porphyria cutanea Tarda (PCT)	Variable[a]	Non-acute Hepatic
Coproporphyrinogen Oxidase	HereditaryCoproporphyria (HC)	Autosomal dominant	Acute Hepatic
Protoporphyrinogen Oxidase	Variegate Porphyria (VP)	Autosomal dominant	Acute Hepatic
Ferrochelatase	Erythropoietic Protoporphyria (EPP)	Autosomal dominant[b]	Non-acute Erythropoietic

[a]Autosomal dominant and recessive inheritances have been reported.
[b]EPP is caused by a co-inheritance of a FECH gene mutation on one allele and a low expressed gene on the second allele; autosomal recessive inheritance has been reported.

human EPP, which is caused by heterogenous mutations (point mutations, null allele mutations, etc…), the ferrochelatase defect in bovine protopophyria is caused only by a missense mutation in the normal termination codon in the ferrochelatase gene which results in a protein with an additional extension on the carboxyl-terminal end (Jenkins et al, 1998).

History of the disease

The disease EPP was first described and named by Magnus et al. in 1961. The genetic nature of this disease was revealed by Haeger and his group in 1963. In 1975, Bonkowsky and co-workers proved that the EPP disease is caused by a deficiency in ferrochelatase, the enzyme responsible for the last step in heme biosynthesis pathway. Since then, studies have been focusing on revealing the different mutations in the FECH gene and currently more than 70 EPP mutations are described (Schneider et al, 2000a; www. HGMB.org).

Clinical features of EPP

EPP is a relatively rare disease with a predicted prevalence estimated at 1 in 75,000-200,000 (Schneider et al, 2000a). The main clinical symptom of the EPP disease is a painful photosensitivity that starts in childhood. Patients suffer from a severe burning pain in the skin of face and hands after a short exposure (in the order of minutes) to sunlight (Todd, 1994). EPP occurs because of the accumulation of the substrate (protoporphyrin) in the skin resulting from the deficiency of ferrochelatase activity. Protoporphyrin accumulation starts in the erythrocytes, from which it can then spread to other cells (Brun et al, 1990). Using fluorescence microscopy, the increased level of protoporphyrin in EPP patients can be detected by the presence of red fluorescence in the epidermis and blister fluid (Gogh and Schothorst, 1973; Miura et al, 1980).

Biochemical studies investigating the role of oxygen in the development of the photosensitivity reaction, suggested that after absorption of energy corresponding to Soret's band wavelength (about 400 nm), the stable protopophyrin molecule becomes unstable in an excited state. The surplus energy of this excited state is transferred to oxygen molecules that become very reactive and give rise to photodynamic cell injury (Thunell et al, 2000). The finding that oxygen deprivation reduces the photochemical sensitivity of protoporphyrin supports these propositions (Spikes, 1975; Lee et al, 1984; Thunell et al, 2000). Patients may develop edema on different areas of the body that in some cases can be associated with small hemorrhagic vesicles and thickening of the skin, especially over the knuckles (Deybach, 2001; Schneider et al, 2000a). Painful cutaneous photosensitivity reduces the sunlight tolerance of individuals with EPP and may influence their lifestyles over their entire lifetime, rendering them detached from their environment (Schneider et al, 2000a; Deybach, 2001).

In less than 10% of EPP patients, hepatotoxic effects of excess protoporphyrin deposition, showed by the presence and random distribution of protoporphyrin crystals in the cytoplasmic compartments of hepatocytes, bile canaliculi, and epithelia of bile ducts cells (Komatsu et al, 2000, Meerman, 2000), may lead to progressive liver dysfunction. Without liver transplantation, this case can be lethal (Deybach, 2001; Schneider et al, 2000a; Thunell et al, 2000).

Diagnosis of EPP

The diagnosis of EPP is based on the clinical symptoms described above and on an abnormal increase in the level of free protoporphyrin in peripheral erythrocytes, which can be detected using fluorescence microscopy (Thunell et al, 2000). Besides this rapid and sensitive

test, the diagnosis of EPP can be confirmed through measuring ferrochelatase activity in peripheral lymphocytes (Deybach, 2001). Monitoring of liver function and protoporphyrin levels are advised, even though liver disease associated with EPP is difficult to identify at an early stage before serious damage has occurred (Todd, 1994).

Inheritance of EPP

EPP is a heterogeneous genetic disorder in which only few mutations can be found in unrelated individuals (Deybach, 2001; Minder et al, 2002; Norris et al, 1990). The inheritance mode of EPP has long been debated. Early studies suggested that EPP is autosomal dominant (Haeger et al, 1968). Although most studies are consistent with this classification, the inheritance of this disorder has now been shown to be more complex and the hypothesis "autosomal dominant disorder with a low clinical penetrance" has been the most favored explanation of EPP inheritance. However, in some instances, the disease has been shown to be autosomal recessive (Lamoril et al, 1991; Sarkany et al, 1994; Goerz et al, 1996). The autosomal dominant inheritance of EPP has been suggested to be associated with an incomplete penetrance because less than 10% of the carriers of a ferrochelatase gene mutation will develop the EPP disease symptoms (Schneider et al, 2001).

The different EPP mutations identified involve only one FECH allele, with the second allele being normal (Gouya et al, 1999). Assuming that EPP is autosomal dominant, one would expect the residual enzyme activity to be around 50% of the normal. Enzyme activity reported in EPP patients was less than 50 % (Bottomley et al, 1975), which is not consistent with the dominant inheritance of the disease. Asymptomatic EPP patients often express higher FECH

enzyme activity than do patients with symptoms (Bonkowsky et al, 1975; Sassa et al, 1982; Deybach et al, 1986).

Gouya et al (1996) suggested a mode of inheritance of EPP in which the clinical expression of the disease requires first, the inheritance of a mutated allele and second the inheritance of a low expressed normal FECH allele. The same group and others supported this model of inheritance in later studies (Gouya et al, 2002; Morris et al, 2002). The identification of FECH gene polymorphic variant sequences was associated with the low expressed allele (Morris et al, 2002). Studies of allelic segregation patterns and quantitation of their transcribed RNA showed that the clinical expression of EPP is the result of co-inheritance of a mutant ferrochelatase allele along with one that is expressed at low level (Gouya et al, 1999). The less than 50% of ferrochelatase activity observed in patients with EPP was recently shown to be caused by trans-inheritance of one deleterious mutation and an IVS3-48T>C transition in intron 3 of the FECH gene. This single polymorphism was suggested to be a modulator of the use of a constitutive abnormal acceptor splice site, resulting in the degradation of the abnormally spliced mRNA with a decreased level of mRNA, ferrochelatase enzyme, and its activity (Gouya et al, 2002). In a more recent study, Wiman et al (2003) investigated different EPP mutations in nine Swedish families with erythropoietic protoporphyria (Wiman et al, 2003). They found that all patients showing EPP symptoms had a mutated allele and IVS3-48C>T polymorphism, providing additional support for the intronic polymorphism. A situation similar to this mechanism of inheritance, in which variation in the expression level accounts for incomplete penetrance, has been documented in many dominantly inherited disorders such as Hirschsprung disease (Hofstra et al, 1997), Campomelic dysplasia or basal cell nevus syndrome (Wolf, 1997). While appealing, this mechanism of low expression of FECH gene needs more investigation.

Coinheritance of a wild-type *FECH* allele and a weakly expressed one is not the only explanation for the clinical and biochemical manifestation of EPP. Went and Klasen (1984) suggested the existence of a third allele that, in association with the mutated allele, leads to the known EPP clinical features. This suggestion remains only a hypothesis even though Gouya et al (1999) argued that if this hypothesis is true, it could explain the rare autosomal recessive form of EPP, and that this third allele has to be a weakly expressed one. Recently, Magness et al. (1998) reported a new region of 2 kb upstream from the transcription start site that may contribute to a high level of erythroid expression of the *FECH* gene by maintaining an active chromatin configuration. They suggested that mutations in the region that contains erythroid-specific regulatory elements are possibly involved in the *FECH* gene low expression. On the other hand, sequencing of the coding regions, as well as parts of intron 1 and 3' UTR, to search for mutations that might decrease *FECH* mRNA steady-state level, failed to detect any other sequence variations (Magness et al, 1998).

FECH gene mutations and ferrochelatase activities in patients with EPP

More than 70 different EPP mutations in human ferrochelatase gene have been described (Schneider et al, 2000a; www. HGMB.org), along with one partial chromosomal deletion (Carolyn et al, 2001). Currently known EPP mutations are summarized in Table 2. Two general classes of mutations have been closely linked to the disease. The first class involves "null allele" mutations including nonsense mutations and frameshift mutations that cause intron/exon splicing errors resulting in an internal deletion in exon 1, 2, 3, 4, 5, 6, 7, 9, or 10 and causing an early termination of translation (Sellers et al, 1998a; Sellers et al, 1998b; Schneider et al, 2000a; Schneider et al, 2000b). The second class includes missense mutations that result in an amino

Table 2. Summary of known mutations in the FECH gene*.

Mutation type	Exon	Codon	Residue mutation	Liver disease	Reference
Nucleotide substitutions (missense/nonsense)					
	2	55	Gly-Cys	+	Lamoril et al. 1991
	2	59	Gln-Stop codon	+/-	Schneider et al.1994
	3	71	Ile-Lys		Rufenacht et al. 1998
	3	96	Gln-Stop codon		Henriksson et al. 1996
	4	115	Arg-Stop codon	+/-	Henriksson et al. 1996
	4	139	Gln-Leu		Elder et al. (manuscript submitted)
	4	151	Ser-Pro		Rufenacht et al. 1998
	5	182	Leu-Arg		Rufenacht et al. 2001
	5	186	Ile-Thr		Tanizawa et al. 1996
	5	191	Tyr-His		Rufenacht et al. 1998
	5	192	Pro-Thr		Rufenacht et al. 1998
	7	236	Cys-Tyr		Elder et al. (manuscript submitted)
	7	260	Phe-Leu		Elder et al. (manuscript submitted)
	7	263	Ser-Pro		Gouya et al. 1999
	7	264	Ser-Leu		Martinez et al. 2001
	7	267	Met-Ile		Lamoril et al. 1991
	8	283	Thr-Ile		Rufenacht et al. 1998
	8	288	Met-lys		Rufenacht et al. 1998
	8	301	Trp-Stop codon		Rufenacht et al. 1998
	9	334	Pro-Leu		Rufenacht et al. 1998
	9	362	Val-Gly		Sarkany et al.1994
	10	379	Lys-stop codon	+/-	Bloomer et al. 1998; Wang 1996
	10	379	Lys-Asn		Elder et al. (manuscript submitted)
	11	386	His-Pro		Gouya et al. 1998
	11	406	Cys-Ser		Schneider et al.2000
	11	406	Cys-Tyr		Schneider et al.2000
	11	411	Cys-Glu		Schneider et al.2000
	11	417	Phe-Ser		Brenner et al. 1992
Nucleotide substitutions (splicing)					
	1	IVS -23	C-T		Nakahashi et al. 1992
	1	IVS +5	G-A		Wang et al. 1999
	2	IVS +11	A-G	+	Bloomer et al. 1998
	3	IVS -48	T-C		Gouya et al. 2002
	3	IVS +2	T-G	+/-	Sarkany et al. 1994
	3	IVS +6	A-C	+	Bloomer et al.1998
	4	IVS -4	A-G		Yotsumoto et al. 2001
	4	IVS +1	G-C		Rufenacht et al. 1998
	4	IVS +1	G-T		Wang et al.1999
	4	IVS -1	G-C		Wang. 1996

	5	IVS +1	G-T		Frank et al. 1999
	6	IVS +1	G-A		Wang et al. 1999
	7	IVS +1	G-A		Nakahashi et al. 1993
	7	IVS +5	G-A		Wang et al. 1994
	8	IVS +1	G-T		Wang et al. 1995
	8	IVS -2	A-G		Rufenacht et al. 1998
	9	IVS -2	A-G		Rufenacht et al. 1998
	9	IVS +1	G-A	+	Nakahashi et al. 1993
	9	IVS +2	T-A		Wang et al.1999
	9	IVS -1	G-A		Wang et al.1999
	10	IVS +1	G-T		Rufenacht et al. 1998
	10	IVS +3	A-G	+	Sarkany et al. 1994
	10	IVS -3	A-T		Wang et al. 1993
Small deletions					
	1	13	Del G40		Todd et al. 1993
	4	112	Del A338		Frank et al. 1999
	4	131	Del ATCAA393		Frank et al. 1999
	4	133	Del A400		Wang et al. 1997
	5	162	Del T488		Frank et al. 1999
	5	162	Del TTCGGTAC GTCCAT		Di Pierro et al. 2001
	5	193	Del TACAG580	+/-	Frank et al. 1999
	6	225	Del G678		Wang et al. 1997
	6	236	Del T709	+	Rufenacht et al. 1998
	7	251	Del GAGAA751		Henriksson et al. 1996
	8	280	Del C843		Gouya et al. 1998
	8	299	Del Del TG899		Schneider et al.1994
	10	373	Del T1122		Henriksson et al. 1996
	10	378	Del A1135	+	Bloomer et al. 1998
	10	379	Del G1138		Gouya et al. 1996
	11	416	Del CTT1248		Rufenacht et al. 1998
Small insertions					
	3	68	Ins A205		Wang et al. 1997
	3	71	Ins T213	+/-	Rufenacht et al. 1998
	3	72	ins T215		Wang et al. 1997
Gross deletions					
	Entire FECH gene				Magness et al. 1994

* Adapted from www.HGMB.org; Schneider et al. 2000a.

acid substitution (point mutation) or in early polypeptide chain termination (Schneider et al, 2000a; Brenner et al, 1992). Studies of ferrochelatase activity in patients with EPP showed that all symptomatic patients had a reduced level of enzyme associated with a residual activity less than 50% of the normal enzyme activity (Goerz et al, 1996). Asymptomatic EPP patients often have higher enzyme activity (about 50% of normal) than those showing the disease symptoms (Gouya et al, 1999; Bottomley et al, 1975; Bonkowsky et al, 1975; Sassa et al, 1982).

Hepatic complications of erythropoietic protoporphyria

Less than 1/4 of the patients with EPP develop liver disease (Bloomer et al, 1998). Liver complications appear with "null allele" mutations that consist of frameshifts and nonsense mutations and result in a truncated protein (Schneider et al, 2000a). Like most EPP patients, those with liver complication are heterozygous for the mutations (Chen et al, 2002; Schneider et al, 2000b). Statistical analyses showed a significant ($p<0.05$) correlation between null allele and liver complication. To date, no missense mutation has been found in association with liver disease (Minder et al, 2002).

Histochemical studies on mice with heterozygous and homozygous point mutations in the FECH gene, suggested that the obstruction of the biliary ducts by protoporphyrin deposits causes the accumulation of protopophyrin in the parenchyma, resulting in a severe damage and loss of hepatocytes (Libbrecht et al, 2003). Patients with cholestatic liver disease resulting from EPP complication, display excessive protoporphyrinemia (Gross et al, 1998). Severe cholestatic hepatic complication can cause the development of liver cirrhosis accompagnied by a very high protopophyrin level (Libbrecht et al, 2003). Studies of patients before and after liver transplantation showed that immediately after liver transplantation, protopophyrin level in

erythrocytes decreased to 46-96% of pre-operative levels (Gross et al, 1998). Without liver transplantation, liver cirrhosis can be lethal (Bloomer et al, 1998). Long-term survival following liver transplantation in patients with EPP was reported, but transplantation does not completely cure the disease since the patient still carries the FECH gene mutation (Meerman, 2000).

Treatment

Since the discovery of EPP in 1961, there has been significant progress in understanding the genetics and the pathogenesis of this disease. Treatment of erythropoietic protopophyria involves the administration of large doses of beta-carotene or L-cysteine-HCl, which are prescribed to ease the sensibility to sunlight by interfering with porphyrin-sensitized photoxidative damage in the skin and delaying the appearance of light-exposure symptoms (Badminton and Elder, 2002; Mathews and Rosner, 2002). Intravenous administration of di-α-tocopherol acetate (vitamin E) results in a significant decrease in the concentration of accumulated protopophyrin in erythrocytes and a progress in liver function, suggesting that vitamin E can be used as a therapeutic option in treating EPP patients with liver complications (Komatsu et al, 2000). Application of reflective sunscreen preparations remains the most prescribed treatment, even though their effectiveness varies among patients with different levels of accumulated protopophyrin, and therefore different levels of photosensitivity (Schneider et al, 2000a). Dietary fish oil rich in omega-3 polyunsaturated fatty acids was suggested as an option in EPP therapy (Chakranarti and Tan, 2002). Many other treatments are described, and in case of intolerance to beta-carotene, α-tocopherol or sunscreens, pyridoxine can be used to reduce photosensitivity in EPP patients (Ross and Moss, 1990).

In EPP patients with liver failure, liver transplant is the only possible therapy, even though transplants are not successful for all patients since some of them die within few months after transplantation due to abdominal bleeding and other complications (Bloomer et al, 1996). In the case of successful liver transplant, patient monitoring showed alleviation of skin photosensitivity and absence of protopophyrin deposits in the transplanted liver (Leone et al, 2000). Nevertheless, these patients still carry the genetic mutations responsible for liver disease development, and the level of erythrocyte protopophyrin remains high after liver transplant, making reappearance of the disease possible (Bloomer et al, 1996). Gordeuk et al (1986) found that oral administration of iron might decrease the free erythrocyte protoporphyrin levels and reestablish normal liver function, suggesting that iron therapy could prevent liver complications in patients with EPP. Because protopophyrin originates mostly from the erythroid cells, bone marrow transplant can be a successful therapy for patients with severe EPP complications. In fact, Lichtin et al (1998) succeeded in curing a patient with EPP by allogenic bone marrow transplant.

None of the prescribed treatments is completely effective, since tolerance of sunlight diminishes when the treatment is stopped (Schneider et al, 2000a). The best way to manage the EPP disease and alleviate its symptoms is by adjusting the life-style and avoiding sunlight to minimize porphyrin phototoxicity (Schneider et al, 2000a).

As mutations associated with EPP continue to be identified, phenotype/genotype correlations should become clear. It may eventually be possible to identify those patients predisposed to develop hepatic failure. With the advances in molecular genetics, gene therapy holds particular promise as a future therapy for EPP. Gene therapy has successfully been used to correct enzyme defects *in vitro* suggesting that ferrochelatase would make a promising target for

gene therapy in the treatment of this disease. Mathews-Roth et al (1995) showed that expression of human ferrochelatase gene in cultured fibroblasts from patients with EPP reduced the enzyme deficiency. In a more recent study, Pawliuk et al (1999) succeeded in transferring the FECH gene into hematopoietic stem cells in a murine with erythropoietic protopophyria and accomplished a long-term cure of skin photosensitivity associated with the disease.

Objectives of the research

There are many possible explanations for the variability in residual activity of ferrochelatase in patients with EPP. One current popular suggestion is that the clinical manifestation of EPP requires the coinheritance of a mutated FECH allele and a weakly expressed normal FECH allele (Gouya et al, 1996, Gouya et al, 1999). This model may explain in part the 10-50% residual activity of some EPP mutations compared to the normal enzyme. However, a molecular explanation for the actual decrease in ferrochelatase activity from missense mutations is lacking. Now that the crystal structure of human ferrochelatase is solved, and we know that it is a homodimeric protein, another possible explanation for the low activity is that ferrochelatase is active only when both monomers are normal. Studies on EPP ferrochelatases have focused on measuring enzyme activity on recombinant homodimeric mutants. In the current study, we report the first investigation of the activity and physical properties of homo- and heterodimeric mutant ferrochelatases.

The objectives of this research were to investigate the activity of homo- and heterodimeric ferrochelatases with EPP mutations, provide a molecular explanation for the decrease in ferrochelatase activity associated with EPP missense mutations, and investigate the effect of most missense mutations on ferrochelatase structure and activity. Twelve EPP missense

mutations were investigated in this study. These mutations were P334L, Y191H, S264L, F260L, M267I, M288K, K379N, Q139L, C236Y, C406S, F417S, and H386P. The major goal was to express, purify and kinetically examine the heterodimeric enzyme to see if the loss of activity is additive or greater than expected. To achieve this objective, we had to develop a system to coexpress wild type and mutant ferrochelatase and to separate heterodimers from homodimers.

CHAPTER 2

PRODUCTION AND CHARACTERIZATION OF ERYTHROPOIETIC PROTOPORPHYRIC HETERODIMERIC FERROCHELATASES

Materials and Methods

Construction of heterodimeric human ferrochelatase

The expression of the heterodimeric mutant human ferrochelatase was carried out using two ferrochelatase producing plasmids. The first plasmid encoding ferrochelatase was previously constructed in our laboratory (Burden et al, 1999). This plasmid contained a 6-histidine-tag and an ampicillin resistance gene along with a ferrochelatase cDNA containing an EPP mutation. The second plasmid contained the wild type ferrochelatase cDNA with a CBP-tag (calmodulin binding protein) and a kanamycin resistance gene. The steps used to construct the second plasmid are summarized in Figure 3.

Step 1: Construction of the pTrcHis-kanamycin plasmid

Both plasmids pTrcHis (Invitrogen, Carlsbad, CA) and pACYC177 (Fermentas, Hanover, MD) were digested with the restriction enzyme *Bsp*HI. The goal of this step was to remove the kanamycin gene (kan) from plasmid pACYC177 and the ampicillin resistance gene (amp) from plasmid pTrcHis. The digested products were separated on TAE gel and purified using the QIAquick Gel Extraction Kit (QIAGEN, Valencia, CA). The kanamycin gene and the pTrcHis

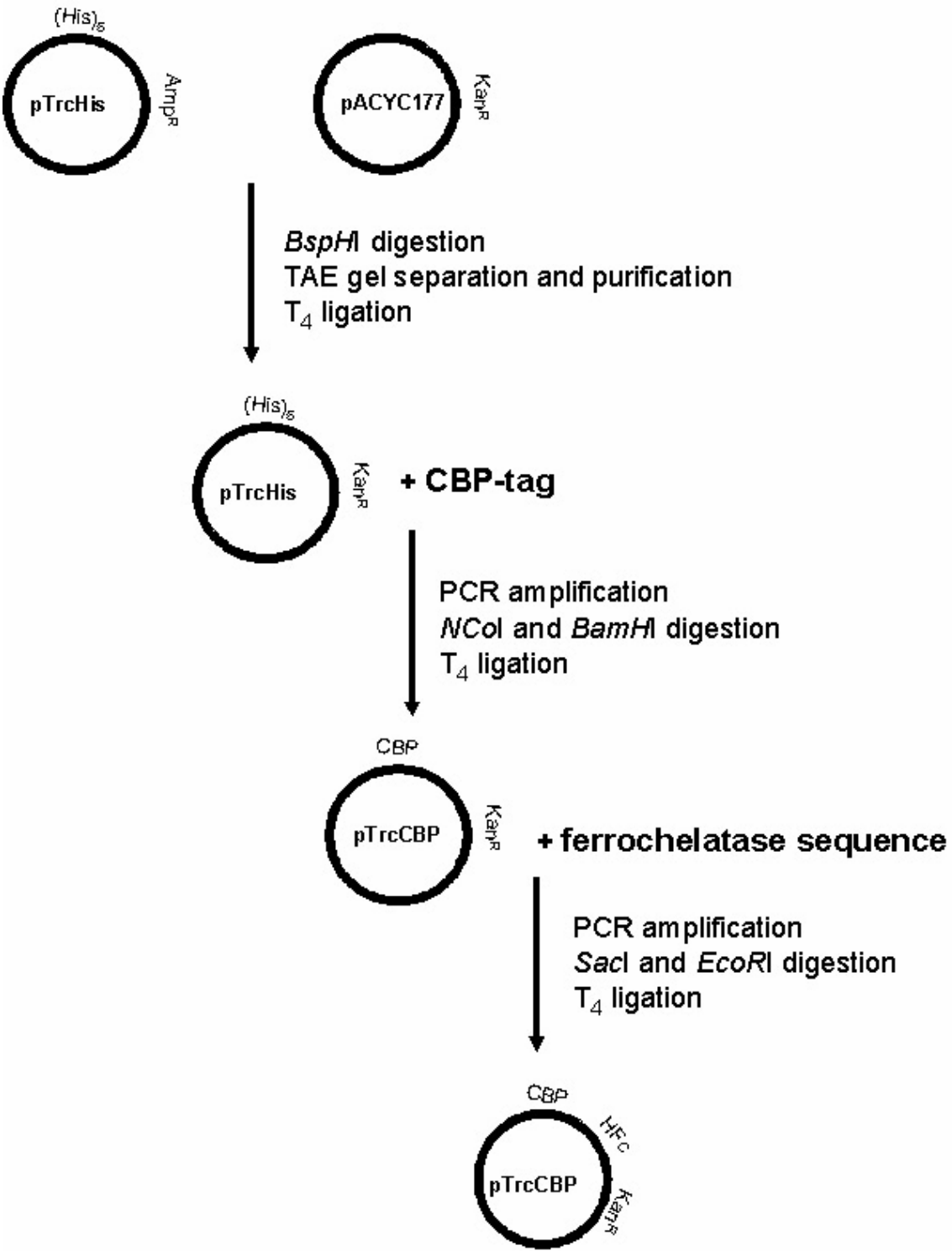

Figure 3. The steps used to construct the pTrc-CBP-kanamycin-human ferrochelatase plasmid.

plasmid lacking the ampicillin resistance gene were then ligated using T4 ligase to form pTrc-His-Kanamycin plasmid.

Step 2: Construction of the pTrc-CBP-kanamycin plasmid

CBP (Calmodulin Binding Protein)-tag sequence was PCR amplified using the following sets of primers: Primer1: Sense: 5' GCG GGG **GCC ATG G**GT AAG GCA CGA TGG AAA AAG AAT TTC ATA GCC GTC TCA GCA GCC AAC 3'; Antisense: 5' GTT GGC TGC TGA GAC GGC TAT GAA ATT CTT TTT CCA TCG TCG CTT AC**C CAT GGC** CCC CGC 3'. The bold sequence indicates the *Nco*I restriction site used for cloning. The underline indicates the CBP-tag sequence. Primer 2: Sense: 5' GTC TCA GCA GCC AAC CGC TTT AAG AAA ATC TCA TCC TCC GGG GCA CTT **GGA TCC** GCG GGG 3'; Antisense: 5' CCC CGC **GGA TCC** AAG TGC CCC GGA GGA TGA GAT TTT CTT AAA GCG GTT GGC TGC TGA GAC 3'. The bold sequence indicates the *Bam*H1 restriction site used for cloning. The underline corresponds to CBP-tag sequence. These sets of primers were used to create the CBP-tag. The third set of primers was used to clone the CBP-tag into the pTrc- kanamycin plasmid. Primer 3: Sense: 5' GCG GGG **GCC ATG G**GT 3'; Antisense: 5' CCC CGC **GGA TCC** AAG 3'. Bold indicates the *Nco*I restriction site used for cloning. Both amplified CBP-tag (PCR product) and the constructed pTrcHis-kanamycin plasmid were digested with *Nco*I and *Bam*HI to eliminate the His-tag sequence from the pTrcHis-kanamycin plasmid. Digest products were purified using the QIAquick Gel Extraction Kit (QIAGEN, Valencia, CA) and then ligated using T4 ligase. The resulting plasmid contained both the CBP-tag and kanamycin resistance gene sequences and was named pTrc-CBP-kanamycin.

Step 3: Construction of the pTrc-CBP-kanamycin-human ferrochelatase plasmid

In order to insert the sequence of human ferrochelatase into the pTrc-CBP-Kanamycin plasmid, the ferrochelatase coding sequence was PCR amplified using the following primers: Sense: 5' GCG GGG **GAG CTC** CAA CCG CAG AAG AGG AAG 3'. Bold indicates the *Sac*I restriction site used for cloning and the underline represents the beginning of human ferrochlatase sequence. Antisense primer: 5' CCC GCG **GAA TTC** TCA CAG CTG CTG GCT GGT 3'. Bold indicates the *EcoR*I restriction site used for cloning; the underline corresponds to the end of human ferrochelatase sequence. The PCR product and the pTrc-CBP-kanamycin plasmid were both digested with *Sac*I and *Eco*RI restriction enzymes, purified using the QIAquick Gel Extraction Kit and then ligated with T4 ligase. The constructed plasmid carried the CBP-tag, kanamycin resistance, and the human ferrochelatase sequences and was named pTrc-CBP-kanamycin-human ferrochelatase.

Expression of His-tag and His-CBP-tag wild-type human ferrochelatases (hFc)

His-tag wild-type ferrochelatase plasmid and CBP-tag wild type ferrochelatase plasmid were co-transferred into *E. coli* strain JM109. Colonies were selected on LB plates containing both amp (His) and kan (CBP) for selection. Mature hFc was expressed by inoculating one colony with both His-tag and CBP-tag plasmids into 100 ml Circlegrow (Bio 101, Montreal, Quebec) containing ampicillin (final concentration 0.2 mg/ml) and kanamycin (final concentration 0.2 mg/ml). Cultures were grown at 30ºC in 500 ml Pyrex^R flasks with shaking at 225 rpm. After 6 hours, the 100 ml culture was transferred into one liter of Circlegrow (Bio101) containing 0.2 mg/ml of ampicillin and 0.2 mg/ml of kanamycin, and cultures were grown at 30ºC for 18-20 hours in 2800 ml Pyrex^R flasks with shaking at 225 rpm. The expression of His-

tag wild-type human ferrochelatase was also conducted as described above, but only one plasmid (His-tag wild-type ferrochelatase) was used and so only ampicillin was necessary for selection.

Purification of wild-type and mutant human ferrochelatase homodimer

Cells were harvested after 18-20 hours by centrifugation at 5000 x g for 15 min at 4ºC. The protein is membrane-bound, thus pelleted cells were resuspended in approximately 60 ml detergent containing solubilization buffer (50mM Tris-MOPS, pH 8.0, 0.1M KCl, 1.0 % sodium cholate, 10 µg/ml phenylmethylsulfonylfluoride (PMSF)). The resuspended cells were sonicated 3-4 times for 30 seconds on ice and centrifuged at 150,000 x g for 35 min at 4ºC. The supernatant containing recombinant hFc was loaded into a column containing 3 ml of Talon-Resin (Clontech, Palo Alto, Ca), metal affinity chromatography resin that uses cobalt ions for purifying recombinant polyhistidine-tagged proteins, that had been previously equilibrated with 5 ml of solubilization buffer. After loading the supernatant, the column was washed with 25 ml solubilization buffer and the protein eluted with elution buffer (6 ml solubilization buffer containing 300 mM imidazole). The protein eluted from this column is the His-tag homodimeric human ferrochelatase.

Construction, expression, and purification of heterodimeric mutant human ferrochelatase

Construction of His-tag mutant human ferrochelatase

To create different hFc mutations, the plasmid R115L was used as the template (Burden et al, 1999) in site directed mutagenesis. Site directed mutagenesis of the R115L plasmid was performed using the QuikChange Site-Directed Mutagenesis kit (Stratagene, LaJolla, Ca). PCR was done using synthetic oligonucleotides containing the desired specific base changes

corresponding to the EPP mutations investigated in this study. The original plasmid DNA was then digested with *Dpn*I. Mutated plasmids were sequenced for confirmation that the desired mutation was present. Oligonucleotides were synthesized by the Molecular Genetics Facilities at the University of Georgia and all mutations were verified by the same facilities.

Expression of heterodimeric mutant ferrochelatase

The steps used to express and purify heterodimeric mutant ferrochelatases are summarized in Figure 4. The expression of heterodimeric mutant ferrochelatase was achieved using the protocol described above for the His-CBP-tag wild type ferrochelatase, except that the His-tag mutant ferrochelatase plasmid, CBP-tag wild type ferrochelatase plasmid, and both ampicillin and kanamycin selection were used. Mature recombinant hFc was obtained by inoculating one colony containing both the His-tag and CBP-tag plasmids into 100 ml Circlegrow (Bio 101).

Purification of wild type and mutant heterodimeric human ferrochelatase

All buffers, solutions, and purification steps were done at 4ºC. Cells were harvested by centrifugation and the pellet was resuspended in 60 ml solubilization buffer. Cells were sonicated and centrifuged as with homodimers. The supernatant was expected to contain a mixture of dimeric proteins containing His-tag homodimeric ferrochelatase with two mutated subunits, CBP-tag homodimeric ferrochelatase with two wild type subunits and His-tag/CBP-tag heterodimeric ferrochelatase where one subunit is wild type and the second subunit has the EPP

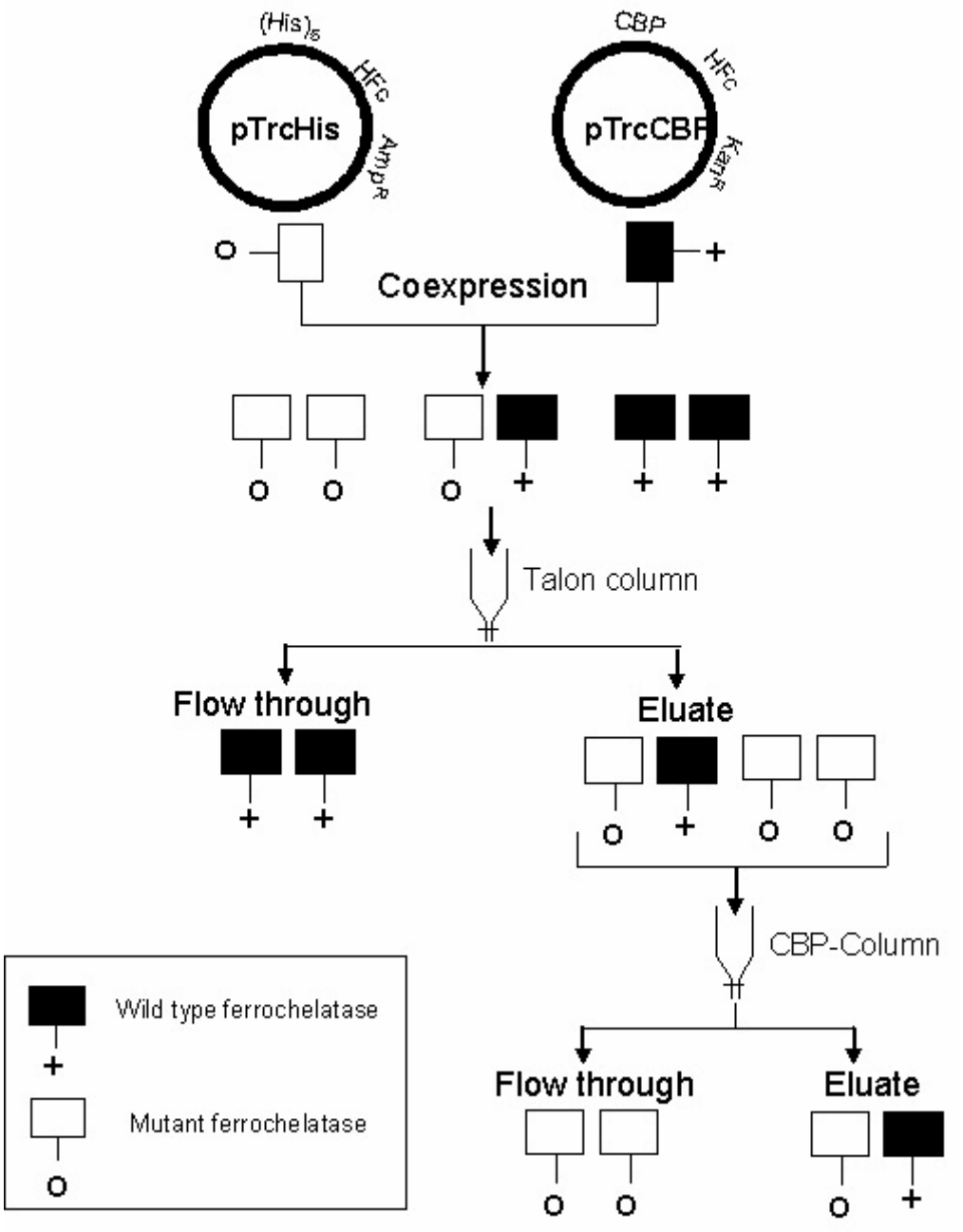

Figure 4. Expression and purification of heterodimeric mutant ferrochelatses.

mutation. The separation of the heterodimers from the homodimers involved four column chromatography steps. The first column was a 3 ml Talon-matrix (Clontech) equilibrated with 5 ml of solubilization buffer. After loading the supernatant, the column was washed with 25 ml solubilization buffer and eluted with an elution buffer (6ml of solubilization buffer containing 300 mM imidazole). The eluted solution from this column contained the His-tag homodimer human ferrochelatase and the His-tag/CBP-tag heterodimer human ferrochelatase. The second column contained 40 ml of Sephadex G-25 (Pharmacia fine chemicals, division of Pharmacia Inc. NJ) equilibrated with the CBP binding buffer (50 mM Tris-HCl, pH 8.0, 150 mM NaCl, 10 mM β-mercaptoethanol, 1.0 mM magnesium acetate, 1.0 mM imidazole, 2 mM $CaCl_2$, 0.1% Tween 20). This column was used to eliminate the imidazole present in the His-tag elution buffer. The eluted protein (mixture of His-tag homodimer and His-tag/CBP-tag heterodimer human ferrochelatases) from the Sephadex G-25 was loaded onto the third 10 ml column of calmodulin affinity resin (Stratagene, LaJolla, CA) equilibrated with the CBP binding buffer. The column was washed with 30 ml of CBP binding buffer. The heterodimer human ferrochelatase was eluted with 30-40 ml of elution buffer (50 mM Tris-HCl, pH 8.0, 10 mM β-mercaptoethanol, 2 mM EGTA, 1M NaCl, 0.1% Tween 20), and concentrated by centrifugation at 3000 rpm for about 1 hr in an Ultrafree centrifugal filter device (Millipore, Billerica, MA). Finally, a 10 ml Sephadex G-25 column was used to eliminate the EGTA present in the CBP elution buffer. This column was equilibrated with the His-tag solubilization buffer (50 mM Tris-MOPS, pH 8.0, 0.1 M KCl, 1.0 % sodium cholate). The purity of ferrochelatase was assessed by UV-visible spectroscopy and SDS-polyacrylamide gel electrophoresis using 12% Tris-HCl Ready Gel (BioRad, Richmond, CA) following the manufacturer's instructions.

Characterization of homodimeric and heterodimeric human ferrochelatases

Characterization by UV-visible spectroscopy

UV-visible spectroscopy was conducted using a Cary-G1 spectrophotometer. Wild type and mutant ferrochelatase concentrations were determined using the extinction coefficient 46,900 $M^{-1} \cdot cm^{-1}$ at 278 nm or the bicinchoninic acid (BCA) procedure (Pierce Chemical Co.). The presence of the [2Fe-2S] cluster was detected by the presence of its characteristic spectra at 330 nm, 460 nm, and 550 nm (Dailey et al. 1994b).

Western blot

Western blots were performed in order to confirm the presence of mutant ferrochelatase heterodimers. The purified protein was separated by polyacrylamide gel electrophoresis on 12% Tris-HCl gel (Bio-Rad, Hercules, CA) including a prestained molecular weight marker (Kaleidoscope prestained standards; Bio-Rad, Hercules, CA) and electrotransferred for 1 hr at 4ºC onto a nitrocellulose membrane. The membrane was blocked with 1% BSA (Bovine Serum Albumin) in TBSC buffer (20 mM Tris-HCl (pH 7.5), 150 mM NaCl, 1 mM $CaCl_2$), then divided into two pieces, one for His-tag detection and the other for CBP-tag detection.

To detect the CBP tag (the wild type subunit), the nitrocellulose membrane was probed with 300 ng of bio-CaM (biotinylated calmodulin) in 1 ml of TBSC for one hour at room temperature. The membrane was washed twice with TBST (TBSC, 0.05% Tween 20) and once with TBSC, then incubated, with shaking, in the appropriate dilution of Streptavidin-AP (alkaline phosphatase; 1:2000 in TBSC) for 1-1.5 hours at room temperature. The nitrocellulose membrane was washed again with TBST and TBSC as before, and then immersed in the NBT-BCIP (NitroBlue Tetrazolium and 5-Bromo-4-chloro-3-indilyl phosphate) color development

solution (0.3 mg/ml of NBT and 0.15 mg/ml of BCIP). The color development reaction was terminated by immersing the nitrocellulose membrane in the stop solution (20 mM Tris-HCl (pH 2.9), 1 mM $CaCl_2$).

To detect the His-tag (the mutant subunit), the nitrocellulose membrane was first probed with a 1: 1000 dilution of the primary antibody (Penta-His antibody mouse IgG) in 1 x TBST (10 mM Tris-HCl (pH 8.0), 150 mM NaCl, 0.5% Tween 20) for 30 minutes. The nitrocellulose membrane was washed 3 times with TBST to eliminate unbound antibody, then transferred to a TBST solution containing the appropriate dilution of the secondary antibody (Rabbit anti-IgG alkaline phosphatase conjugate) and incubated for 30 minutes. The membrane was again washed three times in TBST, and transferred to a NBT-BCIP color development solution. The color development reaction was then stopped by rinsing the membrane in deionized water.

Kinetic analysis of homodimeric and heterodimeric wild type and mutant ferrochelatases

Ferrochelatase activity was assayed aerobically at room temperature by continuous spectrophotometric monitoring of the disappearance of the porphyrin substrate by following the decrease in the absorbance of the porphyrin substrate at 496 nm. The extinction coefficient of 7.5 $mM^{-1} \cdot cm^{-1}$ was used to determine the amount of heme produced. Freshly prepared 10-100 μM ferrous ammonium sulfate and 10-100 μM mesoporphyrin IX (Porphyrin products, Logan, UT) were used as substrates. Mesoporphyrin stock solution was made by mixing 2.5 mg mesoporphyrin IX, 30 μl 2N NH_4OH, 500 μl 10% Triton X-100 in 4.5 ml double distilled water. Mesoporphyrin quantitation was calculated using the extinction coefficient of 445 $mM^{-1} \cdot cm^{-1}$ at 399 nm in 0.1 N HCl. The concentration of ferrous iron in the stock solution was quantitated by employing the ferrous iron chelator ferrozine using the extinction coefficient (278 $mM^{-1} \cdot cm^{-1}$) of

the complex at 562 nm. When preparing 10 ml of the ferrous ammonium sulfate substrate solution 10 mg of ascorbic acid was added to prevent ferrous iron oxidation.

The ferrochelatase assay mixture contained 100 mM Tris-HCl (pH 8.0), 0.5% Tween 20, 1 mM mesoporphyrin, 1 mM ferrous ammonium sulfate and 10 mM β-mercaptoethanol (added to provide a reducing environment). Ferrochelatase (1 nmol/ml) was added last to start the reaction. Ferrochelatase activity from purified samples was expressed as nanomoles of heme per nanomole of ferrochelatase per minute.

Results

Expression and purification of homodimeric and heterodimeric ferrochelatases

Twelve EPP missense mutations (Fig 5) were constructed using site directed mutagenesis and the sequences of the mutants were confirmed by nucleotide sequencing. Wild type and mutant homodimeric ferrochelatases were tagged with 6-histidines at the N-termini, whereas mutant heterodimeric proteins had a His-tag on the mutant subunit and a CBP-tag on the wild type subunit. Wild-type ferrochelatase with either tag was efficiently expressed in the JM109 *E. coli* strain. Recombinant wild type and mutant human ferrochelatases were purified as described in the Materials and Methods. Some mutants had decreased expression levels relative to wild type hFc. For these mutants, individual six-liter cultures were grown and harvested to obtain sufficient protein. Figure 6 shows examples of the purified heterodimeric mutant ferrochelatases.

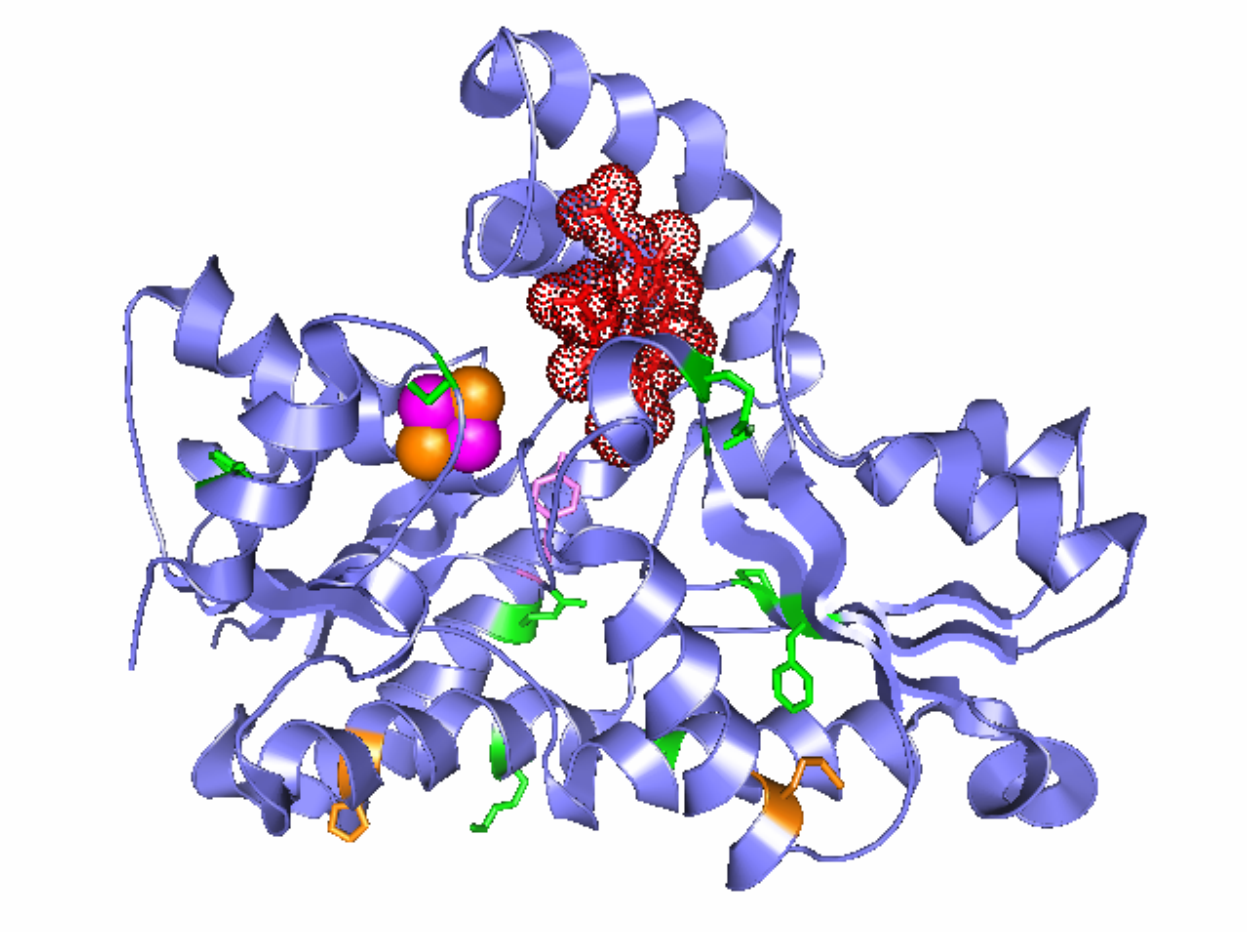

Figure 5: EPP mutations investigated in this study. Porphyrin is shown in dots. The iron-sulfur cluster is shown in spheres. The orange shows the mutations in the dimer interface. The violet shows a mutation in the active site. The green shows the other EPP mutations studied.

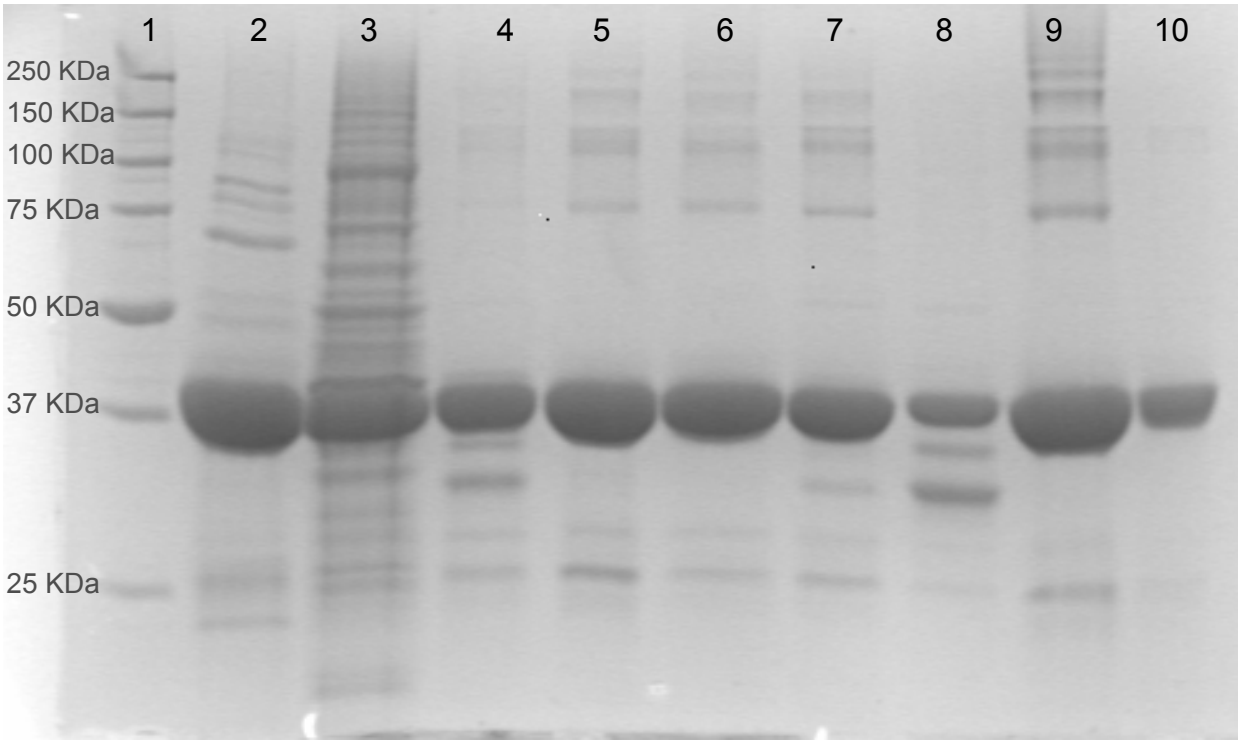

Figure 6. SDS-polyacrylamide gel of purified heterodimeric erythropoietic protoporphyric ferrochelatases. Lane1 , molecular weight markers, lane 2, homodimeric His-tag wild-type ferrochelatase; lane 3, homodimeric CBP-tag wild-type protein; lane 4, His-CBP-tag wild-type; lanes 5, 6, 7, 8, 9, and 10 are the heterodimeric mutants M267I, K379N, Q139L, C236Y, S264L, and F260L respectively.

Characterization of human recombinant ferrochelatases

The visible absorption spectra of human recombinant wild-type ferrochelatases are shown in Figure 7. Wild-type ferrochelatases with a His-tag or a CBP-tag on both subunits or a His-tag on one subunit and a CBP-tag on the other subunit all showed similar spectra, proving that substituting one or both tags did not change the characteristic spectra of the wild type protein.

The recombinant wild type human ferrochelatase and the homodimeric and heterodimeric proteins containing the mutations C236Y, Y191H, K379N, F260L, Q139L, S264L, P334L and M267I had the characteristic reddish color indicative of the presence of the [2Fe-2S] cluster normally found in mammalian ferrochelatases (Dailey et al. 1994b). To provide further evidence for the presence or absence of the [2Fe-2S] cluster in the purified mutant proteins, UV-visible absorbance was measured between the wavelengths of 250 nm and 600 nm. The intactness of the [2Fe-2S] cluster was shown by the presence of its characteristic spectra at 330 nm, 460 nm, and 550 nm (Dailey et al. 1994b). The spectra of the homodimeric and heterodimeric mutant ferrochelatases indicated above were identical to the wild type showing an absorption peak at approximately 330 nm: indicative of an intact [2Fe-2S] cluster (Fig. 8). In contrast, the spectra of the homodimeric mutant ferrochelatases with the mutations F417S, C406S, H386P, and M288K lacked the characteristic spectra of the [2Fe-2S] cluster (Fig. 9). These purified proteins were colorless and in addition, mutants F417S and C406S had little detectable enzyme activity. The lack of color would indicate that the clusters were not assembled or that they were assembled but were not stable. The same results were obtained with the heterodimeric forms of these mutants, except F417S, which did appear to have a very light reddish color during purification, but precipitated after elution from the last column, rendering it unstable for kinetic studies.

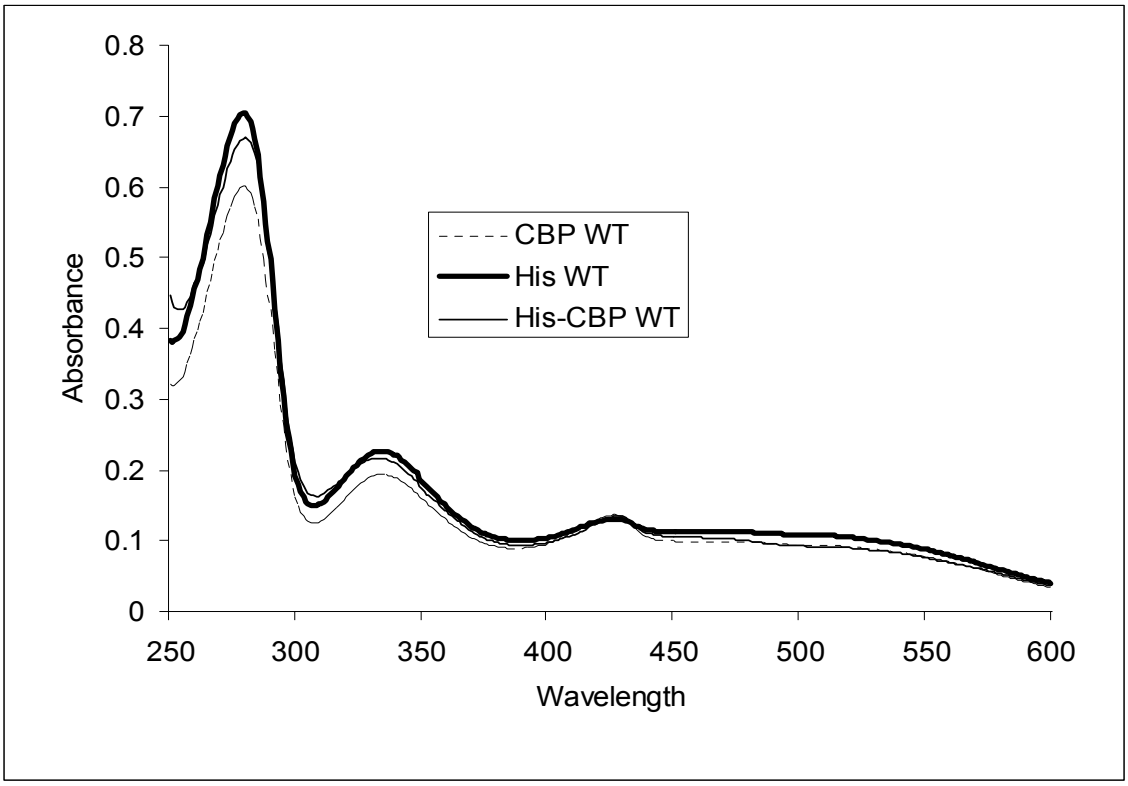

Figure 7. UV-visible spectra for purified His-tag, CBP-tag and His-CBP-tag wild type human ferrochelatases. The top line represents His-tag homodimeric ferrochelatase (His WT), the middle line is for the His-CBP wild type protein (His-CBP WT), and the bottom line represents the CBP-tag homodimeric ferrochelatase (CBP WT).

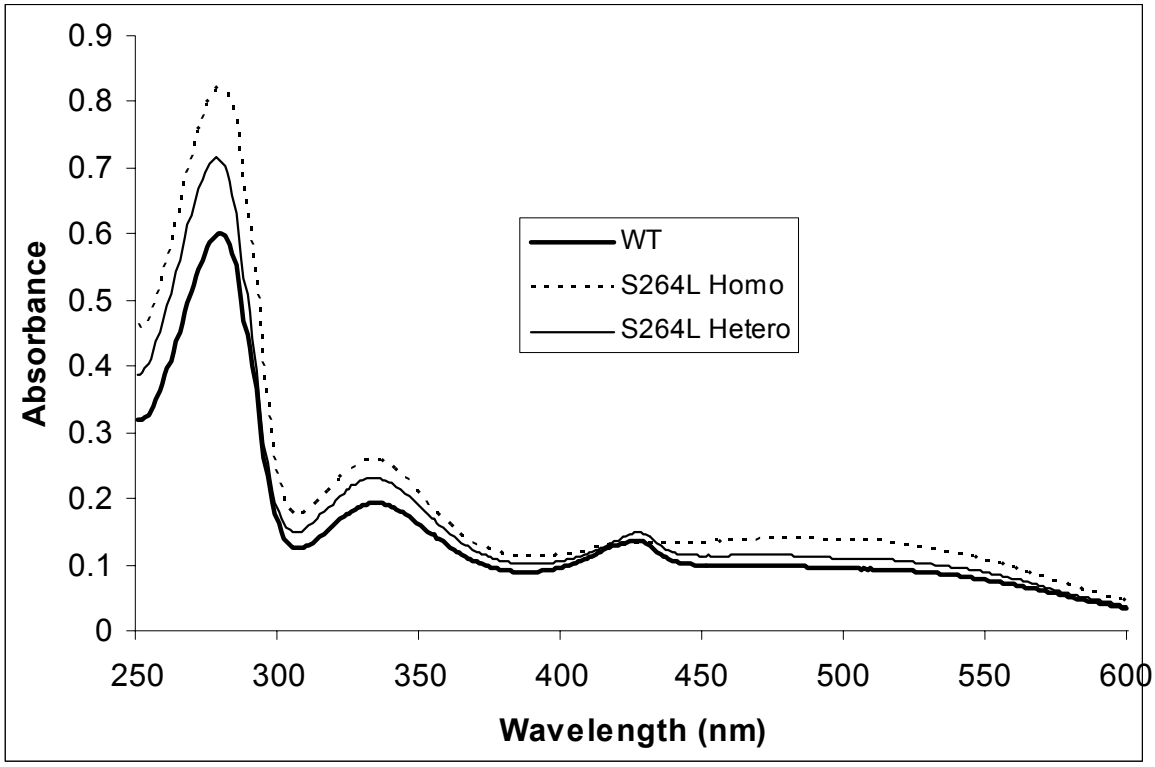

Figure 8. UV-visible spectra for purified wild type and mutant human ferrochelatases. The top line represents the homodimeric mutant S264L (S264L homo), the middle line is for the heterodimeric mutant S264L (S264L hetero), and the bottom line represents the wild-type ferrochelatase (WT). All other mutant proteins showed similar spectra except for the proteins with the mutations M288K, H386P, C406S, and F417S. (See text).

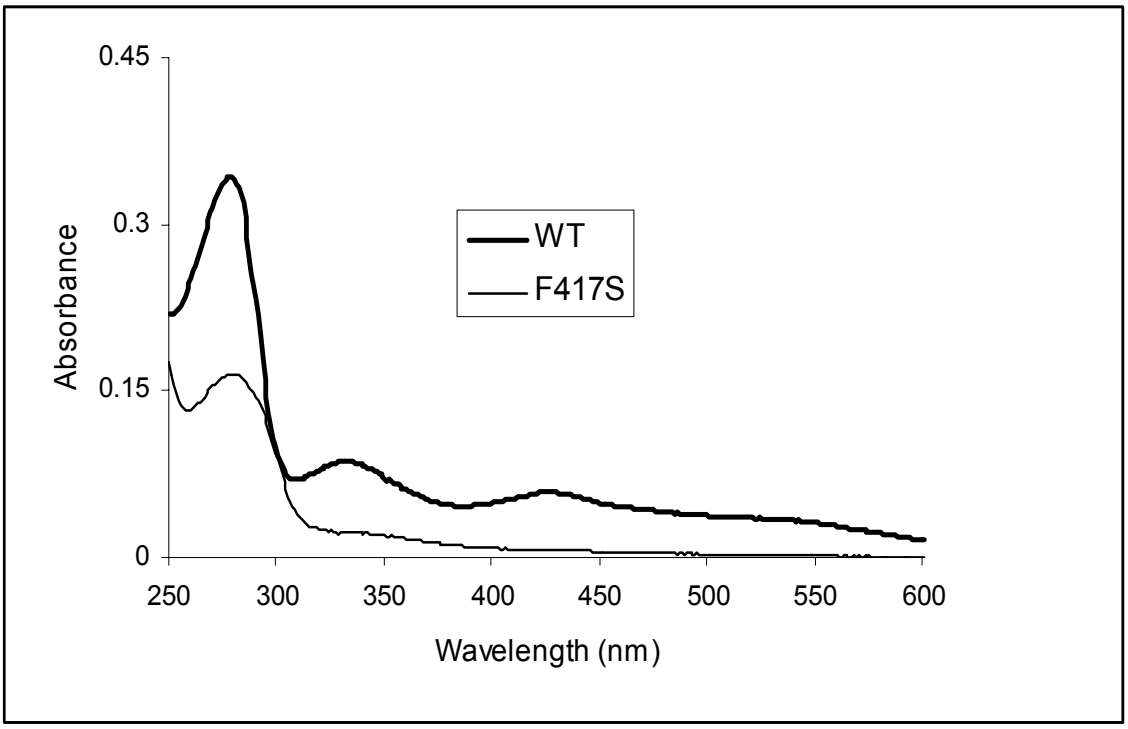

Figure 9. UV-visible spectra for purified wild type and mutant human ferrochelatases. The top line represents the His-tag homodimeric wild type and the bottom line represents the homodimeric mutant F417S. This spectrum shows the lack of the [2Fe-2S] cluster peak around 330 nm for the mutant F417S. The other proteins with the mutations M288K, H386P, and C406S showed similar spectra compared to the mutant F417S (See text).

All mutants with intact iron-sulfur clusters had the characteristic peak at approximately 330 nm. This peak, as well as the red color, diminished upon storage at 4ºC within 1-4 days (Dailey et al, 1994b).

Western blots

The formation of the dimeric wild-type ferrochelatase (one His-tagged monomer + one CBP-tagged monomer) and the heterodimeric mutant ferrochelatases (one normal CBP-tagged monomer + one mutated His-tagged monomer) was evaluated using western blot (Fig 10). Western blot results are summarized in Table 3. These results showed that only heterodimeric mutants H386P and M288K were not isolated, suggesting that the ferrochelatases with these mutations may dimerize, but that they may have a short lifetime because of instability.

Ferrochelatase assays and kinetic parameters

Characterization of His-tag, CBP-tag, and His-CBP-tag wild type ferrochelatases

To verify that the substitution of one or both His-tag on the wild type ferrochelatase by a CBP-tag does not have any effect on the characteristics of the wild type protein, the His-CBP-tagged, His-tagged and CBP-tagged wild type ferrochelatases were expressed, purified and characterized spectroscopically and kinetically. As indicated above, all three forms of wild-type ferrochelatases (His-tag/His-tag, CBP-tag/CBP-tag and His-tag/CBP-tag) had the same characteristic spectra (Fig 7). Kinetic results showed that the wild type ferrochelatases had similar apparent K_ms for iron and mesoporphyrin substrates (Table 4, Fig 11 and Fig 12).

Table 3: Summary of the western blot analysis of the heterodimeric EPP ferrochelatases.

Mutant	Heterodimer Formation
Y191H	+
F260L	+
C236Y	+
K379N	+
S264L	+
Q139L	+
M267I	+
F417S	+
P334L	+
C406S	+
M288K*	-
H386P*	-

* Heterodimeric mutants that could not be isolated. Western blots were conducted on purified enzymes for the first ten mutants and on crude extracts and eluant from the last purification column for the two last mutants (M288K and H386P).

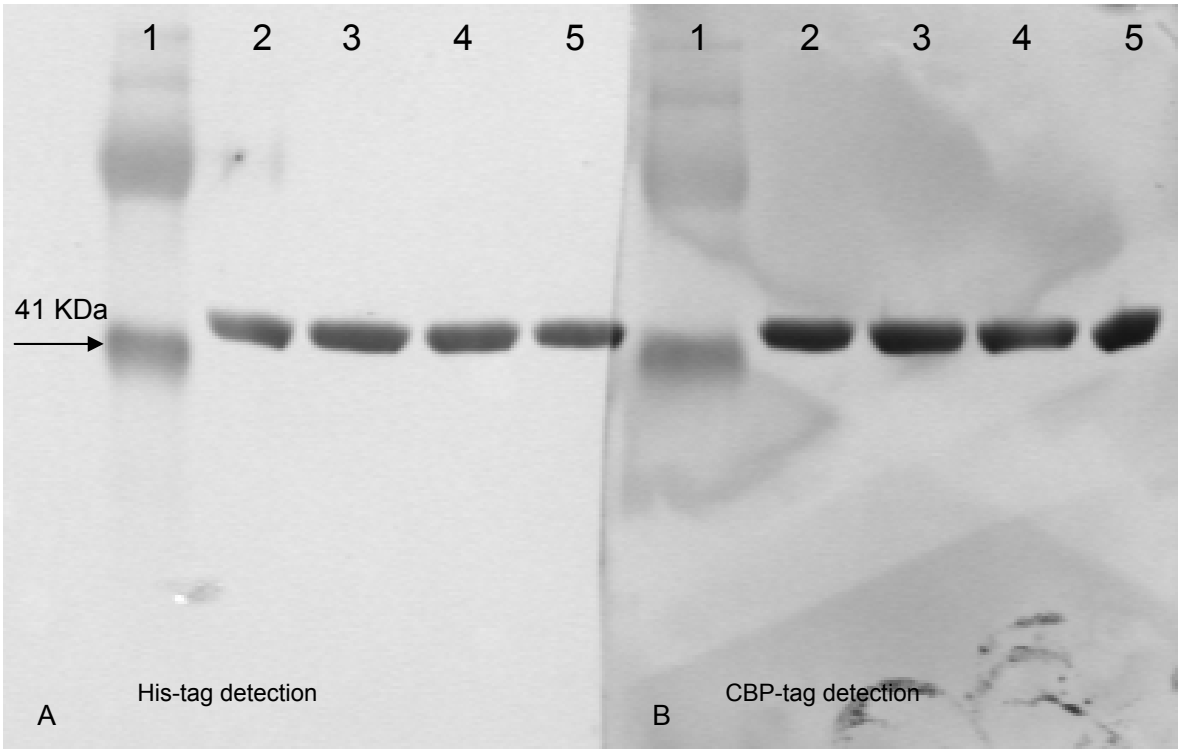

Figure 10. Western blot for the wild type and heterodimeric mutant (F260L) ferrochelatases.
A: Western blot for His-tag detection. Lane 1 is the marker (Kaleidoscope prestained standards (BioRad)), Lanes 2 and 3 are the His-CBP-tag wild type ferrochelatase, lanes 4 and 5 are the heterodimeric mutant (F260L).
B: Western blot for CBP-tag detection. Lane 1 is the marker, lanes 2 and 3 are the His-CBP-tag wild type, lanes 4 and 5 are the heterodimeric mutant (F260L).

A

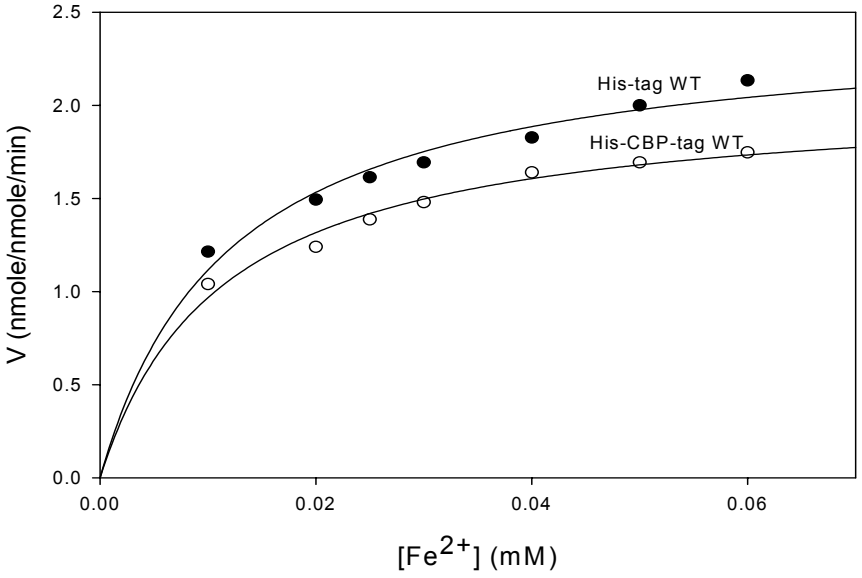

B

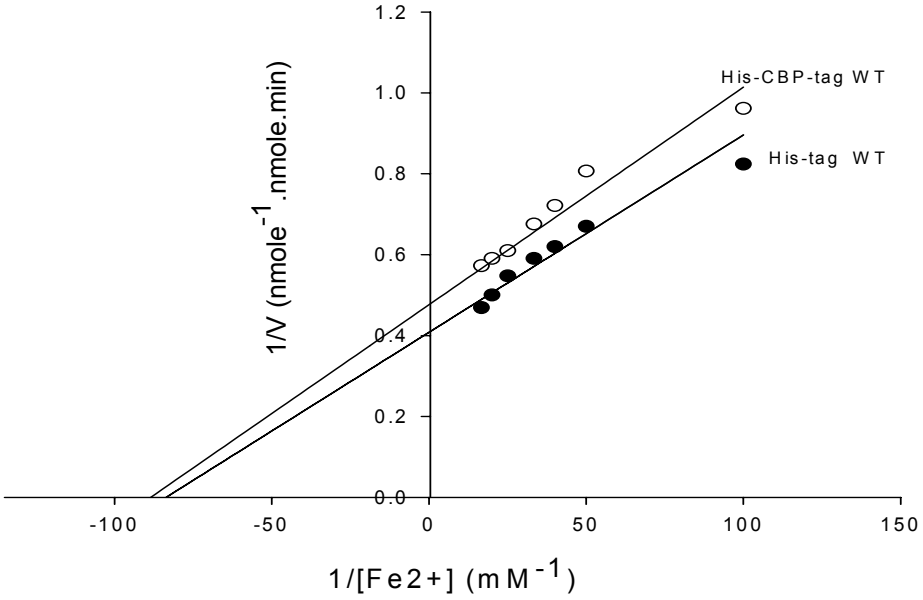

Figure 11. Apparent V_{max} and apparent K_m of ferrous iron for homodimeric his-tag and his-CBP-tag wild type ferrochelatases
(A) Rate (V) vs [Fe2+] for His-tag and His-CBP-tag wild type ferrochelatases.
(B) Lineweaver-Burk (LB) or double reciprocal plot.

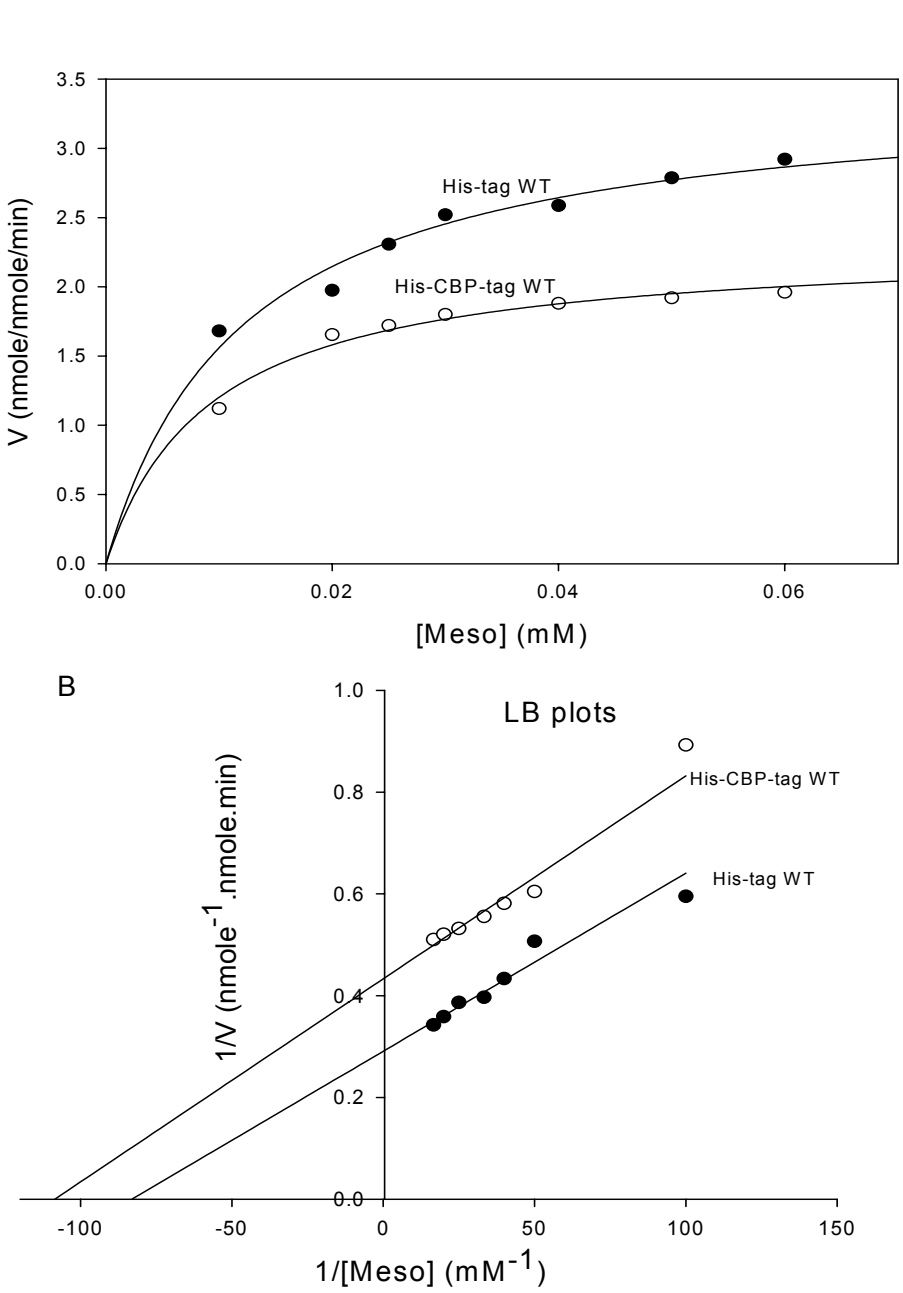

Figure 12. Determination of apparent V_{max} and apparent K_m of mesoporphyrin for homodimeric his-tag and his-CBP-tag wild type ferrochelatases.
(A) Rate (V) vs [Meso] for His-tag and His-CBP-tag wild-type ferrochelatases.
(B) Lineweaver-Burk (LB) or double reciprocal plot.

The V_{max} of the wild-type heterodimer is 25% lower than that of the homodimer wild type. This may be explained by the differences in the purification procedures. Heterodimeric wild type hFc was purified through a long procedure involving four different columns. Heterodimers were also concentrated for about one hour before use in kinetic analysis. In contrast, the homodimeric wild type was purified through a single column and did not need to be concentrated (see Materials and Methods). These different purification methods of hetero- versus homodimers may also explain the decrease in activity of heterodimeric mutants compared to homodimeric mutants.

Kinetic characterization of homodimeric and heterodimeric mutant ferrochelatases

The apparent kinetic parameters of the wild type and mutant ferrochelatases for iron and mesoporphyrin are summarized in Table 4. EPP mutations investigated in this study were divided into five classes according to their location in the human ferrochelatase structure. The first class included mutations in or near the active site pocket, the second class had mutations in the dimer interface, the third class consisted of mutations in the protein surface, the fourth class had internal mutations, and the fifth class included mutations in the C-terminal end of the protein.

Complementation of E. coli ΔhemH by F417S, C406S, H386P, M288K, and S264L

The goal of these experiments was to detect enzyme activity of mutants that had no measurable activity during the enzyme assays. The ferrochelatase deficient *E.coli* strain (ΔhemH) grows poorly in the absence of heme supplementation. Plasmids carrying the ferrochelatase gene with the various mutations were electroporated into ΔhemH cells to determine if any of these mutants could rescue the cell's mutant phenotype. Normal growth

would indicate complementation and expression of ferrochelatase in the deficient strain. The data of this experiment showed that among the various mutants investigated; only F417S and C406S complemented the ferrochelatase deficient *E. coli.* Therefore, these proteins had retained some of their activities. The complementation of ΔhemH by H386P, M288K, and S264L was negative, indicating that ferrochelatases with these mutations were completely inactive (Table 5).

Table 4. Effect of EPP mutations on homodimeric and heterodimeric human ferrochelatases kinetic parameters.

Mutant	Homodimers			Heterodimers		
	K_m^{Fe}(μM)	K_m^{Meso}(μM)	V_{max} (min^{-1})	K_m^{Fe}(μM)	K_m^{Meso}(μM)	V_{max} (min^{-1})
WT	11.96	12.07	3.44	11.41	9.45	2.61
P334L	48.81	18.23	0.56	ND	ND	0
Y191H	25.07	129.1	2.57	37.97	17.18	1.83
S264L	ND	ND	0	23.48	13.83	1.67
F260L	76.27	14.6	1.82	44.14	9.71	0.94
M267I	11.71	12.35	3.18	8.3	6.1	2.53
M288K	ND	ND	0	ND	ND	0
K379N	110.11	22.4	2.03	23.22	25.28	1.57
Q139L	26.2	26.7	0.6	21.87	9.17	1.65
C236Y	14.1	30.2	0.93	17.9	12.9	0.69
C406S	ND	ND	0	ND	ND	0
F417S	ND	ND	0	ND	ND	0
H386P	ND	ND	0	ND	ND	0

ND = Not Determined

Table 5. Characteristics of homodimeric mutant ferrochelatases.

Mutation	ΔhemH complementation	Presence of the [2Fe-2S] cluster
C406S	+	–
F417S	+	–
H386P	–	–
M288K	–	–
S264L	–	+

ΔhemH complementation tests were conducted using purified enzymes.

Discussion

Mutations in the gene coding for ferrochelatase are the cause of erythropoietic protoporphyria (EPP). The mode of inheritance of this disease is still controversial, especially after the discovery of putative cases of recessive inheritance (Sarkany et al, 1994). Early investigations of ferrochelatase activity in various pedigrees suggested an autosomal dominant inheritance with 50% decrease in the activity. However, later studies indicated that patients with EPP have a residual activity that is only between 10-50% of normal (Todd, 1994). Early attempts to explain the variability in the inheritance and expression of the disease suggested that the inheritance of a FECH gene mutation from one parent is necessary, but not sufficient, to cause the disease; since in many cases both parent and child have the same mutation of the FECH gene but only the child develops clinical symptoms of the disease (Norris et al, 1990; Sarkany et al, 1994). This suggests that additional factors are required to produce the clinical features of the disease. Several recent studies have focused on identifying these factors and several theories have emerged. The best supported of these theories suggests a mode of inheritance of EPP in which the clinical expression of the disease requires both the inheritance of a mutated allele (e.g. a missense mutation in the coding region) and a weakly expressed normal FECH allele (Gouya et al, 1996).

To date, 71 EPP mutations have been identified (www. HGMB.org; Schneider et al. 2000a). These mutations include 21 missense mutations, four of which have not yet been published (Elder, personal communication). The majority of EPP mutations are "null allele" mutations including nonsense mutations that result in nucleotide deletions or insertions and exon skipping and frameshift mutations that result in truncated inactive protein.

Genetically, the coinheritance of a normal weakly expressed ferrochelatase allele and a mutant allele may explain the 10-50% enzyme activity of EPP mutations compared to the wild type enzyme. While the low-expression model is appealing and may explain some EPP mutations, a molecular explanation for the decrease in ferrochelatase activity of most missense mutations is lacking. A small number of missense mutations causing residue replacement in the enzyme have been identified in patients with EPP. Now that the crystal structure of human ferrochelatase is solved, and we know that it is a homodimeric protein, another possible explanation for the low activity is that ferrochelatase is active only when both monomers are normal. Most studies have focused on measuring enzyme activity in homodimeric mutants. In the current study, we report the first investigation of the activities and physical properties of homo- and heterodimeric mutants. Herein, we investigate 12 missense mutations because, unlike "null allele" mutations that produce truncated proteins, point mutations may provide information about the function of individual residues in the enzymatic catalysis.

All EPP mutations investigated in this study were identified in patients who were clinically diagnosed based on cutaneous photosensitivity and increased levels of erythrocyte protoporphyrin (www.HGMD.org, Schneider et al, 2000a; Rufenacht et al, 1998).

Characteristics of mutations in or near the active site pocket

All the missense mutations located in or near the active site pocket are shown in Fig 13.

Mutation P334L

The EPP mutation P334L was first identified by Rufenacht et al. (1998). When expressed in a bacterial system, this mutant showed a large reduction in ferrochelatase activity (less than 19% of the normal) (Rufenacht et al. 1998).

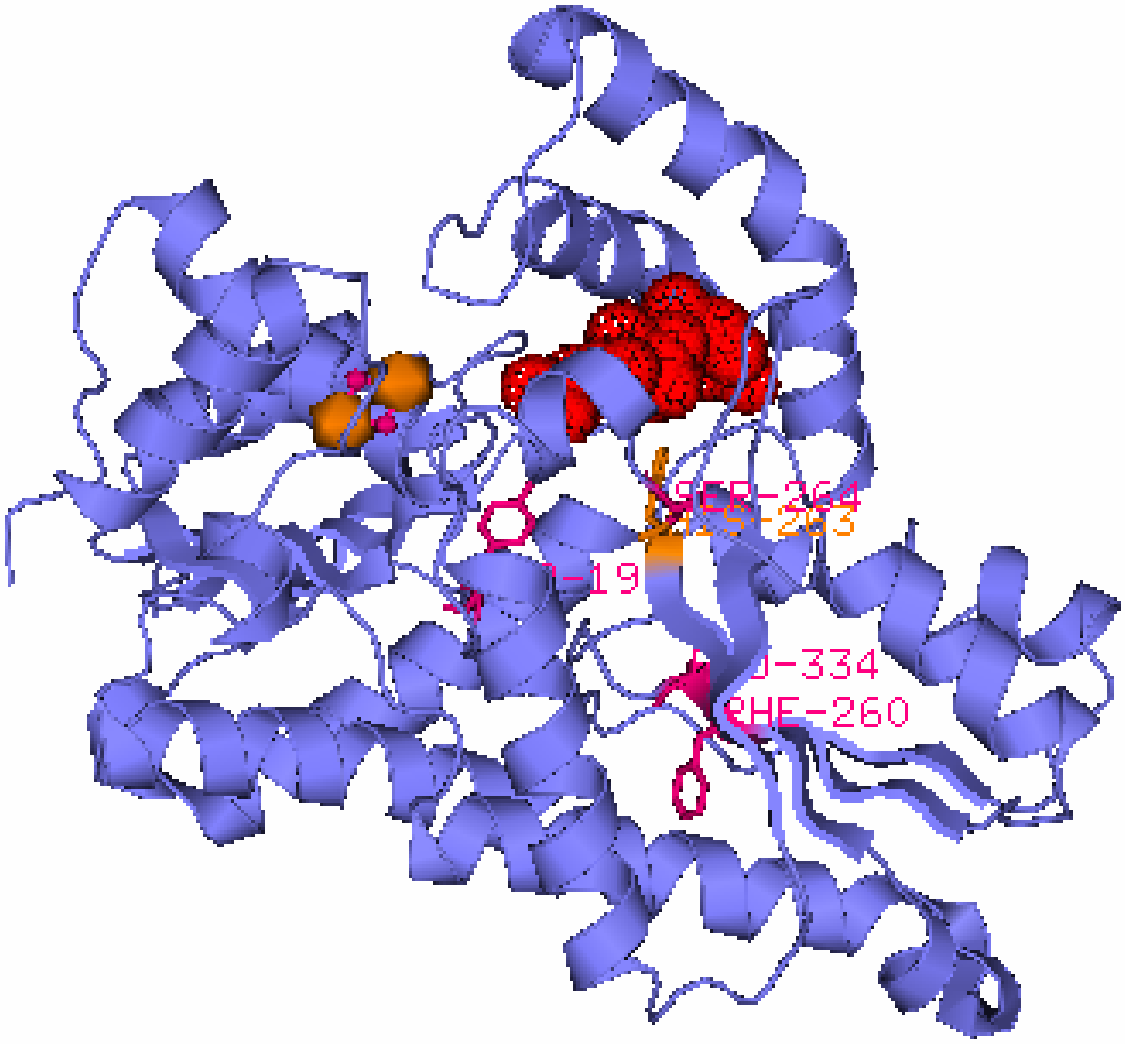

Figure 13. Location of erythropoietic protoporphyria (EPP) mutations (P334L, Y191H, S264L, and F260L). A single monomer is shown to demonstrate the location of the residues in or near the active site pocket that have been reported to be modified in EPP patients. The mutations are shown in violet sticks. The center of the active site pocket represented by the residue His-263 is shown in orange. The porphyrin substrate is shown in red dots and the [2Fe-2S] cluster is shown in spheres.

Our data for the homodimeric mutant were consistent with those described by Rufenacht et al. (1998) showing a considerable change in the apparent V_{max} and Fe K_m (Table 4). The visible spectrum of the homodimeric mutant showed the characteristic feature of an [2Fe-2S] cluster. We were unable to isolate the heterodimeric mutant suggesting a decrease in the structural stability of the protein.

The highly conserved P334 residue is at the bottom of the active site (Table 6, Fig 14), but appears to be too distant (12.6Å) from H263 and other residues suggested to be involved in the metal ion coordination and porphyrin proton abstraction and metallation during catalysis (Sellers et al, 2001). The proline to leucine substitution might affect the structural aspects of the protein and its stability.

Mutation Y191H

The residual activity of this mutant as a homodimer was approximately 74% of the wild type and was consistent with the results reported by Rufenacht et al (1998) and Sellers et al (2001). The residue Y191 is located in the active site, about 9Å from the center of the active site represented by the residue H263 (Fig 13). It is approximately 3Å from R164 in the wild type enzyme and is aligned so that a hydrogen bond can exist between the –OH of Y191 and the guanido group of R164. We speculate that the mutation Y191H disrupts or at least reorients the H-bond with R164. R164 has been proposed to be involved in the substrate iron binding prior to porphyrin metallation (Sellers et al, 2001). The mutant Y191H had altered apparent K_ms for both substrates, contrary to the finding of Sellers et al. (2001), where this mutant had a similar porphyrin K_m compared to the wild type and only the K_m for the iron was altered.

Table 6. Conserved residues of ferrochelatase*. The residues have the human numbering.

Identical residues	Highly conserved residues	
G77	V85	L265
P79	F88	G273
D95	L89	D274
R115	L107	V287
Y123	I111	W301
S130	I132	G306
P131	G127	L311
H263	G128	D316
P266	R164	P334
Y276	Y165	D340
Q302	P168	I342
S303	M177	T344
W310	P192	L345
L311	S195	E347
P313	W227	I348
F337	I241	L381
E343	S261	V385

*Adapted from (Dailey and Dailey, 2003). The analysis is based on the comparison of 44 eukaryotic and prokaryotic ferrochelatase sequences in public databases. The identical residues are observed in 95% of the sequences or more. The highly conserved residues occur with conservative replacements in more than 95% of sequences.

```
human               1 MRSLGANMAAALRAAGVLLRDPLASSSWRVCQPWRWKSGAAAAAVTTCTAQHAQGAKPQV
bovine              1 ~~~~~~~MAAALRSAGVLLRDRLLYGGSRACQPRRCQSGAATAAAATETAQRARSPKPQA
mouse               1 MLSASANMAAALRAAGALLREPLVHGSSRACQPWRCQSGAA.VAATTEKVHHAKTTKPQA
chicken             1 ~~~~~~~MAAAGRAA.....RPLVAGGRQLRVPLRWRGQVAAAAPST.........KPQA
xenopus             1 ~~~~~~~~MAAFRAAHRLLGHILRNESSAGLVTQRWSSSAAVAS.....VPKSSDPKPHA
drosophila          1 ~~~~~~~~~~~~~~~~~~~~~~~~~~~~~~~~~~~~~~~~~MFLHNTKFCRLASGLAGGV
s_cerevesiae        1 ~~~~~~~~~~~~~~~~~~~~~~~~~~~~~~MLSRTIRTQGSFLRRSQLTITRSFSVTFNM
s_pombe             1 ~~~~~~~~~~~~~~~~~~~~~~~~~~~~~~~~~~~~MSVSSYSSDASSTVMDESPPNGVT
b_subtilis          1 ~~~~~~~~~~~~~~~~~~~~~~~~~~~~~~~~~~~~~~~~~~~~~~~~~~~~~~~~~~~~
e_coli              1 ~~~~~~~~~~~~~~~~~~~~~~~~~~~~~~~~~~~~~~~~~~~~~~~~~~~~~~~~~~~~
c_crescentus        1 ~~~~~~~~~~~~~~~~~~~~~~~~~~~~~~~~~~~~~~~~~~~~~~~~~~~~~~~~~~~~
m_tuberculosis      1 ~~~~~~~~~~~~~~~~~~~~~~~~~~~~~~~~~~~~~~~~~~~~~~~~~~~~~~~~~~~~

human              61 QP.QKRKPKTGILMLNMGGPE..TLGDVHDFLLRLFLDRDLMTL.P.IQNKLAP.FIAKR
bovine             54 QP.GNRKPRTGILMLNMGGPE..TVEEVQDFLQRLFLDQDLMTL.P.VQDKLGP.FIAKR
mouse              60 QP.ERRKPKTGILMLNMGGPE..TLGEVQDFLQRLFLDRDLMTL.P.IQNKLAP.FIAKR
chicken            40 EP.ETRKPKTGILMLNMGGPE..RLDDVHDFLLRLFLDRDLMTL.P.AQNKLAP.FIAKR
xenopus            48 QP.DKRKPKTGILMLNMGGPE..TLDDVHGFLLRLFLDKDLMTL.P.AQSKLAP.FIAKR
drosophila         20 RNLSGQKPKTAILMLNMGGPT..HTDQVHDYLLRIMTDRDMIQL.P.VQSRLGP.WIAQR
s_cerevesiae       31 QNAQKRSP.TGIVLMNMGGPS..KVEETYDFLYQLFADNDLIPISAKYQKTIAK.YIAKF
s_pombe            25 KSVSGKGP.TAVVMMNMGGPS..NLDEVGPFLERLFTDGDIIPL.GYFQNSLGK.FIAKR
b_subtilis          1 ~~~~MSRKKMGLLVMAYGTPYKE..EDIERYYTHIRRGRK...............PEPE
e_coli              1 ~~~~MRQTKTGILLANLGTPDAPTPEAVKRYLKQFLSDRRVVDTSRLLWWPLLRGVILPL
c_crescentus        1 ~~~~~MTQKLAVVLFNLGGPD..GPDAVRPFLFNLFRDPAIIGAPALIRYPLAA.LISTT
m_tuberculosis      1 ~~~~~~MQFDAVLLLSFGGPEGP..EQVRPFLENVTRGRG...............VPAE

                                                 *
human             115 RTPKIQEQYRRI..GGGSPIKIWTSKQGEGMVKLLDELSPNTAPHKYYIGFRYVHPLTEE
bovine            108 RTPKIQEQYRRI..GGGSPIKMWTSKQGEGMVKLLDELSPHTAPHKYYIGFRYVHPLTEE
mouse             114 RTPKIQEQYRRI..GGGSPIKMWTSKQGEGMVKLLDELSPATAPHKYYIGFRYVHPLTEE
chicken            94 RTPRIQEQYSRI..GGGSPIKKWTAVQGEGMVKLLDSMSPQTAPHKYYIGFRYVHPLTEE
xenopus           102 RTPKIQEQYSKI..GGGSPIKKWTEQQGEGMVKLLDELSPATAPHKYYIGFRYVRPLTEA
drosophila         75 RTPEVQKKYKEI..GGGSPILKWTELQGQLMCEQLDRISPETAPHKHYVGFRYVNPLTEN
s_cerevesiae       87 RTPKIEKQYREI..GGGSPIRKWSEYQATEVCKILDKTCPETAPHKPYVAFRYAKPLTAE
s_pombe            80 RTPKVQNHYSDI..GGGSPILHWTRIQGSEMCKILDKKCPESAPHLPFVAFRYAPPLTED
b_subtilis         39 MLQDLKDRYEAI..GGISPLAQITEQQAHNLEQHLNEIQDEIT.FKAYIGLKHIEPFIED
e_coli             57 RSPRVAKLYASVWMEGGSPLMVYSRQQQQALAQRLPEM.PVA......LGMSYGSPSLES
c_crescentus       53 REKSAKANYAIM..GGGSPLLPETEKQARALEAALALAMPGVEA.KCFIAMRYWHPLTDE
m_tuberculosis     37 RLDAVAEHYLHF..GGVSPINGINRTLIAEL.....EAQQEL...PVYFGNRNWEPYVED

                                        *
human             173 AIEEMERDGLERAIAFTQYPQYSCSTTGSSLNAIYRYYNQVGRKPTMKWSTIDRWPTHHL
bovine            166 AIEEMERDGLERAVAFTQYPQYSCSTTGSSLNAIYRYYNEVGRKPTMKWSTIDRWPTHPL
mouse             172 AIEEMERDGLERAIAFTQYPQYSCSTTGSSLNAIYRYYNEVGQKPTMKWSTIDRWPTHPL
chicken           152 AIEEMEDDGIERAIAFTQYPQYSCSTTGSSLNAIYRYYNKKGKKPKMKWSIIDRWPTHPL
xenopus           160 AIEEMERDGVERAIAFTQYPQYSCSTTGSSLNAIYRYYNAKGTQPKMKWSVIDRWPTHPL
drosophila        133 TLAEIEKDKPERVVLFSQYPQYSCATSGSSFNSIFTHYRSNNLPSDIKWSIIDRWGTHPL
s_cerevesiae      145 TYKQMLKDGVKKAVAFSQYPHFSYSTTGSSINELWRQIKALDSERSISWSVIDRWPTNEG
s_pombe           138 MLDELKKANVSRAVAFSQYPQWSCATSGASLNELRRKLIEKGMEKDFEWSIVDRWPLQQG
b_subtilis         96 AVAEMHKDGITEAVSIVLAPHFSTFSVQSYNK...RAKEEAEKLGGLTITSVESWYDEPK
e_coli            110 AVDELLAEHVDHIVVLPLYPQFSCSTVGAVWDELARILARKRSIPGI..SFIRDYADNHD
c_crescentus      110 TARQVAAFAPDQVVLLPLYPQFSTTTTGSSLKAWKKTYKGSGVQ.....TTVGCYPTEGG
m_tuberculosis     87 AVTAMRDNGVRRAAVFATSAWSGYSSCTQYVEDIARARRAAGR.DAPELVKLRPYFDHPL

                         *                       *  *  *                       *
human             233 LIQCFADHILKELDHFPLEKRSEVVILFSAHSLPMSVVNRGDP..YPQEVSATVQKVMER
bovine            226 LIQCFADHILKELDHFPPEKRREVVILFSAHSLPMSVVNRGDP..YPQEVGATVQRVMDK
mouse             232 LIQCFADHILKELNHFPEEKRSEVVILFSAHSLPMSVVNRGDP..YPQEVGATVHKVMEK
chicken           212 LIQCFADHIQKELDLFPPDKRKDVVILFSAHSLPMSVVNRGDP..YPQEVGATVQRVMEK
xenopus           220 LIQCFADHIQKELNMFPADKRGEVVILFSAHSLPMSVVNRGDP..YPQEVGATVQKVMER
drosophila        193 LIKTFAQRIRDELAKFVETKRNDVVILFTAHSLPLKAVNRGDA..YPSEIGASVHMVMQE
s_cerevesiae      205 LIKAFSENITKKLQEFPQPVRDKVVLLFSAHSLPMDVVNTGDA..YPAEVAATVYNIMQK
s_pombe           198 LINAFAENIEETLKTYPEDVRDDVVIVFSAHSLPMSQVAKGDP..YVYEIAATSQAVMKR
b_subtilis        153 FVTYWVDRVKETYASMPEDERENAMLIVSAHSLPEKIKEFGDP..YPDQLHESAKLIAEG
e_coli            168 YINALANSVRASFAKHGEPD....LLLLSYHGIPQRYADEGDD..YPQRCRTTTRELASA
c_crescentus      165 LIEAHARMIRESWEK..AGSPTNIRLLFSAHGLPEKVILAGDP..YQKQVEATAAAVAAH
```

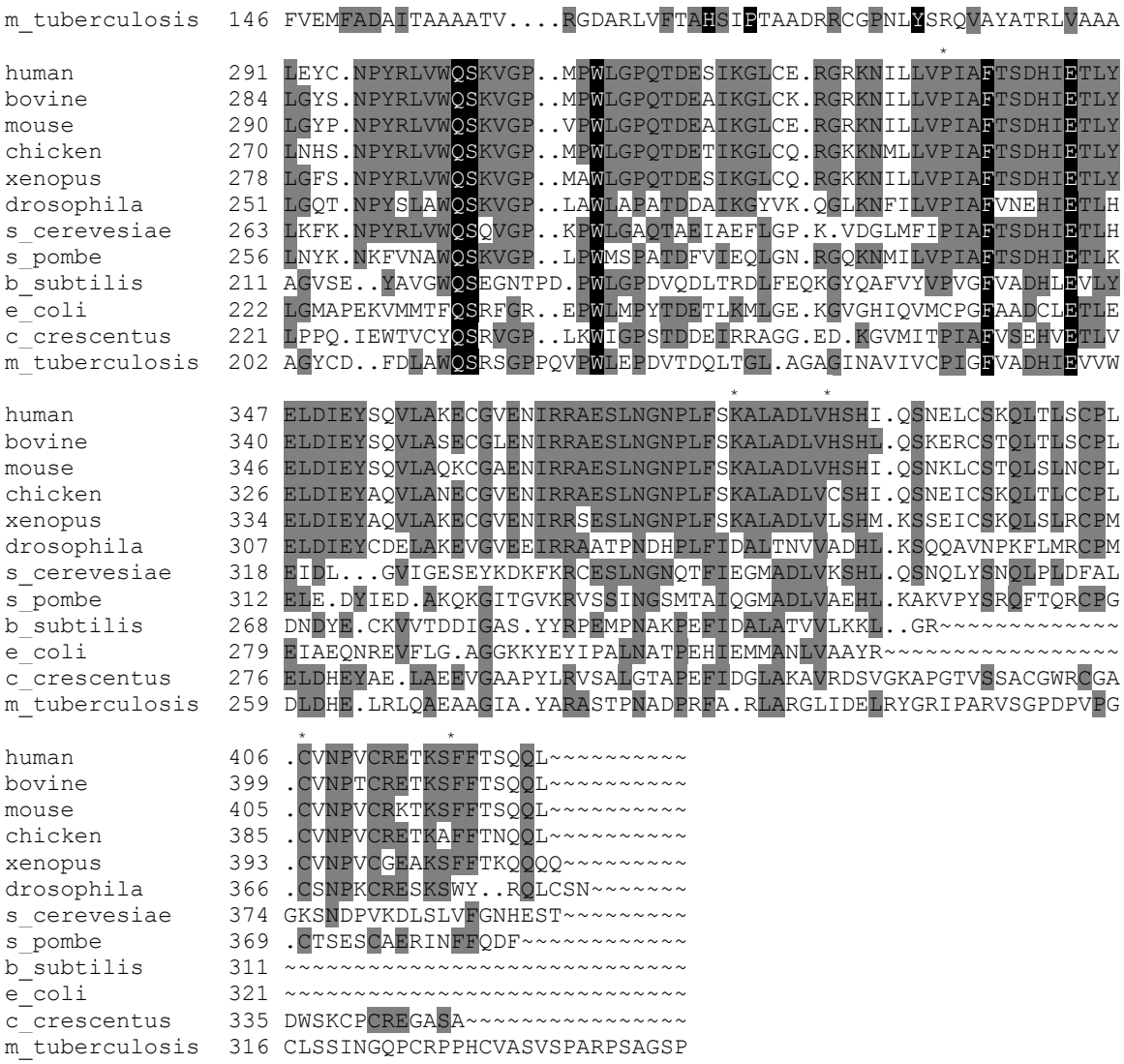

Figure 14. Pileup of selected eukaryotic and prokaryotic ferrochelatase sequences. Sequences shown are for the human, bovine, mouse, chicken, Xenopus, Drosophila, yeast *S. cerevisiae*, *S. pombe*, the bacteria *B. subtilis*, *E. coli*, *C. crescentus* and *M. tuberculosis*. These sequences represent soluble and membrane associated monomeric ferrochelatases and membrane associated dimeric ferrochelatases. Black boxes show the identical residues between all selected systems, gray boxes show the conserved residues. The asterisks show the location of the human EPP mutations in the FECH gene, investigated in this study.

The authors also presented data showing that mutating this residue along with R164, W227 and Y165 altered only the affinities for the metal ion substrate, indicating that they are possibly involved in the metal ion binding (Sellers et al. 2001). Our data suggest that this residue (Y191) is not necessarily directly involved in the metal substrate coordination, but may be involved in the stabilization of the active site pocket by maintaining a stable H-bond with R164 involved in the coordination of the metal ion.

This mutant, even as a homodimer, retained most of the normal activity (74 %), which is inconsistent with the less than 50% activity characteristic of EPP. However, when first discovered by Rufenacht et al. (1998), this mutation was found to be associated with a second mutation on the same FECH allele, and this likely causes the dramatic decrease in the enzyme activity, suggesting that Y191H mutation may play a minor role in the enzyme deficiency.

Mutation S264L

This mutation was first identified by Martinez et al. (2001). Kinetic analysis in the present study indicates that the homodimeric form of this mutant is inactive. This was in spite of the fact that near normal levels of protein with intact [2Fe-2S] cluster (Fig 8) were produced in the recombinant system. The ferrochelatase deficient *E. coli* (Δhem) strain was not complemented by the expressed mutated enzyme indicating that this mutant has no enzyme activity (Table 5). The heterodimeric mutant exhibited an apparent K_m for mesoporphyrin similar to the wild type while the apparent K_m for iron was two-fold higher than that of the wild type (Fig 15 and 16) and had about 64% of wild type enzyme activity. The residue S264 is adjacent to the central residue H263, a key residue suggested to be involved in porphyrin proton

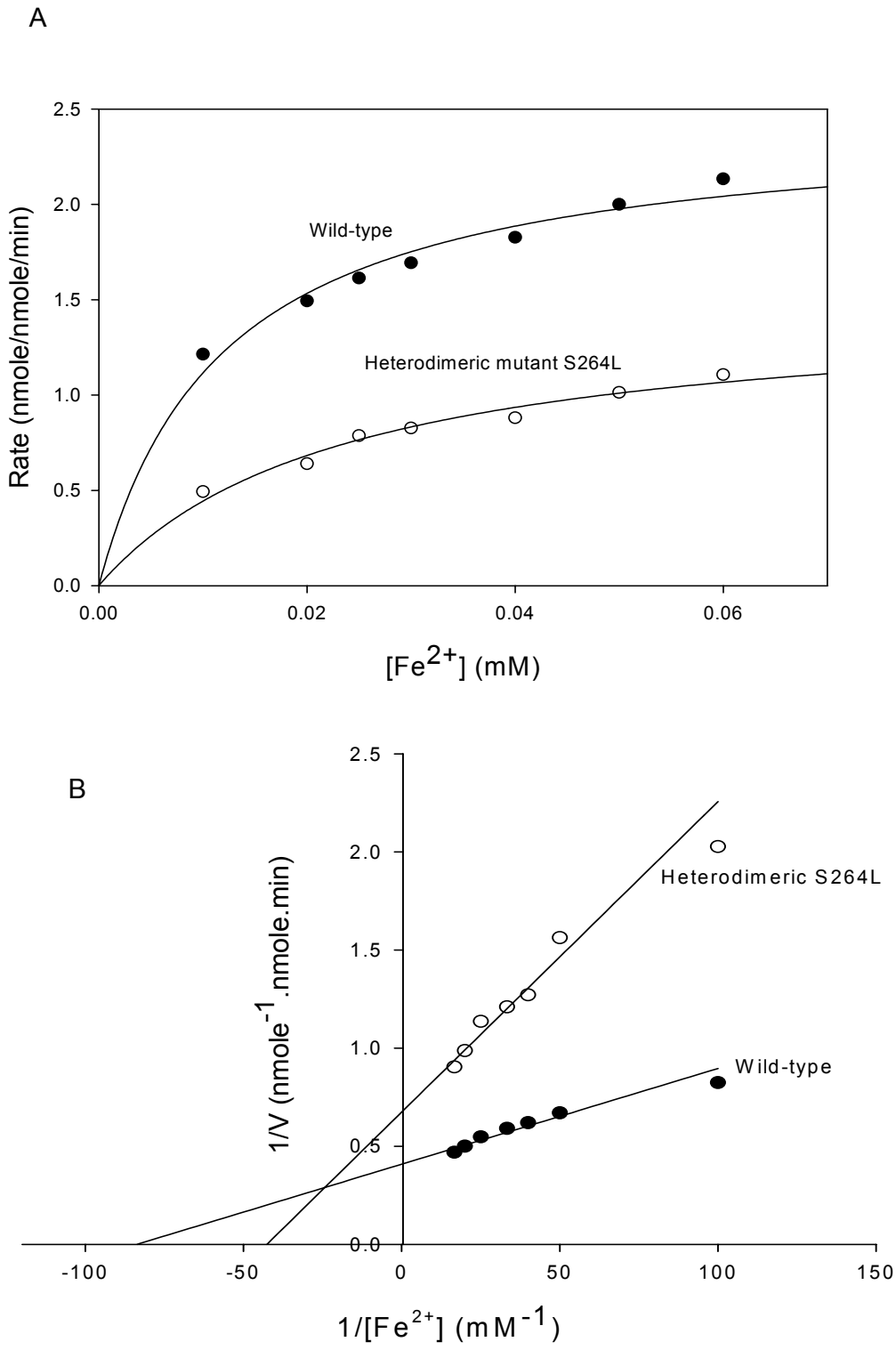

Figure 15. Apparent V_{max} and apparent K_m of ferrous iron for wild type and heterodimeric mutant S264L ferrochelatases.
(A) Rate (V) vs [Fe2+] for wild type and heterodimeric mutant S264L ferrochelatases
(B) Lineweaver-Burk (LB) or double reciprocal plot.

A

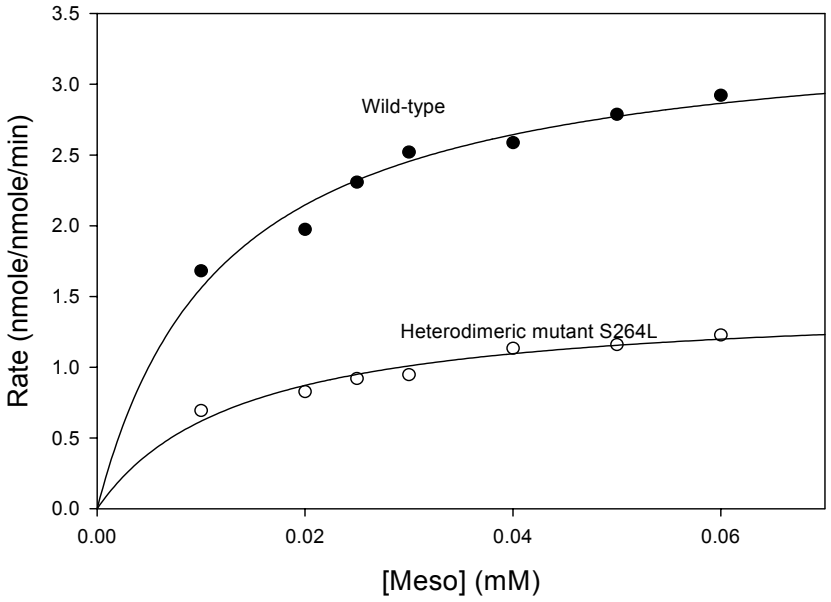

B

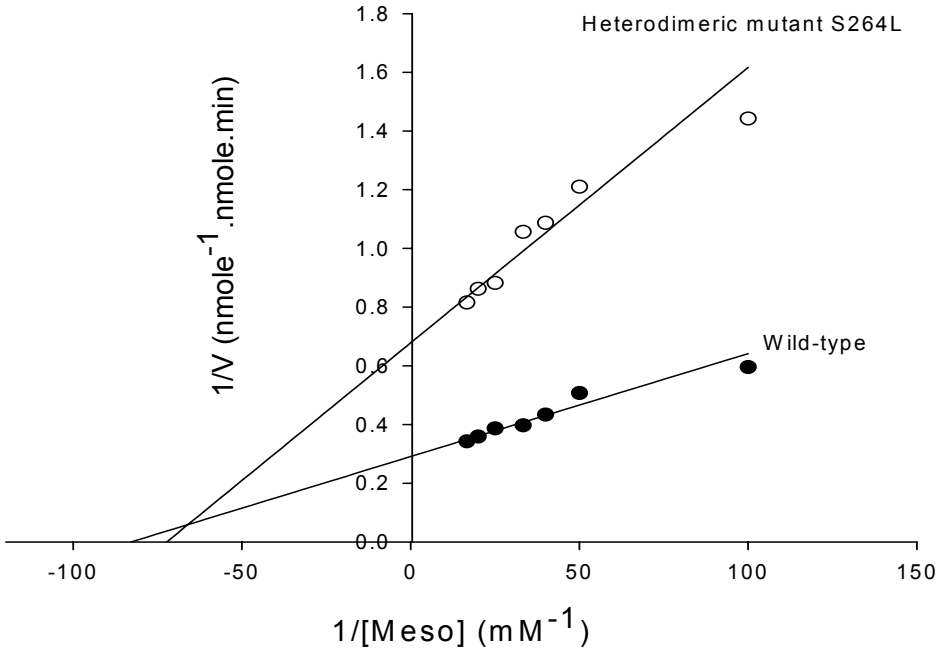

Figure 16. Apparent V_{max} and apparent K_m of mesoporphyrin for wild type and heterodimeric mutant S264L ferrochelatases.
(A) Rate (V) vs [Meso] for wild type and heterodimeric mutant S264L ferrochelatases.
(B) Lineweaver-Burk (LB) or double reciprocal plot.

abstraction (Labbe-Bois and Camadro, 1994; Dailey et al, 2000; Sellers et al, 2001; Dailey and Dailey, 2003). The substitution of a serine to a Leucine might disrupt the structural aspect of this region of the active site pocket by substituting a linear side chain by a bulky one such as leucine. An interesting finding is that the heterodimer had a significantly altered K_m for iron, an unexpected observation if both subunits function independently.

Mutation F260L

The substitution of F260 by leucine produced a 6-fold increase in the apparent K_m of iron for the homodimeric mutant and about 4-fold increase for the heterodimeric mutant, but little change was detected in the apparent K_ms of porphyrin for both homodimeric and heterodimeric proteins. The V_{max} was decreased approximately 52% in the homodimer (Table 4). Unlike other known missense mutations, this mutation was identified in a compound heterozygote (the second allele has an early termination) patient who developed a liver disease (G. Elder, personal communication), which is a complication of EPP. From this, one would expect a very low *in vivo* activity of the mutant enzyme since only F260L ferrochelatase would be formed at one-half of the normal amount resulting in about 25% total activity. The homodimeric mutant ferrochelatase retained nearly 52% of the normal activity while the heterodimeric mutant protein retained only 36% of the normal activity. This suggests that this mutation caused some protein instability that resultd in denaturation/inactivation of the heterodimer during the extended purification procedure required to isolate heterodimers.

The residue F260 is located close to the active site in a β-sheet at the end of which the central residue H263 is located (Fig. 13). We speculate that F260 may participate in maintaining the conformational state of the active site pocket and that a substitution of phenylalanine to

leucine may affect the structure of this region. This substitution can affect the structural aspects of the β-sheet and the active site pocket rendering it less suitable for the incoming metal ion.

Characteristics of mutations in the dimer interface

Mutation M267I

Our data show that both homodimeric and heterodimeric mutants exhibited similar kinetic parameters compared to the wild type (Table 4). A previous study found that the M267I ferrochelatase was more thermolabile than the wild-type enzyme (Dailey et al. 1994a). M267 is located in the interface between the two monomers and both residues are only 3.8 Å from each other (Fig 17). Based on its location, it is possible that this residue may play a role in the stabilization of the dimer. However, at the temperature we examined (30 ºC) the protein was stable.

The fact that there is no difference in the kinetic parameters between homodimeric and heterodimeric mutants compared to the wild type, provides further evidence that this residue is not directly involved in the catalytic mechanism of the enzyme. It is worth noting that not all EPP mutations dramatically reduce enzyme activity. Another example is the mutation Y191H (described above), which retained ~ 74% of the normal activity. When first identified by Lamoril et al (1991), M267I was found associated with another mutation in the FECH gene suggesting another possibility that this mutation was most likely responsible for the EPP disease and that M267I might have only a minor role in the disease (Lamoril et al. 1991).

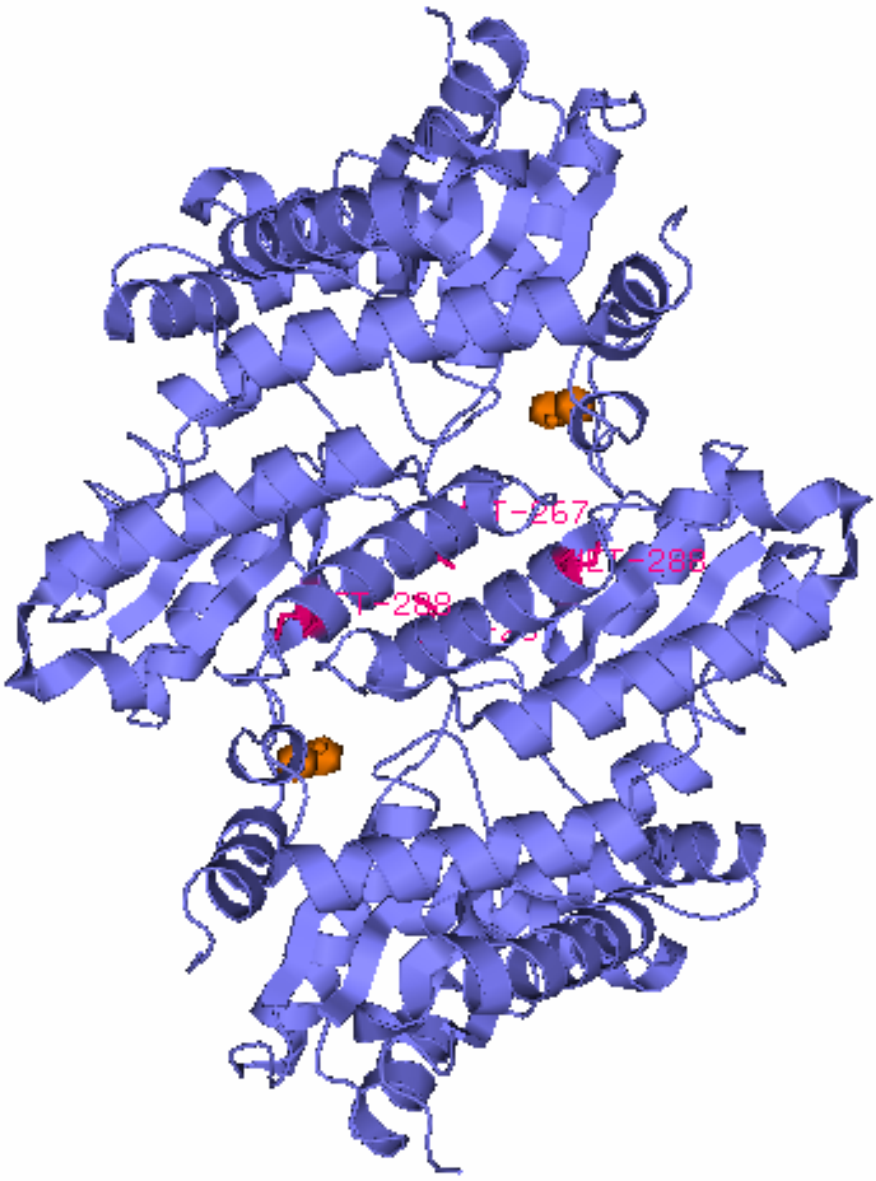

Figure 17. Location of human erythropoietic protoporphyria (EPP) mutations (M267I and M288K). The dimer is shown to demonstrate the location of the residues in the dimer interface of ferrochelatase that have been reported to be modified in EPP patients. The [2Fe-2S] clusters are also shown.

Mutation M288K

When first identified and expressed *in vitro*, this recombinant homodimeric mutant (M288K) resulted in a protein with a residual activity less than 19% of the normal (Rufenacht et al. 1998). Our data show that this mutation produced an inactive enzyme that failed to complement the ferrochelatase deficient (Δhem) *E. coli* strain (Table 5) suggesting that the residue M288 is essential for ferrochelatase functionality. Dynamic light scattering (DLS) was carried using DynaPro MS system (DYNAPRO, Charlottesville, VA) at 4ºC to examine the homodimeric mutant M288K. DLS analysis showed a high polydispersity in size distribution indicating that ferrochelatase with the mutation M288K was unstable and aggregating.

Western blot analysis of crude extract and eluate from the last purification column demonstrated that recombinant heterodimeric mutant ferrochelatase could not be isolated, suggesting that this mutant failed to form the dimer, or possibly dimerized but had a short lifetime because of instability (Fig 18). The residue M288 is highly conserved between all eukaryotic systems where ferrochelatases are dimeric proteins (Fig 14). We speculate that this residue, among others, may be required for the dimerization of eukaryotic ferrochelatases. This may explain why ferrochelatases from species where this residue is not conserved, such as *B. subtilis,* are monomeric proteins (Fig 14).

M288 is located at the end of the helix α11, in the interface between the two monomers, and is buried by hydrophobic residues where water is completely excluded (Fig 17). The helix α11 is critical for hydrogen bonding and hydrophobic interactions at the dimer interface (Wu et al, 2001). The mutation M288K changes a linear uncharged residue (methionine) into a basic charged amino acid (lysine). This chemical and structural change might disrupt the hydrophobic core in this region and the structural aspects of the helix in the interface.

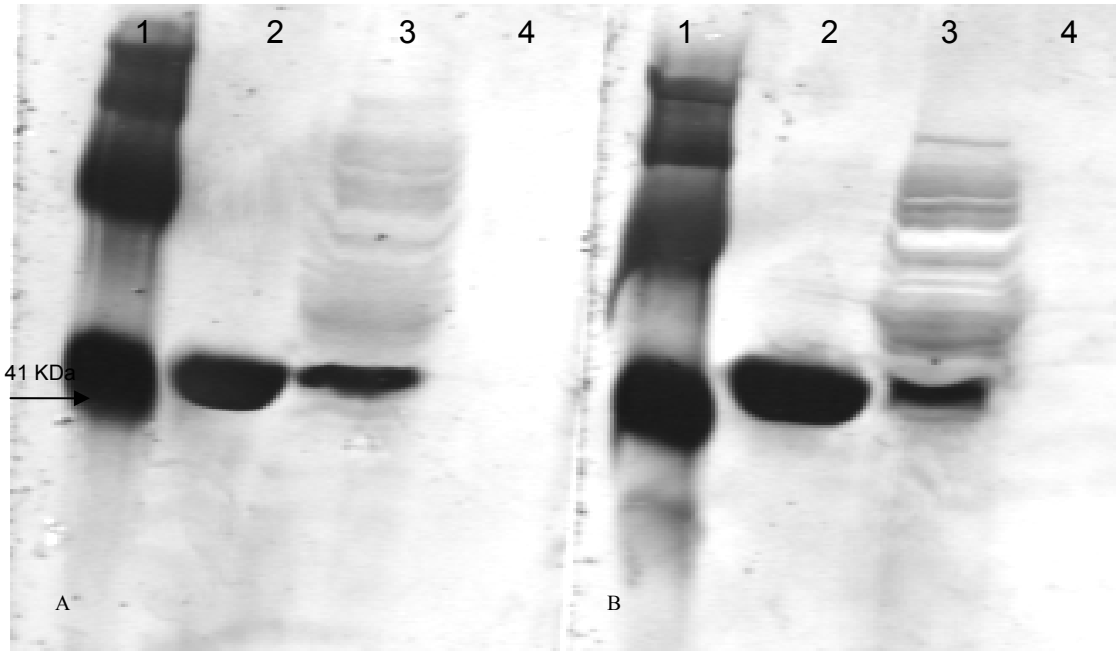

Figure 18. Western blot for wild type and heterodimeric mutant (M288K) ferrochelatases.
A: Western blot for His-tag detection. Lane 1 is the marker (Kaleidoscope prestained standards (BioRad)), Lane 2 is the His-CBP-tag wild type ferrochelatase used as positive control, lane 3 is the crude cell extract of heterodimeric mutant M288K, lane 4 is the eluate from the last column.
B: Western blot for CBP-tag detection. Lane 1 is the marker, lane 2 is the His-CBP-tag wild type, lane 3 is the crude cell extract of the heterodimeric mutant M288K, lane 4 is the eluate from the last column.

Characteristics of mutations on the surface

Mutation K379N

This mutation has been identified recently (Elder et al. personal communication). Our data show that both recombinant homodimeric and heterodimeric mutants had a V_{max} nearly 60% of normal and both had intact [2Fe-2S] clusters. Both homodimeric and heterodimeric mutants exhibited close apparent K_ms for mesoporphyrin, which were increased ~2-fold compared to the wild type ferrochelatase. The affinity for iron was dramatically affected for the homodimeric mutant (10-fold decrease compared to the wild type) and only a 2-fold decrease for the heterodimeric mutant (Table 4).

The residue K379 is located on the back surface of the protein with respect to the opening of the active site (Fig 19). It is too distant from the active site (at least 26Å from H263) to be involved in the catalytic mechanism, but the mutation K379N might cause a structural change that interferes with the overall folding of the protein. The dramatic decrease in the apparent K_m for iron in the homodimeric mutant suggests that this residue (K379) may be involved in metal ion coordination. K379 is exposed to the surface in the back of the active site of the protein, facing the mitochondrial matrix not far from D383, which was suggested to be involved in the initial binding of the metal ion substrate (Wu et al. 2001; Sellers et al. 2001). We speculate that the residue K379 may be involved in the initial binding of the metal ion substrate and that substituting a basic charged amino acid with a polar, non-charged side chain (asparagine), could impair interactions of this residue with other residues or its ability to bind the metal ion substrate.

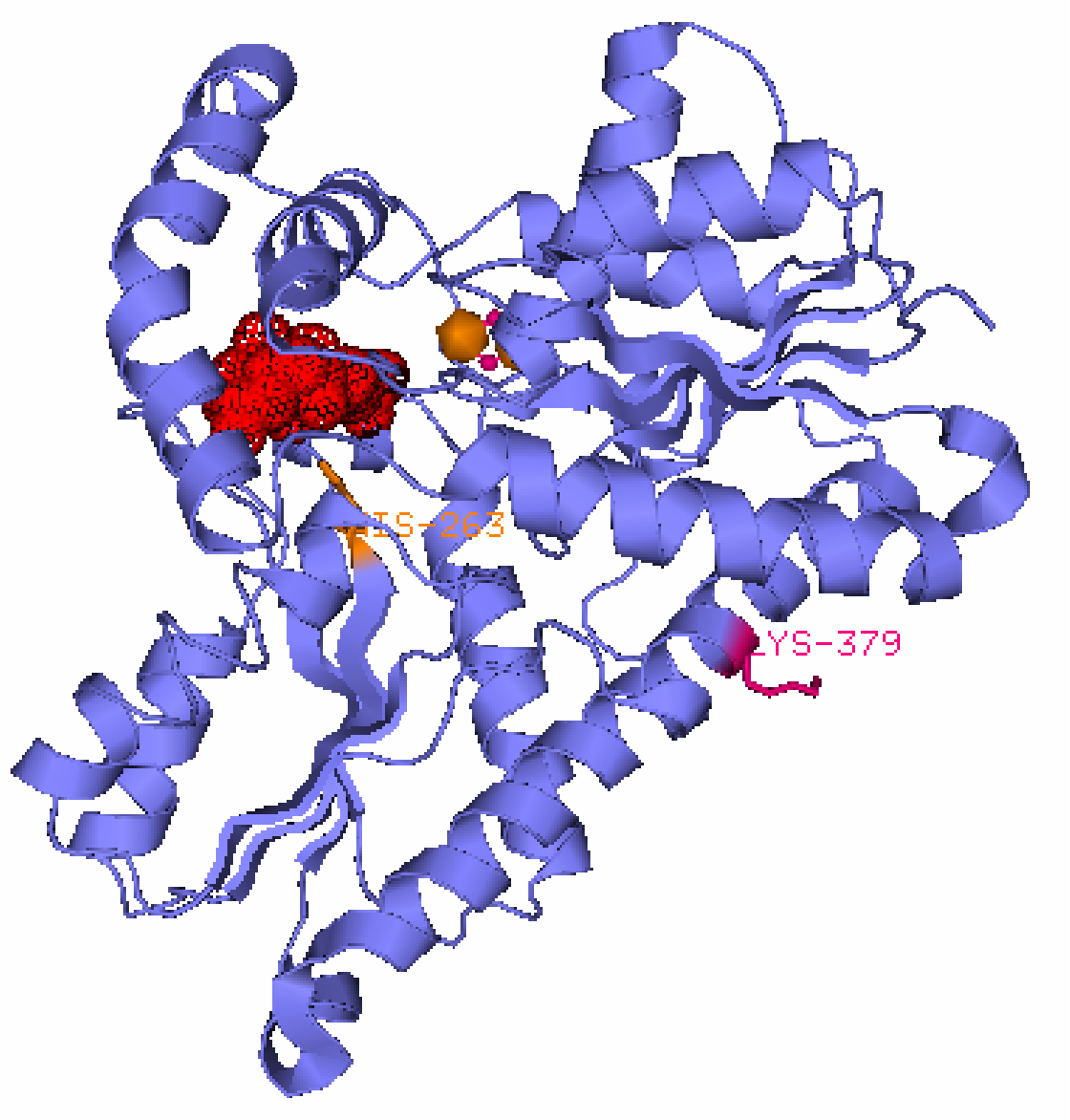

Figure 19. Location of human erythropoietic protoporphyria (EPP) mutation K379N that is on the surface of ferrochelatase. A single monomer is shown in which the porphyrin substrate is shown in red dots and the [2Fe-2S] is shown in orange and purple spheres.

Characteristics of internal mutations

Mutation Q139L

This human EPP mutation has been identified by Elder et al. (personal communication). The homodimeric mutant Q139L had altered affinities for both substrates and a V_{max} approximately 15% of the normal enzyme (Table 4, Fig 20, and Fig. 21). This mutation substitutes a polar amino acid (glutamine) with a hydrophobic one (leucine) which might have an effect on structural aspects of the protein. Q139 is located near the back surface of the protein distant from the active site. Its distance from the active site rules out direct participation in the catalysis of the protein (Fig. 22).

The heterodimeric mutant retained almost 63% of the normal activity, indicating that the less than 50% residual activity, necessary for the development of EPP clinical manifestations, requires that this EPP mutation be in both monomers. This suggestion is confirmed by the finding that the EPP patient carrying this mutation was homozygous for this missense mutation in exon 4 (G. Elder, personal communication).

Mutation C236Y

This EPP mutation was identified in a patient with an elevated concentration of protopophyrin in erythrocytes and plasma (G. Elder, personal communication). Kinetic analysis of this mutant showed that V_{max} for the homodimeric and heterodimeric mutants was 27% of the normal. The apparent K_m for iron increased slightly. However, the apparent K_m for the porphyrin substrate in the homodimeric mutant increased almost 3-fold, but was increased only slightly in the heterodimeric mutant (Table 4). Both homodimeric and heterodimeric mutants retained their [2Fe-2S] clusters.

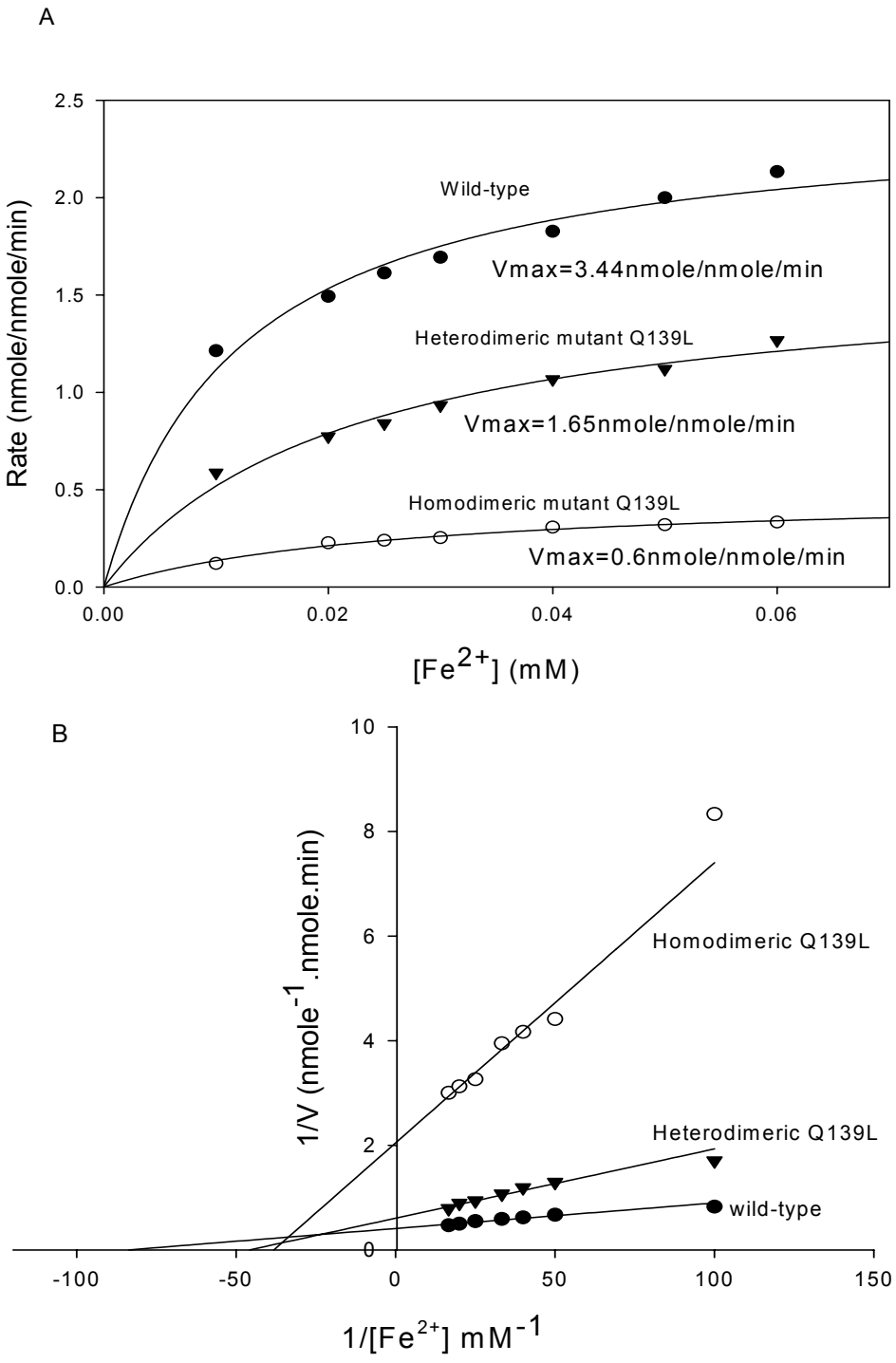

Figure 20. Apparent V_{max} and apparent K_m of ferrous iron for wild type and Q139L mutant ferrochelatases.
(A) Rate (V) vs [Fe2+] for wild type and mutant ferrochelatases.
(B) Lineweaver-Burk (LB) or double reciprocal plot.

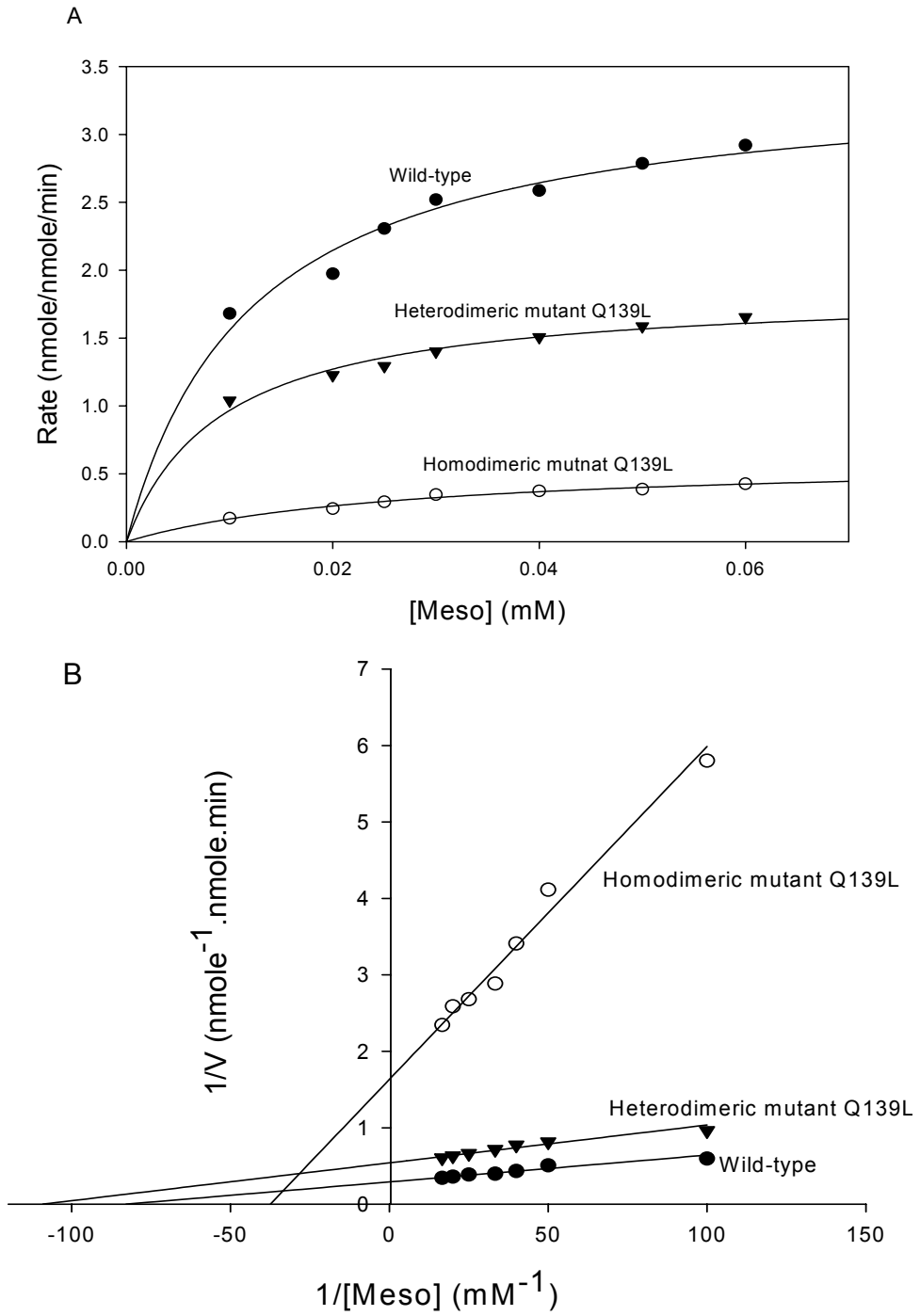

Figure 21. Apparent V_{max} and apparent K_m of mesoporphyrin for wild type and Q139L mutant ferrochelatases.
(A) Rate (V) vs [Meso] for wild type and mutant ferrochelatases.
(B) Lineweaver-Burk (LB) or double reciprocal plot.

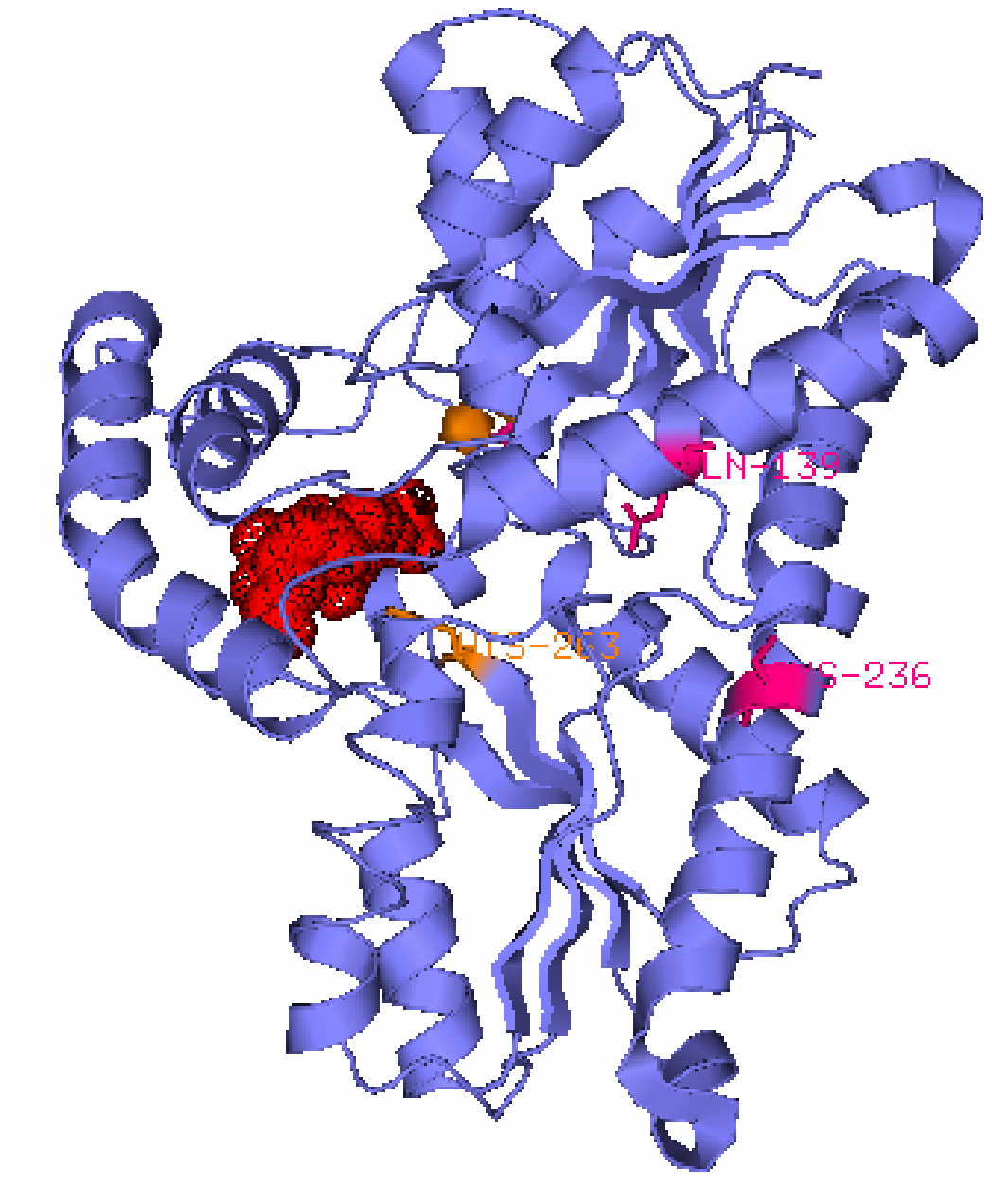

Figure 22. Location of human erythropoietic protoporphyric (EPP) mutations Q139L and C236Y. A single monomer is shown to demonstrate the position of internal residues that have been reported to be modified in EPP patients.

The kinetic data showed that the mutation C236Y affected only the affinity of the protein for its porphyrin substrate, suggesting a possible role in protein catalysis. However, C236 is an internal residue (Fig 22) that is distant from the active site. The decrease in the affinity for the porphyrin substrate and in activity may be explained by a structural change in the overall folding of each monomer, since cysteine, which has a short side chain, is substituted by an aromatic amino acid.

When first identified, this mutation was found associated with another missense mutation (K379N, discussed above) in a compound heterozygote patient. The distance between K379 and C236 is about 11Å, excluding any possible direct interaction between these two residues. This patient, in contrast to most symptomatic EPP patients, did not inherit the FECH low expression allele, suggesting that the association of these two missense mutations may be responsible for EPP.

Characteristics of mutations in the C-terminal end

Mutation C406S

Schneider et al (2000b) identified one of the four-cluster ligand mutations (C406S) of human ferrochelatase in an EPP patient. This mutant ferrochelatase had no detectable activity as a homodimer, which was expected since previously Crouse et al. (1996) had produced and characterized this mutation during their identification of the cluster ligands. The mutation C406S produced an enzyme that failed to assemble its [2Fe-2S] cluster; it was unstable and had no activity (Crouse et al. 1996). Data from the present study show that the recombinant homodimeric human ferrochelatase expressed in *E.coli* JM109, lacked the reddish color indicative of an intact cluster. This was confirmed by UV-spectroscopy, which showed the

absence of the cluster peak at approximately 330 nm. The mutant enzyme had no detectable activity, but when expressed in the ferrochelatase deficient *E.coli* strain (Δhem), it did rescue its growth (Table 5). This suggests that *in vivo* a small amount of active enzyme with intact clusters may exist and retain some activity, or that the protein might have some activity in the absence of the cluster. In either case, this activity is minimal and is only sufficient to rescue *E. coli* Δhem growth.

Dynamic light scattering (DLS) data for the homodimeric mutant C406S showed the presence of two different molecular weights. The first had a hydrodynamic radius of 4.09 nm, corresponding to a molecular weight of 91 KDa and suggesting that ferrochelatase with the mutation C406S is still able to form a dimer in the absence of its [2Fe-2S] clusters. However, the stability of the dimer is questionable. The second molecular weight exhibited a hydrodynamic radius of 10.6 nm corresponding to a higher molecular weight of 984 KDa, suggesting that ferrochelatase is possibly succeptible to aggregation because of this mutation.

The heterodimeric mutant lacked the reddish color during its purification and had no measurable kinetic parameters. Having only one mutated monomer, one might expect that the protein would have one cluster bound to the normal monomer. However, the absence of any cluster could be confirmed by spectroscopy. No spectral features characteristic of the cluster were detected. This is possibly due to one or several reasons: (i) the protein aggregated because of the lack of the second cluster, (ii) the protein failed to assemble both clusters because of this mutation or (iii) the protein assembled the cluster *in vivo* but it was rendered unstable during the extended purification procedure.

Western blot analysis of the eluate from the last purification column showed that the heterodimeric mutant C406S forms a dimer (Table 3, Fig 23), suggesting that ferrochelatase can

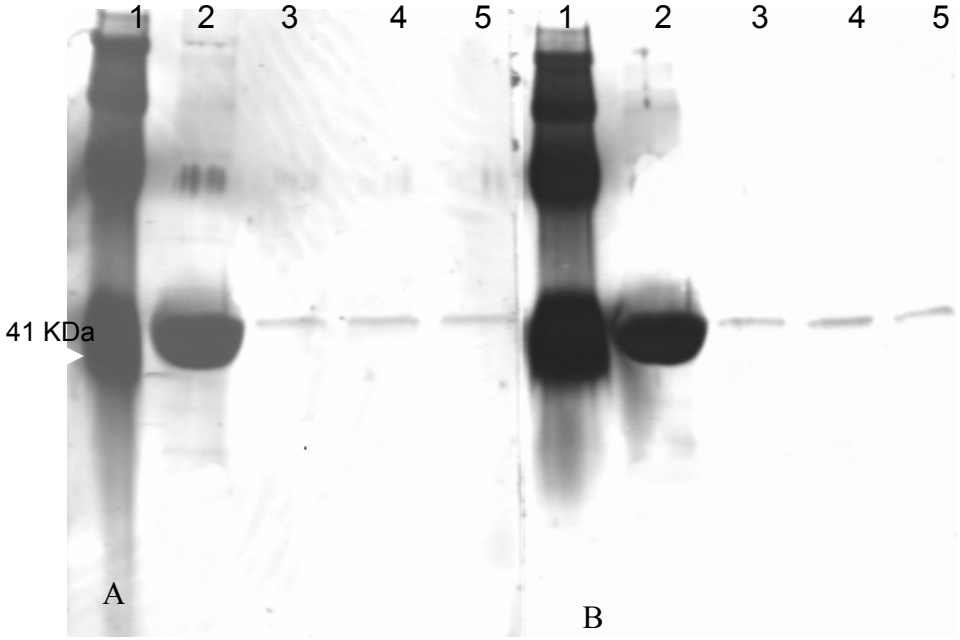

Figure 23. Western blot for wild type and heterodimeric mutant (C406S) ferrochelatases. A: Western blot for His-tag detection. Lane 1 is the marker (Kaleidoscope prestained standards (BioRad)), Lane 2 is the His-CBP-tag wild type ferrochelatase, used as positive control, lane 3 and 4 are the purified heterodimeric mutant C406S.
B: Western blot for CBP-tag detection. Lane 1 is the marker, lane 2 is the His-CBP-tag wild type, lanes 3 and 4 are the purified heterodimeric mutant C406S.

form a dimer with one or no [2Fe-2S] cluster, but it needs both clusters to be stable and, therefore, remain active.

Mutation F417S

The human EPP mutation F417S was identified by Brenner et al. (1992) who found a very low enzyme activity associated with it. Dailey et al. (1994a) suggested that this mutation affects the structural aspects of the enzyme without being directly involved in the catalytic mechanism. To further study the role of F417, a number of point mutations (F417L, F417Y and F417W) were introduced via site-directed mutagenesis (Dailey et al. 1994a). These mutations produced proteins with no measurable activities except for the F417L, which had altered apparent K_m and V_{max} for both ferrous iron and mesoporphyrin substrates suggesting that F417 is not an active site residue and that its mutation affects the structural aspects of the protein. Further investigations of the F417S mutant were conducted after discovering the presence of the [2Fe-2S] clusters in human ferrochelatase (Dailey et al. 1994b). Dailey et al. (1994a) found that when purified, this mutant lacked its [2Fe-2S] clusters which provided additional support for the suggestion that this mutation affects the stability of the [2Fe-2S] clusters and thus of the protein (Sellers et al. 1998b).

In our study, the homodimeric mutant F417S lacked the spectral characteristics of intact clusters (Fig. 9) and had no measurable activity. However, when expressed in the ferrochelatase deficient *E. coli* strain (ΔhemH), this mutant showed enough activity to enable cell growth (Table 5), indicating that *in vivo* a small amount of active enzyme may exist and has sufficient activity for cell growth.

The heterodimeric mutant F417S exhibited different features from the homodimeric mutant. During its purification, a slight reddish color was visible indicative of the presence of the [2Fe-2S] cluster. However, the protein precipitated as it eluted off the last column. Thus, the heterodimeric protein may have one cluster bound to the normal monomer, which explains the reddish color. However, a single cluster dimer is not sufficient to maintain dimer stability. Western blot data of purified protein showed that this mutant was present as a dimer (Fig. 24), indicating that ferrochelatase is possibly able to form a dimer with only one cluster but it needs both clusters to maintain its stability and activity.

The residue F417 is located near the carboxyl terminal end in exon 11 (Fig 25). This residue is contained in the helix harboring C411, which is one of the four [2Fe-2S] cluster ligands. This mutation could possibly disrupt the helical conformation and can cause an overall structural modification of the C-terminal extension, and thus of the protein, thereby impairing the Fe-S cluster assembly.

Mutation H386P

The prokaryotic expression of the homodimeric and heterodimeric ferrochelatases with this mutation indicated that the substitution of His-386 by a Pro dramatically impaired the catalytic function of the enzyme (Table 5). These results are consistent with those found by Gouya et al (1998). The authors suggested that the His-386 to Pro substitution might disrupt an α-helix and cause a structural change that impairs the enzyme activity. The human ferrochelatase tertiary structure (Wu et al. 2000) demonstrates that this residue is located in the helix α-15 close to the C-terminal end of the protein. This is where three of the iron-sulfur cluster ligands reside and is close to the dimer interface where most of the residues involved in the

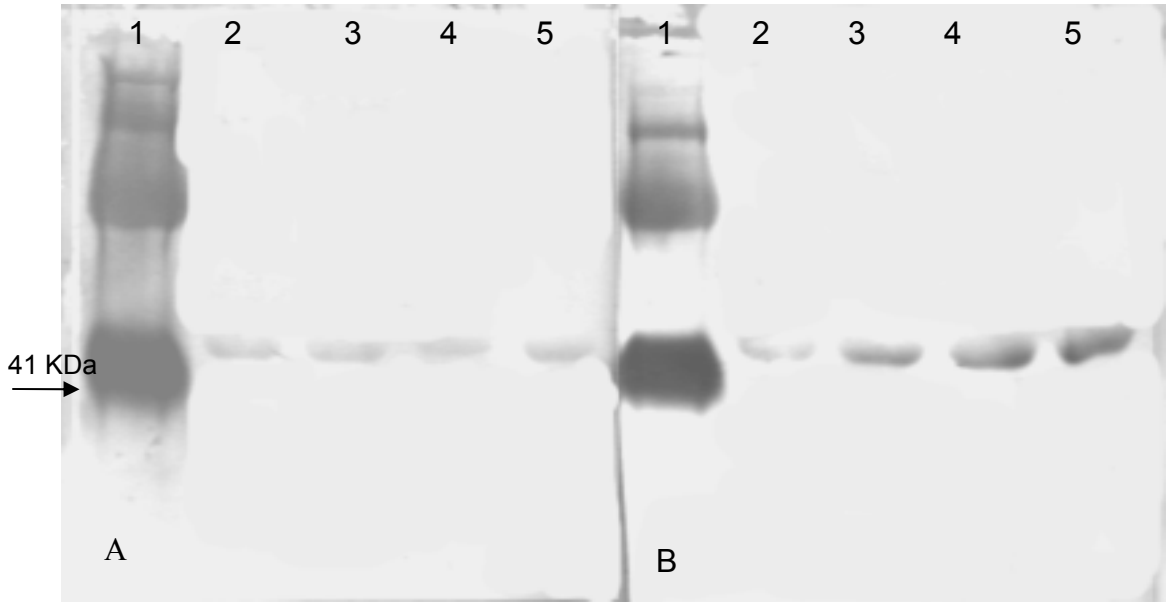

Figure 24. Western blot for wild type and heterodimeric mutant (F417S) ferrochelatases. A: Western blot for His-tag detection. Lane 1 is the marker (Kaleidoscope prestained standards (BioRad)), Lanes 2, 3, 4, and 5 are the purified heterodimeric mutant F417S. B: Western blot for CBP-tag detection. Lane 1 is the marker, lanes 2, 3, 4, and 5 are the purified heterodimeric mutant F417S.

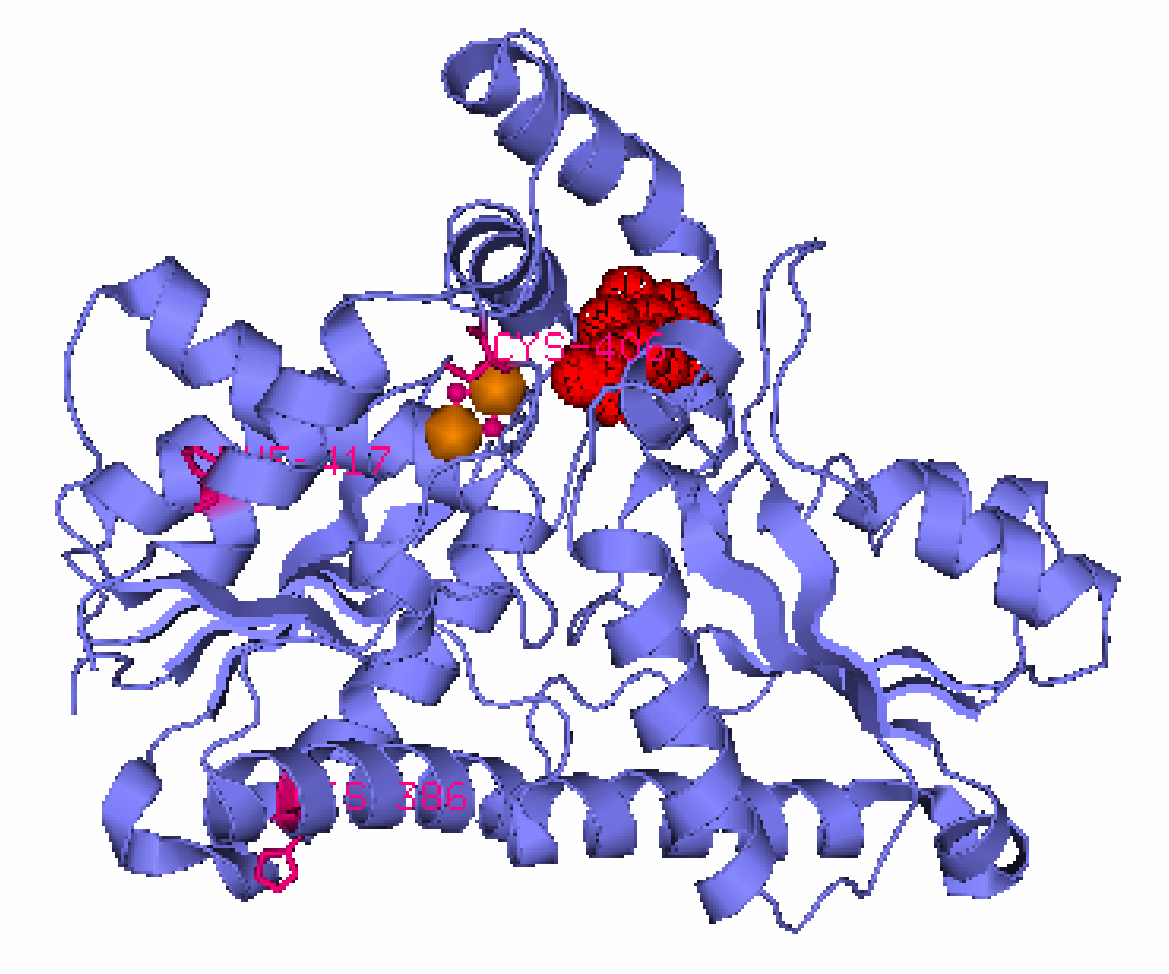

Figure 25. Location of human erythropoietic protoporphyria (EPP) mutations (C406S, F417S, and H386P). A single monomer is shown to demonstrate the locations of the residues in the C-terminal end that have been found mutated in EPP patients.

hydrogen bonding between the two monomers are located (Fig 25) (Crouse et al, 1996; Wu et al, 2000). The substitution of His-386, which is a polar amino acid, by the hydrophobic amino acid proline might disrupt the helical structure and the stability of the carboxyl terminal extension, thereby affecting the ability of the protein to maintain its iron-sulfur clusters and its hydrogen bonds in this region.

Western blot analysis of the crude extract and the eluate from the last purification column showed that the heterodimeric mutant failed to associate its monomers (Table 3), suggesting that this missense mutation affects the ability of the protein to dimerize and providing evidence that the C-terminal end of ferrochelatase is required for protein dimerization.

CHAPTER 3

EXAMINATION OF SITE-DIRECTED MUTANTS OF HUMAN FERROCHELATASE

Introduction

Ferrochelatase is the enzyme involved in catalyzing the last step of the heme biosynthesis pathway. It inserts ferrous iron into protoporphyrin IX to form protoheme (Dailey, 1997; Dailey et al, 2000). In eukaryotes, ferrochelatase is associated with the inner mitochondrial membrane and its active site is on the mitochondrial matrix side of the membrane (Dailey, 1990). It is synthesized in the cytosol as a high molecular weight precursor and proteolytically processed during its translocation into the mitochondria to form the mature protein (Dailey et al, 2000). The human enzyme exists as a homodimer with a molecular weight of 86 kDa (Wu et al, 2001).

Mammalian ferrochelatase utilizes only dicarboxylate porphyrins of the IX isomer (Dailey and Smith, 1984; Honeybourne et al, 1979; Dailey and Fleming, 1986). Ferrochelatase can use proto-, meso- deutero-, and hematoporphyrin as substrates (Dailey and Smith, 1984). Porphyrins that are not substrates may be competitive inhibitors of the enzyme.

Ferrochelatase utilizes ferrous iron but not ferric iron (Dailey, 1990). It catalyzes the insertion of a variety of divalent cations such as cobalt and zinc, but not monovalent or trivalent metals (Dailey, 1990, Dailey, 1996). Ferric iron is neither a substrate nor an inhibitor of the enzyme. Many divalent cations like manganese, cadmium, lead, and mercury are competitive inhibitors of ferrochelatases (Dailey, 1987).

While the catalytic mechanism of the enzyme is currently not fully understood, portions of a proposed mechanistic model appear to be confirmed by data obtained from co-crystallization of *B. subtilis* ferrochelatase with a potent inhibitor, N-methylmesoporphyrin (N-MeMP). Previously, it was suggested that metallation involves porphyrin macrocycle distortion. The crystallographic studies found that "the enzyme holds pyrrole rings B, C and D in a vice-like grip and forces a 36˚ tilt on ring 'A' (Lecerof et al, 2000)". Porphyrin enters the active site from the enzyme surface that faces the mitochondrial membrane, whereas the iron entry site has been suggested to be from the surface facing the mitochondrial matrix, and from there, it is transported to the site of metallation via a series of highly conserved residues (Dailey, 1982; Sellers et al, 2001).

Several models regarding the ferrochelatase catalytic mechanism have been suggested. The most recent model suggests that the first steps consist of iron binding and porphyrin binding and distortion by conserved residues within the enzyme. This distortion is followed by the abstraction of protons using His 263 as the first acceptor (Sellers et al, 2001). The next step in this model consists of metal transport to the active site, where it is incorporated into the porphyrin substrate. The entry site of the metal ion is believed to be opposite the site of His 263 and the active site, where iron binds first to H231 and D383, and then is translocated via highly conserved residues including W227 and Y191 into the active site of the protein. After protoporphyrin distortion, the metallation occurs via R164 and Y165. H263 is the first acceptor of the two abstracted protons, which will then be released via conserved carboxylates including E343, H341 and D340 (Sellers et al, 2001). Bain-Ackerman and Lavallee (1979) had originally suggested that iron insertion in a distorted protoporphyrin substrate displaces the two pyrrole protons, which are then released via highly conserved residues.

In the current study, conserved and non-conserved residues were mutated via site-directed mutagenesis and kinetic analysis was conducted to evaluate the effect of these mutations on ferrochelatase activity in order to understand its catalytic mechanism.

Materials and Methods

Expression of wild type and mutant human ferrochelatases (hFc)

Plasmids producing mutant ferrochelatases were constructed using site-directed mutagenesis kit (Stratagene, LaJolla, Ca) and PCR with synthetic oligonucleotides containing the desired base change. Oligonucleotides were then digested with *Dpn*I. Mutated plasmids were sequenced for confirmation that the desired mutation was present. Wild type and mutant ferrochelatase plasmids were transferred into JM109 E-coli strain. Colonies were selected on LB plates containing ampicillin. Mature hFc was expressed by inoculating one colony containing His-tag plasmid into 100 ml Circlegrow (Bio 101, Montreal, Quebec) supplemented with ampicillin (final concentration 0.2 mg/ml). Cultures were grown at 30º C with shaking at 225 rpm. After 6 hours, the 100 ml culture was used to inoculate one liter of Circlegrow (Bio101) supplemented with ampicillin (final concentration 0.2 mg/ml) and incubated at 30ºC for 18-20 hours with shaking at 225 rpm.

Purification of wild type and mutant human ferrochelatases

Cells were harvested after 18-20 hours by centrifugation at 5000 x g for 15 min at 4º C. Since the human ferrochelatase protein is membrane associated, pelleted cells were resuspended in 60 ml detergent containing solubilization buffer (50 mM Tris-MOPS, pH 8.0, 0.1 M KCl, 1.0 % sodium cholate, 10 μg/ml phenylmethylsulfonylfluoride (PMSF)). Cell suspension was

sonicated 3-4 times for 30 seconds on ice and centrifuged at 150,000 x g for 35 min at 4ºC. The supernatant was loaded onto a column containing 3 ml of Talon-matrix (Clontech, Palo Alto, Ca) equilibrated with 5 ml of solubilization buffer. After loading the supernatant, the column was washed with 25 ml solubilization buffer, and the protein eluted with elution buffer (6ml of solubilization buffer containing 300 mM imidazole).

Characterization of human ferrochelatases

UV-visible spectroscopy was conducted using a Cary-G1 spectrophotometer. Wild type and mutant ferrochelatase concentrations were determined using the extinction coefficient 46900 $M^{-1}\cdot cm^{-}1$ at 278 nm. The presence of the [2Fe-2S] cluster was detected by the presence of its characteristic spectra at 330 nm, 460 nm, and 550 nm (Dailey et al, 1994b).

Kinetic analysis of wild type and mutant ferrochelatases

Ferroechelatase activity was assayed aerobically at 25º C by continuous spectrophotometric monitoring of the disappearance of the porphyrin substrate by measuring the decrease in its absorbance at 496 nm. The slope given was used to determine the amount of heme produced using the extinction coefficient 7.5 $mM^{-1}\cdot cm^{-1}$.

Enzyme activity was measured using freshly prepared 10-100 μM ferrous ammonium sulfate and 10-100 μM mesoporphyrin IX (Porphyrin products, Logan, UT) as substrates. Mesoporphyrin stock solution was made by mixing 2.5 mg mesoporphyrin IX, 30 μl 2N NH_4OH, 500 μl 10% Triton X-100 in 4.5 ml double distilled water. Mesoporphyrin quantitation was calculated using the extinction coefficient of 445 $mM^{-1}\cdot cm^{-1}$ at 399 nm in 0.1 N HCl. The concentration of ferrous iron in the stock solution was quantitated by employing the ferrous iron

chelator ferrozine and the extinction coefficient of the complex (278 $mM^{-1} \cdot cm^{-1}$) at 562 nm. When preparing the 10 ml of ferrous ammonium sulfate substrate solution, approximately 10 mg of ascorbic acid was added to prevent ferrous iron oxidation.

The ferrochelatase assay mixture contained 100 mM Tris-HCl (pH 8.0), 0.5% Tween 20, 0.1 mM mesoporphyrin, 0.1 mM ferrous ammonium sulfate, and 10 mM β-mercaptoethanol (added to provide a reducing environment). Ferrochelatase (1nM) was added last to start the reaction. Ferrochelatase activity from purified samples was expressed as nanomoles of heme per nanomole of ferrochelatase per minute.

Results

Expression, purification and characterization of wild type and mutant ferrochelatases

The recombinant wild type and mutant human ferrochelatases containing the mutations H240A, F337A, S339A, and T414N were efficiently expressed in the JM109 *E. coli* strain and they all had the characteristic reddish color indicative of the presence of the [2Fe-2S] cluster in mammalian ferrochelatases (Dailey et al. 1994b).

To provide further evidence for the presence of the [2Fe-2S] cluster in the purified mutant proteins, UV-visible absorbance of wild type and mutant ferrochelatases were measured between the wavelengths of 250 nm and 600 nm. The absorption spectra of human recombinant wild type and mutant ferrochelatases are shown in Figure 26. The presence of the [2Fe-2S] cluster was investigated by the presence of its characteristic spectra at 330 nm (Dailey et al. 1994b). The spectra of mutant ferrochelatases were identical to the wild type showing an absorption peak at approximately 330 nm indicative of the [2Fe-2S] cluster.

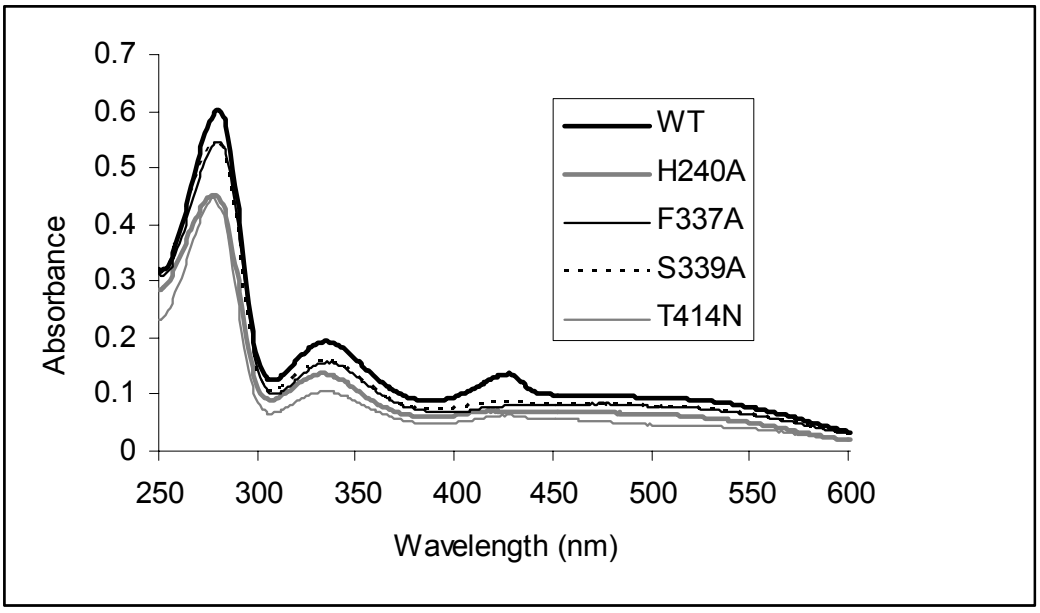

Figure 26: UV-visible spectra for purified wild type and mutant human ferrochelatases. The top line represents the wild type, the second line is mutant S339A, the third line represents mutant F337A, the fourth line represents mutant H240A, and the bottom line represents mutant T414N.

Kinetic characterization

The apparent kinetic parameters of the wild type and mutant ferrochelatases using iron and mesoporphyrin as substrates are summarized in Table 7. The mutant H240A exhibited similar V_{max} and apparent K_m for porphyrin substrate compared to the wild type. The apparent K_m of iron increased 2.3 fold compared to that of the wild type. The residue F337 (Table 6) that was mutated to alanine using site directed mutagenesis had a significantly different V_{max} from that of the wild type and altered apparent K_ms for both substrates. The V_{max} was 20 % of the wild type. The apparent K_m for iron increased 1.5 fold compared to that of the wild type, while the apparent K_m of porphyrin increased 2 fold (Fig 27 and Fig 28). In mutant S339A, the apparent K_m for iron increased approximately 4 fold while the apparent K_m for porphyrin increased 3.5 fold. The V_{max} decreased approximately 27% compared to wild-type ferrochelatase. The residue T414 was mutated to T414N and found to have a 3-fold increase in the apparent K_m for mesoporphyrin, but little change in the V_{max} and the apparent K_m for iron.

Table 7: Effect of site directed mutagenesis on ferrochelatase activity.

Mutant	K_m^{Fe}(μM)	K_m^{Meso}(μM)	V_{max} (min^{-1})
WT	11.96	12.07	3.44
H240A	27.57	12.06	3.42
F337A	16.75	24.6	0.71
S339A	47.57	42.66	2.51
T414N	16.73	37.17	4.28

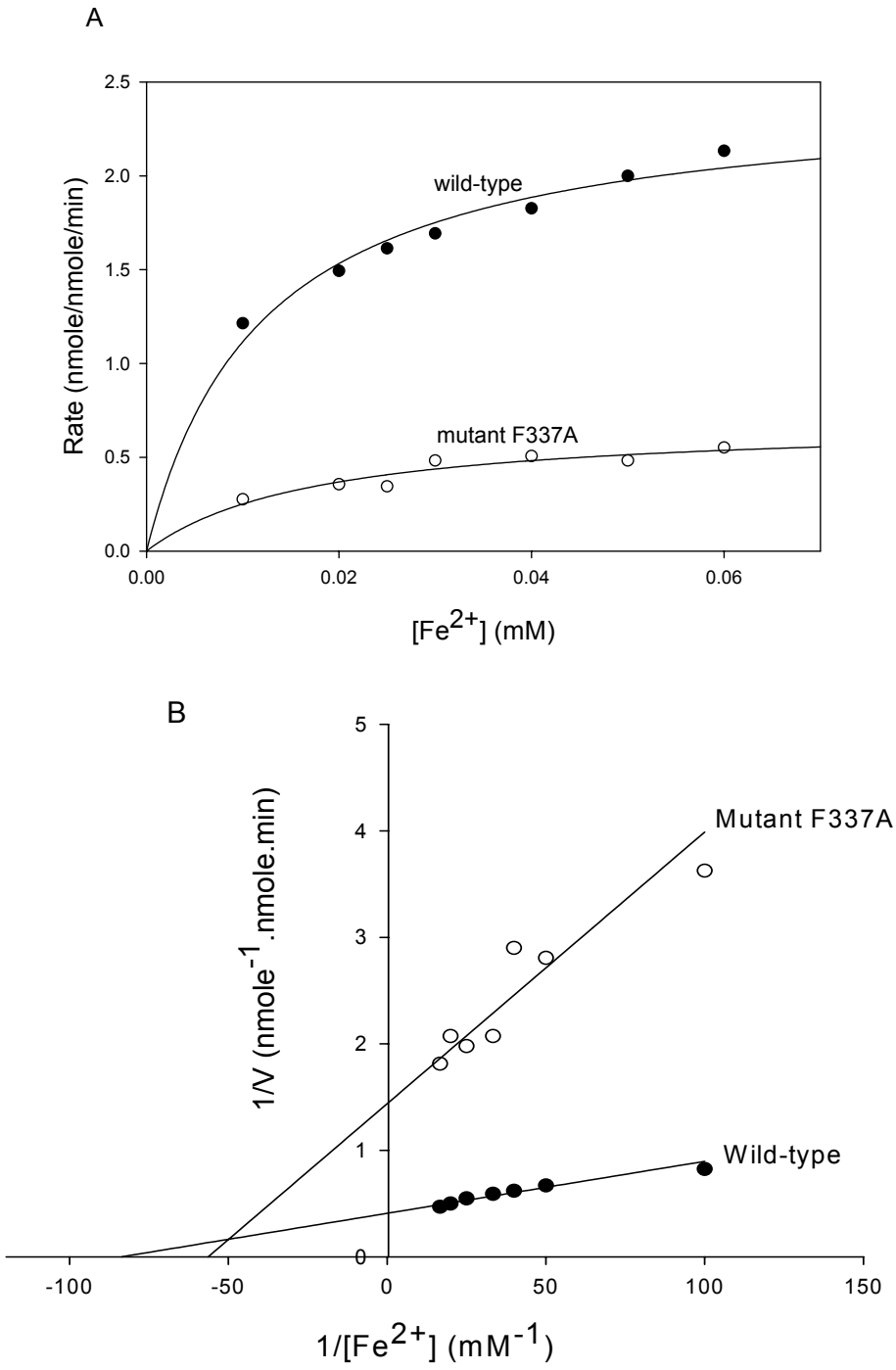

Figure 27: Determination of apparent V_{max} and apparent K_m of iron for wild type and F337A mutant ferrochelatases.
(A) Rate (V) vs [Fe^{2+}] for wild type and mutant ferrochelatases.
(B) Lineweaver-Burk (LB) or double reciprocal plot.

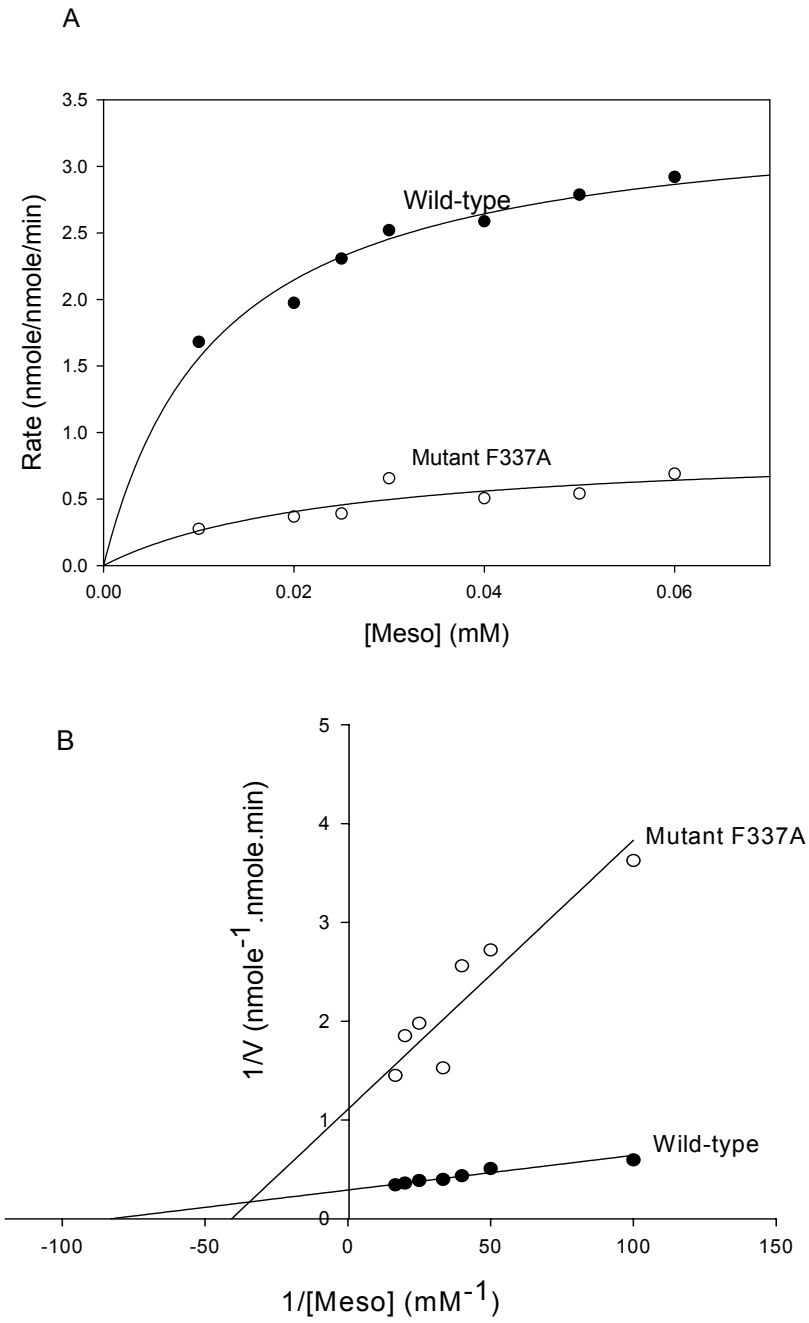

Figure 28: Determination of apparent V_{max} and apparent K_m of mesoporphyrin for wild type and F337A mutant ferrochelatases.
(A) Rate (V) vs [Meso] for wild type and mutant ferrochelatases.
(B) Lineweaver-Burk (LB) or double reciprocal plot.

Discussion

Alignment of known ferrochelatase sequences revealed that they have only 5% identity among their 330 core residues (Dailey et al, 2000) and less than 10% highly conserved residues (Olsson et al, 2002). It was suggested that these few conserved residues are most likely involved in the function of the enzyme (Olsson et al, 2002). A variety of studies concerning ferrochelatase catalytic mechanism has been conducted. However, despite these studies, the catalytic mechanism of ferrochelatase is still not fully understood. While most of these models agree about the entry path of porphyrin substrate into the active site, the entry site and the channeling of the metal ion substrate is still debated. In 2001, Sellers et al. suggested a model for human ferrochelatase catalytic mechanism, in which iron binds first to H230 and D383, and then is translocated via highly conserved residues including W227 and Y191 into the active site of the protein.

Our data suggest that another entry site for the metal ion is possible in which the residue H240 might be involved in the initial binding. This residue is located in the back surface of the protein and seems to be too distant from the residues suggested in Sellers's model, indicating that other residues might be involved in channeling the metal ion from H240 to the porphyrin metallation site. These residues are likely located in a tunnel that expands from the surface of the protein where it starts with residue H240 to the center of the active site specified by residue H263. The highly conserved residue F337 opens this tunnel to the active site (Fig 29). The mutation F337A had very low activity and altered apparent K_ms for both substrates, suggesting that this mutation changes the structural aspects of the tunnel and surroundings.

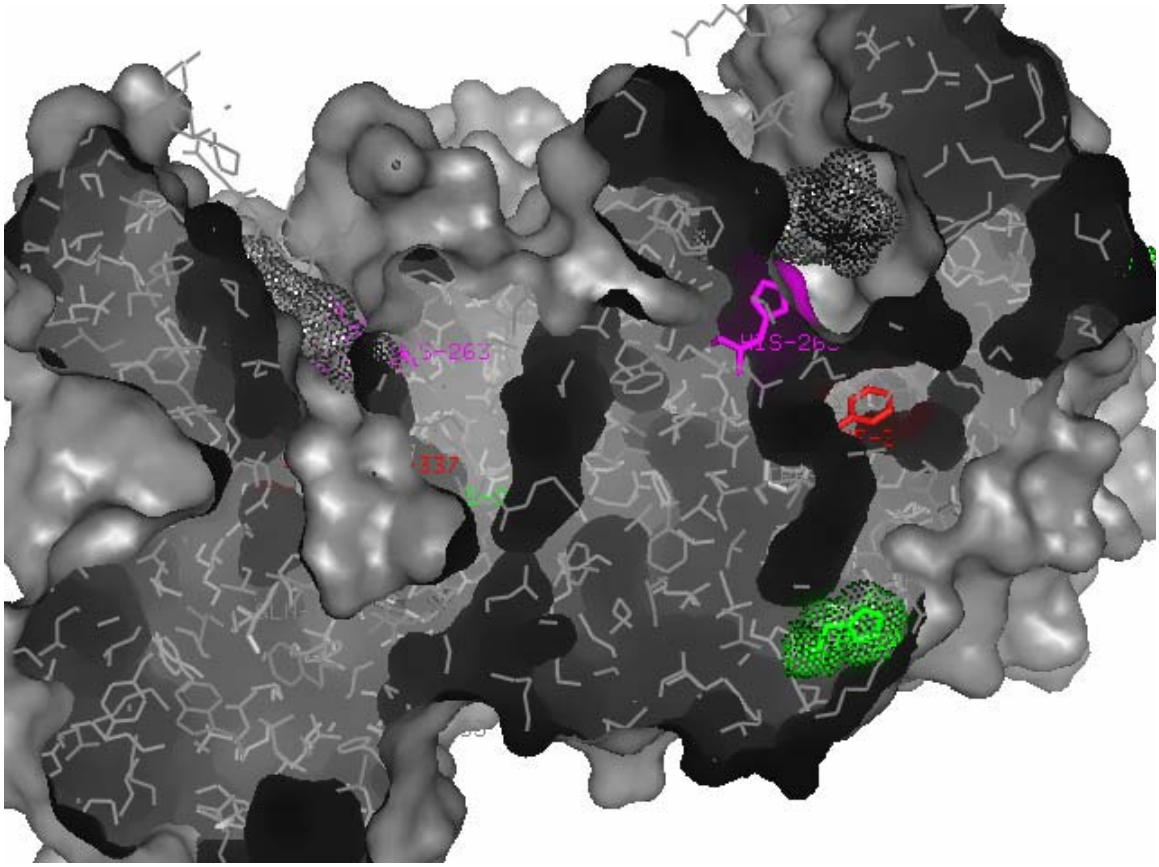

Figure 29: The entry site and movement of iron to the active site. The figure shows the suggested tunnel which extends from H240 (shown in green dots) to the center of the active site specified by the residue H263 (shown in purple sticks). The residue F337 that opens the tunnel to the active site is shown in red sticks. The porphyrin substrate is shown in grey dots.

Our data also suggest that since F337 is near the active site (within9Å), it might be involved in maintaining the stability of the active site. We infer from the results of this study that the highly conserved residue F337 probably has a dual role, both in opening the tunnel through which the metal ion substrate is transported to the active site (Fig 29), and in maintaining the stability of the active site and its ability to bind the porphyrin substrate

Based on the results of this study, we suggest that the initial binding of the metal ion may occur at the His 240 site on the matrix side of the protein. This site is located in the back of the enzyme, ~20Å from H263 specified as the center of the active site (Sellers et al, 2001). Additional residues are needed for the movement of iron into the active site. The highly conserved residues Q302, S303, E347, and S261 possibly exist in the tunnel that expands from H240 to the center of the active site, suggesting that these residues and others may be involved in iron transportation into the active site (Fig 29). The involvement of these residues in iron transportation needs to be confirmed by site-directed mutagenesis and kinetic studies. The residue F337 plays a role in opening this tunnel to the active site and it probably also has a role in porphyrin binding and/or distortion (Dailey and Dailey, 2003). The bound iron will displace the two hydrogens from the porphyrin and these will be transported to the enzyme exterior via conserved residues. These conserved residues may be those in the model suggested by Sellers et al. (2001).

The mutant S339A retained 73% of the normal activity but showed altered apparent K_ms for both substrates. The substitution of the internal polar residue S339 by a hydrophobic residue like alanine disrupts the chemical aspects of this region and affects its stability. S339 seems to be too distant from the active site to be involved in the catalytic mechanism and as an internal

residue, it is probably involved in maintaining the stability of the overall structure of ferrochelatase.

The residue T414 is located in the C-terminal end. Mutations of other residues in this region (like F417S and H386P) showed a loss of the [2Fe-2S] cluster and of enzyme activity (see chapter 2). Previous studies showed that the elimination of the C-terminal extension results in an inactive enzyme suggesting that the carboxyl-terminal end is required for enzyme functionality (Dailey et al, 1994a). Our data show that the mutant T414N retained its [2Fe-2S] cluster (Table 7, Fig 26) as well as a normal activity, suggesting that this mutation does not affect ferrochelatase functionality.

CHAPTER 4

SUMMARY AND CONCLUSIONS

It has long been accepted that human EPP is an autosomal dominant disease, even though several cases showed recessive inheritance (Sarkany et al, 1994). However, it has always been found that symptomatic EPP patients have only about 20-30% of normal activity and that individuals with 50% activity have no clinical symptoms. These observations raised doubts about the pattern of inheritance of this disease and left unexplained the low penetrance of EPP. Different hypotheses have been suggested to explain this, including the possibility of a third allele for ferrochelatase (Went and Klasen, 1984). The most appealing hypothesis suggested the co-inheritance of a FECH gene mutation in one allele and a low expression in the second (Gouya et al, 1999). Despite these hypotheses, a molecular explanation of the EPP disease is lacking because most of the previous studies have focused on investigating the activity of homogenous mutants and none have examined the possibility of mixed dimeric ferrochelatases in patients with this disease. The current study investigates the activities and physical properties of both homo- and heterodimeric ferrochelatases with EPP mutations and shows that FECH gene mutations in patients with protoporphyria, whose clinical diagnosis of EPP shows cutaneous photosensitivity and increased erythrocytes protopophyrin concentration, can have structural alterations in ferrochelatase protein. This is associated with a significant decrease in the enzyme activity that is associated in some cases with a loss of the [2Fe-2S] cluster.

The fact that some of the mutations investigated in this study, and others, showed a residual activity higher than the 50% expected in patients with EPP, and that a considerable

molecular heterogeneity exists in the FECH gene variants identified in EPP patients, suggest that there is no clear and strict correlation between the FECH gene defect and the residual activity of the produced protein. This suggests that additional factors such as association with other mutations and environmental factors may be associated with the known mutations and lead to different levels of *in vivo* expression of the protein, and thus to different levels of disease severity.

We also showed in this study that the metal ion substrate of ferrochelatase possibly has a different entry path to the active site pocket than previously reported. The kinetic studies showed that residue H240 is probably involved in the initial binding of the metal ion and from there this substrate is transported via conserved residues to the active site. These residues possibly exist in the tunnel that expands from H240 to the center of the active site. Our data suggest the involvement of residue F337 in opening the tunnel to the active site and probably in the binding and distortion of the porphyrin substrate.

REFERENCES

Al-Karadaghi S, Hansson M, Nikonov S, Jönsson B, Hederstedt L: Crystal structure of ferrochelatase: the terminal enzyme in heme biosynthesis. Structure 5:1501-1510, 1997

Al-Karadaghi S: Metal Binding to Saccharomyces cerevisiae Ferrochelatase. Biochemistry 41:13499 –13506, 2002

Andrews SC: Iron storage in bacteria. Adv Microb Physiol 40:281-351, 1998

Badminton MN, Elder GH: Management of acute and cutaneous porphyrias. Int J Clin Pract 56:272-278, 2002

Bain-Ackerman MJ, Lavallee DK: Kinetics of metal-ion comlexation with N-methyltetraphenylporphyrin. Evidence concerning a general mechanism of porphyrin metelation. Inorg Chem 18:3358-3364, 1979

Blackwood ME, Rush TS, Medlock A, Dailey HA, Spiro TG: Resonance raman spectra of ferrochelatase reveal porphyrin distortion upon metal binding. J Am Chem Society 119:12170-12174, 1997

Blackwood ME, RushTS, Romesberg F, Schultz PG, Spiro TG: Alternative modes of substrate distortion in enzyme and antibody catalyzed ferrochelation reactions. Biochemistry 37:779-782, 1998

Bloomer J, Bruzzone C, Zhu L, Scarlett Y, Magness S, Brenner D: Molecular defects in ferrochelatase in patients with protoporphyria requiring liver transplantation. J Clin Invest 102:107-114, 1998

Bloomer JR, Hill HD, Morton KO, Anderson-Burnham LA, Straka JG: The enzyme defect in bovine protoporphyria. Studies with purified ferrochelatase. J Biol Chem 262: 667-671, 1987

Bloomer JR, Morton KO, Reuter RJ, Ruth GR: Bovine protoporphyria: documentation of autosomal recessive inheritance and comparison with the human disease through measurement of heme synthase activity. Am J Hum Genet 34:322-330, 1982

Bloomer JR, Rank JM, Payne WD, Snover DC, Sharp HL, Zwiener RJ, Carithers RL: Follow-up after liver transplantation for protoporphyric liver disease. Liver Transpl Surg 2:269-75, 1996

Bonkowsky HL, Bloomer JR, Ebert PS, Mahoney MJ: Heme synthetase deficiency in human protoporphyria: demonstration of the defects in liver and cultured Erythrobroblasts. J Clin Invest 56:1139–1148, 1975

Bottomley S, Tanaka M, Everett M: Diminished erythroid ferrochelatase activity in protoporphyria. J Lab Clin Med 86:126-131, 1975

Brenner DA, Didier JM, Frasier F, Christensen SR, Evans GA, Dailey HA: A molecular defect in human protoporphyria. Am J Hum Genet 50:1203-1210, 1992

Brenner DA, Frasier F: Cloning of murine ferrochelatase. Proc Natl Acad Sci USA 88:538–849, 1991

Brun A, Western A, Malik Z, Sandberg S: Erythropoietic protoporphyria: photodynamic transfer of protoporphyrin from intact erythrocytes to other cells. Photochem Photobiol. 51:573-577, 1990

Burden AE, Wu C K, Dailey TA, Busch JLH, Dhawan I K, Rose JP, Wang BC, Dailey HA: Human ferrochelatase: crystallization, characterization of the [2Fe-2S] cluster and determination that the enzyme is a homodimer. Biochem Biophys Acta 1435: 191–197, 1999

Camadro JM , Labbe P: Purification and properties of ferrochelatase from the yeast. *Saccharomyces cerevisiae*. Evidence for a precursor form of the protein. J Biol Chem 263:11675-11682, 1988

Carolyn A, Whatley D, ThompsonP , Hoy T, Fisher P, Singer C, Lovell CR., Elder GH: Late-Onset Erythropoietic porphyria Caused by a Chromosome 18q Deletion in Erythroid cells. J Invest Dermatol 117:1647-1649, 2001

Chakranarti A, Tan CY. Dietary fish oils as a therapeutic option in erythropoietic protoporphyria. Clinical & Experimental Dermatol 27:324-327, 2002

Chen FP, Risheg H, Liu Y, Bloomer J: Ferrochelatase gene mutations in erythropoietic protoporphyria: focus on liver disease. Cell Mol Biol 48:83-89, 2002

Chow KS, Singh DP, Walker AR Smith AG: Two different genes encode ferrochelatase in Arabidopsis: mapping, expression and subcellular targeting of the precursor proteins. Plant J 15: 531 – 541, 1998

Crouse BR, Sellers VM, Finnegan MG, Dailey HA, Johnson MK: Site-directed mutagenesis and spectroscopic characterization of human ferrochelatase: identification of residues coordinating the [2Fe-2S] cluster. Biochemistry 35:16222–16229, 1996

Dailey HA, Dailey TA, Wu CK, Medlock AE, Wang KF, Rose JP, Wang BC: Ferrochelatase at the millennium: structures, mechanisms and [2Fe-2S] clusters. Cell Mol Life Sci57:1909-1926, 2000

Dailey HA, Finnegan MG, Johnson MK: Human ferrochelatase is an iron-sulfur protein. Biochemistry. 33:403-407, 1994

Dailey HA, Fleming JE: Bovine ferrochelatase. Kinetic analysis of inhibition by n-methylprotoporphyrin, manganese, and heme. J Biol Chem 258: 11453-11459, 1983

Dailey HA, Fleming JE: The Role of Arginyl Residues in Porphyrin Binding to Ferrochelatase. J Biol Chem 261:7902-7905, 1986

Dailey HA, Sellers VM, Dailey TA: Mammalian ferrochelatase. Expression and characterization of normal and two human protoporphyric ferrochelatases. J Biol Chem 269:390-395, 1994a

Dailey HA, Smith A: Differential interaction of porphyrins used in photoradiation therapy with ferrochelatase. Biochem J 223:441-445, 1984

Dailey HA., Finnegan MG, Johnson MK: Human ferrochelatase is an iron-sulfur protein. Biochemistry 3: 403–407, 1994b

Dailey HA: Ferrochelatase. In Hausinger R. P., Eichorn G.L. and Marzilli L.G:, eds. Mechanisms of Metallocenter Assembly VCH, New York,, 1996:pp 77–pp 98

Dailey HA, Dailey TA: Ferrochelatase. In Kadish K.M., Smith K.M., Guillard R:, eds. The Porphyrin Handbook Elsevier Science, California, USA,, 2003:pp93-pp121

Dailey HA: Conversion of coproporphyrinogen to protoheme in higher eukaryotes and bacteria. In Dailey HA:, ed. Biosynthesis of Heme and Chlorophylls McGraw-Hill, New York,, 1990 :pp123–pp155

Dailey HA: Effect of sulfhydryl group modification on the activity of bovine ferrochelatase. J Biol Chem 259:2711-2715, 1984

Dailey HA: Enzymes of heme biosynthesis. J Biol Inorg Chem 2: 411-417, 1997.

Dailey HA: Metal inhibition of ferrochelatase. Ann NY Acad Sci 514:81–86, 1987

Dailey HA: Purification and characterization of membrane-bound ferrochelatase from Rhodopseudomonas sphaeroides. J Biol Chem 257:14714-8, 1982

Dailey HA: Spectroscopic examination of the active site of bovine ferrochelatase. Biochemistry 24:1287-1291, 1985

Dailey HA, Jones CS, Karr SW: Interaction of free porphyrins and metalloporphyrins with mouse ferrochelatase. A model for the active site of ferrochelatase. Biochim Biophys Acta 999:7-11, 1989

Dailey HA: Conversion of coproporphyrinogen to protoheme in higher eukaryotes and bacteria: Terminal three enzymes. In: Dailey, HA:, ed. Biosynthesis of Heme and Chlorophylls McGraw-Hill, New York,, 1990: pp:123-pp161

Dailey TA, Dailey HA: Identification of [2Fe-2S] Clusters in Microbial Ferrochelatases. J Bacteriol 184: 2460 – 2464, 2002

Day AL, Parsons BM, Dailey HA: Cloning and characterization of Gallus and Xenopus ferrochelatases: presence of the [2Fe-2S] cluster in nonmammalian ferrochelatase. Arch Biochem Biophys 359:160-169, 1998

De Matteis F, Gibbs AH, Harvey C: Studies on the inhibition of ferrochelatase by N-alkylated dicarboxylic porphyrins. Steric factors involved and evidence that the inhibition is reversible. Biochem J 226:537-544, 1985

Deybach J C: Painful photosensitivity**.** Lancet 358 :49, 2001

Deybach JC, Da Silva V, Pasquier Y, Nordmann Y. Ferrochelatase in human erythropoietic protoporphyria: the first case of a homozygous form of the enzyme defeciency. In: Nordmann Y:, ed. Porphyrins and Porphyrias John Libbey ,Paris,, 1986: pp173-pp193

Deybach JC, Silva V, Grandchamp B, Nordmann Y: Mitochondrial location of protoporphyrinogen oxidase. Eur J Biochem 149:431-435, 1985

Eldridge MG, Dailey HA: Yeast ferrochelatase: expression in a baculovirus system and purification of the expression protein. Prot Sci 1:271–277, 1992

Ferreira GC, Andrew TL, Karr SW, Dailey HA: Organization of the terminal two enzymes of the heme biosynthetic pathway. J Biol Chem 263:3835-3839, 1988

Ferreira GC, Franco R, Lloyd SG, Moura I, Moura JJ, Huynh BH: Structure and function of ferrochelatase. J Bioenerg Biomembr 27:221-229, 1995

Ferreira GC, SBl, Francosfl R, Lloydll SG, Pereira AS, Moural I, Moural JJG , and Huynh BH: Mammalian Ferrochelatase, a New Addition to theMetalloenzyme Family. J Biol Chem 269: 7062-7065, 1994.

Frank J, Nelson J, Wang X, Yang L, Ahmad W, Lam H, Jugert FK, Kalka K, Poh-Fitzpatrick MB, Goerz G, Merk HF, Christiano AM: Erythropoietic protoporphyria: identification of novel mutations in the ferrochelatase gene and comparison of biochemical markers versus molecular analysis as diagnostic strategies. J Investig Med 47:278-284, 1999

Frustaci J, O'Brian MR: Characterization of a Bradyrhizobium japonicum ferrochelatase mutant and isolation of the hemH gene. J Bacteriol 174:4223-4229, 1992

Goerz G, Bunselmeyer S , Bolsen K, Schurer NY: Ferrochelatase activities in patients with erythropoietic protoporphyria and their families. British J Dermato 134: 880-885, 1996

Gogh van H, Schothorst AA: Determination of very small amounts of protoporphyrin in epidermis, plasma and blister fluids. J Invest Dermatol 61:42-45, 1973

Goldberg A, Ashenbrucker M, Cartwright GE, Wintrobel M: Studies on the biosynthesis of heme in vitro by avian erythrocytes. Blood 11:821–833, 1956

Gora M, Grzybowska E, Rytka J, Labbe-Bois R: Probing the active-site residues in Saccharomyces cerevisiae ferrochelatase by directed mutagenesis. In vivo and in vitro analyses. J Biol Chem 271:11810-11816, 1996

Gordeuk VR, Brittenham GM, Hawkins CW, Mukhtar H, Bickers DR.: Iron therapy for hepatic dysfunction in erythropoietic protoporphyria. Ann Intern Med 105:27-31, 1986

Gouya L, Deybach JC, Lamoril J, Da Silva V, Beaumont C, Grandchamp B, Nordmann Y: Modulation of the phenotype in dominant erythropoietic protoporphyria by a low expression of the normal ferrochelatase allele. Am J Hum Genet 58:292-299, 1996

Gouya L, Puy H, Lamoril J, Da Silva V, Grandchamp B, Nordmann Y, Deybach JC: Inheritance in erythropoietic protoporphyria: a common wild-type ferrochelatase allelic variant with low expression accounts for clinical manifestation. Blood 93:2105-2110, 1999

Gouya L, Puy H, Robreau AM, Bourgeois M, Lamoril J, Da Silva V, Grandchamp B, Deybach JC: The penetrance of dominant erythropoietic protoporphyria is modulated by expression of wild type FECH. Nat Genet 30:27-28, 2002

Gouya L, Schneider-Yin X, Rufenacht U, Herrero C, Lecha M, Mascaro JM, Puy H, Deybach JC, Minder EI: Mutations in the ferrochelatase gene of four Spanish patients with erythropoietic protoporphyria. J Invest Dermatol 111:406-409, 1998

Gross U, Frank M, Doss MO: Hepatic complications of erythropoietic protoporphyria. Photodermatol Photoimmunol Photomed 14:52-57, 1998

Grzybowska E, Monika Góra M, Plochocka D, Rytka J: *Saccharomyces cerevisiae* Ferrochelatase Forms a Homodimer. Arch Biochem Biophys 398:170-178, 2002

Harbin BM, Dailey HA: Orientation of ferrochelatase in bovine liver mitochondria. Biochemistry 24:366-70, 1985

Haeger-Aronsen B, Stathers G, Swahn G: Hereditary coproporphyria. Study of a Swedish family. Ann Int Med 69:221–227, 1968

Haeger-Aronsen B: Erythropietic protoporphyria: a new type of inborn error of metabolism. Am J Med 35:450-454, 1963

Hansson M, Hederstedt L: Cloning and characterization of the Bacillus subtilis hemEHY gene cluster, which encodes protoheme IX biosynthetic enzymes. J Bacteriol 174:8081-8093, 1992

Heike L, Kispal G, Lill R: Mechanism of Iron Transport to the Site of Heme Synthesis insideYeast Mitochondria. J Biol Chem 274:18989–18996, 1999

Henriksson M, Timonen K, Mustajoki P, Pihlaja H, Tenhunen R, Peltonen L, Kauppinen R: Four novel mutations in the ferrochelatase gene among erythropoietic protoporphyria patients. J Invest Dermatol 106:346-50, 1996

Hofstra RMW, Osinga J, Buys CHCM: Mutations in Hirschsprung disease: When does a mutation contribute to the phenotype? Eur J Hum Genet 5:180-185, 1997

Honeybourne CL, Jackson JT, Jones OT: The interaction of mitochondrial ferrochelatase with a range of porphyrin substrates. FEBS Lettm 98:207-210, 1979

Imoto S, Tanizawa Y, Sato Y, Kaku K, Oka Y: A novel mutation in the ferrochelatase gene associated with erythropoietic protoporphyria. Br J Haematol 94:191-197, 1996

Jenkins MM, LeBoeuf RD, Ruth GR, Bloomer JR: A novel stop codon mutation (X417L) of the ferrochelatase gene in bovine protoporphyria, a natural animal model of the human disease. Biochim Biophys Acta 1408:18-24, 1998

Jones MS, Jones OT: The structural organization of haem synthesis in rat liver mitochondria. Biochem J 113:507-514, 1969

Karlberg T, Lecerof D, Gora M, Silvegren G, Labbe-Bois R, Hansson M, Al-Karadaghi S: Metal Binding to *Saccharomyces cerevisiae* Ferrochelatase. Biochemistry 41:13499–13506, 2002

Karr SR, Dailey HA**:** The synthesis of murine ferrochelatase in vitro and in vivo. Biochem J 254:799-803, 1988

Kohno H, Okuda M, Furukawa T, Tokunaga R, Taketani S: Site-directed mutagenesis of human ferrochelatase: identification of histidine-263 as a binding site for metal ions. Biochim Biophys Acta 1209:95-100, 1994

Komatsu H, Ishii K, Imamura K, Maruyama K, Yonei Y, Masuda H, Tsuchihashi T, Sajima Y: A case of erythropoietic protoporphyria with liver cirrhosis suggesting a therapeutic value of supplementation with a-tocopherol . Hepat Res 18:298–309, 2000

Komatsu H, Sajima Y, Imamura K, Masuda H, Yonei Y, Dohmori K, Kokutoh M, Ishii K, Ishii H: An ultrastructural study of the liver in erythropoietic protoporphyria. Med Electron Microsc 33:32-38, 2000

Labbe-Bois R, Camadro JM: Ferrochelatase in *Saccharomyces cerevisiae*. In G. Winkelmann and D. R. Winge:, ed. Metal ions in fungi. Marcel Dekker Inc., New York,, 1994: pp 413-pp 453

Labbe-Bois R: The ferrochelatase from Saccharomyces cerevisiae. Sequence, disruption, and expression of its structural gene HEM15. J Biol Chem 265:7278-7283, 1990

Lamoril J, Boulechfar S, de Verneuil H, Grandchamp B, Nordmann Y, Deybach JC: Human erythropoietic protoporphyria: two point mutations in the ferrochelatase gene. Biochem Biophys Res Commun 181:594-599, 1991

Lecerof D, Fodje M, Hansson A, Hansson M, Al-Karadaghi S: Structural and Mechanistic Basis of Porphyrin Metallation by Ferrochelatase. J Mol Biol 297:221-232, 2000

Lee See K, Forbes IJ, Betts WH: Oxygen dependency of phototoxicity with haematoporphyrin derivatives. Photochem Photobiol 39:631-634, 1984

Leone N, Marzano A, Cerutti E, Actis GC, Marchesa PE, David E, Salizzoni M, Rizzetto M: Liver transplantation for erythropoietic protoporphyria: report of a case with medium-term follow-up. Dig Liver Dis 32:799-802, 2000

Libbrecht L, Meerman L, Kuipers F, Roskams T, Desmet V, Jansen P: Liver pathology and hepatocarcinogenesis in a long-term mouse model of erythropoietic protoporphyria. J Pathol 199:191-200, 2003

Lichtin A *et al*: Correction of erythropoietic protoporphyria (EPP) phenotype by allogenic bone marrow transplant. Blood 92 (Suppl. 1): 532, 1998

Ma JG, Zhang J, Franco R, Jia SL, Moura I, Moura JJG, Kroneck PMH, Shelnutt JA: The structural origin of nonplanar heme distortions in tetraheme ferricytochromes c3. Biochemistry 37: 12431-12442, 1998

Magness ST, Tugores A, Christensen SR, Wagner-Mcpherson C, Evans GA, Naylor EW, Brenner DA: Deletion of the ferrochelatase gene in a patient with protoporphyria. Hum Mol Genet 3;1695-1697, 1994

Magness ST, Tugores A, Diala ES, Brenner DA: Analysis of the human ferrochelatase promoter in transgenic mice. Blood 92:320-328, 1998

Magnus IA, Jarret A, Prankerd TAJ, Rimington C: Erythropoietic protoporphyria(EPP). A new porphyria syndrome with solar urticaria due to protoporphyrinemia. Lancet II:448-451, 1961

Martinez FDM, Di Pierro ED, Biolcati G, Florelli G, Cappellini MD: Human Gene Mutation. Hum Genet 109:241, 2001

Mathews-Roth M, Michel J, Wise R: Ameliorartion of the metabolic defect in erythropoietic protoporphyria by expression of human ferrochelatase in cultured cells. J Invest Dermatol 104:497-499, 1995

Mathews-Roth MM, Rosner B: Long-term treatment of erythropoietic protoporphyria with cysteine. Photodermatol Photoimmunol Photomed 18:307-309, 2002

Medlock AE, Dailey HA: Examination of the carboxyl-terminal chimeric constructs of human and yeast ferrochelatases. Biochemistry 39: 7461–7467, 2000

Meerman L: Erythropoietic protoporphyria. An overview with emphasis on the liver. Scand J Gastroenterol Suppl 232:79-85, 2000

Minder EI, Deybach JC: Systematic analysis of molecular defects in the ferrochelatase gene from patients with erythropoietic protoporphyria. Am J Hum Genet 62:1341-1352, 1998

Minder EI, Gouya L, Schneider-Yin X, Deybach JC: A geneotype-phenotype correlation between null-allele mutations in the ferrochelatase gene and liver complication in patients with erythropoietic protoporphyria. Cell Mol Biol 48:91-96, 2002

Miura T, Torinuki W, Morihana Y: A high skin protoporphyrin level in erythropoietic protoporphyria. Tohoku J Exp Med 130:97-100, 1980

Miyamoto K, Nakahigashi K, Nishimura K, Inokuchi H: Isolation and characterization of visible light-sensitive mutants of Escherichia coli K12. J Mol Biol 219:393-398, 1991

Miyamoto K, Tanaka R, Teramoto H, Masuda T, Tsuji H., Inokuchi H: Nucleotide sequences of cDNA clones encoding ferrochelatase from barley and cucumber. Plant Physiol 105:769-770, 1994

Morris SD, Mason NG, Elder GH, Hawk JL, Sarkany RP: Ferrochelatase gene polymorphism analysis for accurate genetic counselling in erythropoietic protoporphyria. Br J Dermatol 147:572-574, 2002

Nakahashi Y, Fujita H, Taketani S, Ishida N, Kappas A, Sassa S: The molecular defect of ferrochelatase in a patient with erythropoietic protoporphyria. Proc Natl Acad Sci USA 89:281-5, 1992

Nakahashi Y, Miyazaki H, Kadota Y, Naitoh Y, Inoue K, Yamamoto M, Hayashi N, Taketani S: Human erythropoietic protoporphyria: identification of a mutation at the splice donor site of intron 7 causing exon 7 skipping of the ferrochelatase gene. Hum Mol Genet 2:1069-1070, 1993

Nakahashi Y, Miyazaki H, Kadota Y, Naitoh Y, Inoue K, Yamamoto M, Hayashi N, Taketani S: Molecular defect in human erythropoietic protoporphyria with fatal liver failure. Hum Genet 91:303-306, 1993

Nakahashi Y, Taketani S, Okuda M, Inoue K, Tokunaga R: Molecular cloning and sequence analysis of cDNA encoding human ferrochelatase. Biochem Biophys Res Commun 173:748-755, 1990

Norris P, Nunn A, Hawk J, Cox T: Genetic heterogeneity in erythropoietic protoporphyria. a study of the enzymatic defect in nine affected families. J Invest Dermatol 95:260-263, 1990

Olsson U, Billberg A, Sjövall S, Al-Karadaghi S, Hansson M: In Vivo and In Vitro Studies of *Bacillus subtilis* Ferrochelatase Mutants Suggest Substrate Channeling in the Heme Biosynthesis Pathway. J Bacteriol 184:4018–4024, 2002

Pawliuk R, Bachelot T, Wise R, Mathews-Roth M, Leboulch P: Long-term cure of the photosensitivity of murine erythropoietic protopophyria by preselective therapy. Nat Med 5:768-773, 1999

Perutz F: Regulation of Oxygen Affinity of Hemoglobin: Influence of structure of the Globin of the heme iron. Annu Rev Biochem *48:327*-386, 1979

Porra RJ, Jones OTG: Studies on ferrochelatase. Assay and properties of ferrochelatase from a pig-liver mitochondrial extract. Biochemistry 87:181-185, 1963

Porra RJ, Lascelles J: Studies on ferrchelatase: the enzyme formation of haem in proplastid, chloroplasts and plant mitochondria. Biochem J 108:343-348, 1968

Porra RJ, Vitols KS, Labbe RF, Newton NA. Studies on ferrochelatase : The effects of thiols and other factors on the determination of activity. Biochem J 104:321-327, 1967

Poulson R., Polglase WJ: The enzymic conversion of protoporphyrinogen IX to protoporphyrin IX. Protoporphyrinogen oxidase activity in mitochondrial extracts of Saccharomyces cerevisiae. J Biol Chem *260:1269*-1274, 1975

Prasad ARK , Dailey HA: Effect of Cellular Location on the Function of Ferrochlatase J Biol Chem 270:18198–18200, 1995

Proulx KL, Woodard SI, Dailey HA: In situ conversion of coproporphyrinogen to heme by murine mitochondria: terminal steps of the heme biosynthetic pathway. Protein Sci 2:1092-1098, 1993

Punekar NS, Gokhale RS: Factors influencing the stability of heme and ferrochelatase: role of oxygen. Biotechnol Appl Biochem 14:21–29, 1991

Qi Z, O'Brian MR: Interaction between the Bacterial Response Regulator and Ferrochelatasee Mediates Genetic Control of Heme Biosythesis. Molecular Cell 9:155-162, 2002

Ross JB, Moss MA: Relief of the photosensitivity of erythropoietic protoporphyria by pyridoxine. J Am Acad Dermatol 22:340-342, 1990

Rufenacht UB, Gouya L, Schneider-Yin X, Puy H, Schafer BW, Aquaron R, Nordmann Y, Minder EI, Deybach JC: Systematic analysis of molecular defects in the ferrochelatase gene from patients with erythropoietic protoporphyria. Am J Hum Genet 62:1341-1352, 1998

Rufenacht UB, Gregor A, Gouya L, Tarczynska-Nosal S, Schneider-Yin X, Deybach JC: New missense mutation in the human ferrochelatase gene in a family with erythropoietic protoporphyria: functional studies and correlation of genotype and phenotype**.** Clin Chem 47:1112-1113, 2001

Sarkany RP, Alexander GJ, Cox TM. Recessive inheritance of erythropoietic protoporphyria with liver failure. Lancet 343:1394-1396, 1994

Sarkany RP, Whitcombe DM, Cox TM: Molecular characterization of a ferrochelatase gene defect causing anomalous RNA splicing in erythropoietic protoporphyria. J Invest Dermatol 102:481-484, 1994

Sarkany RP: Porphyria. From Sir Walter Raleigh to molecular biology. Adv Exp Med Biol 455:235-241, 1999

Sassa S: Hematologic aspects of the porphyrias. Int J Hematol 71:1-17, 2000

Sassa S, Zalar GL, Poh-Fithpatrick MB, Anderson KE, Kappas A: Studies in porphyria. Functional evidence for a partial deficiency of ferrochelatase activity in mitogen-stimulated lymphocytes from patients with erythropoietic protoporphyria. J Clin Invest 69:809-815, 1982

Schneider-Yin X, Gouya L, Dorsey M, Rufenacht U, Deybach JC, Ferreira GC: Sarkany RP, Alexander GJ, Cox TM: Recessive inheritance of erythropoietic protoporphyria with liver failure. Lancet 343:1394-1396, 1994

Schneider-Yin X, Gouya L, Meier-Weinand A, Deybach JC, Minder EI: New insights into the pathogenesis of erythropoietic protoporphyria and their impact on patient care. Eur J Pediatr 159: 719-725, 2000a

Schneider-Yin X, Gouya L, Dorsey M, Rüfenacht U, Deybach JC, Ferreira GC: Mutations in the iron-sulfur cluster ligands of the human ferrochelatase lead to erythropoietic protoporphyria. Blood 96:1545-1549, 2000b

Schneider-Yin X, Rüfenacht UB, Hergersberg M, Schnyder C, Deybach JC, Minder E I : Haplotype Analysis in Determination of the Heridity of Erythropoietic Protoporphyria among Swiss Families. J Invest Dermatol 117:1521-1525, 2001

Schneider-Yin X, Schafer BW, Mohr P, Burg G, Minder EI: Molecular defects in erythropoietic protoporphyria with terminal liver failure. Hum Genet 93:711-713, 1994

Schneider-Yin X, Schafer BW, Tonz O, Minder EI: Human ferrochelatase: a novel mutation in patients with erythropoietic protoporphyria and an isoform caused by alternative splicing. Hum Genet 95:391-396, 1995

Sellers VM, Johnson MK, Dailey HA: Function of the [2Fe-2S] cluster in Mammalian Ferrochelatase: A possible Role as a Nitric Oxide Sensor. Biochemistry 35: 2699–2704, 1996

Sellers, VM, Wang KF, Johnson MK, Dailey HA: Evidence that the fourth ligand to the [2Fe-2S] cluster in animal ferrochelatase is a cysteine. Characterization of the enzyme from *Drosophila melanogaster*. J Biol Chem 273:22311-22316, 1998a

Sellers VM, Dailey TA, Dailey HA: Examination of ferrochelatase mutations that cause erythropoietic protoporphyria. Blood 91:3980–3985, 1998b

Sellers VM, Wu CK, Dailey TA, Dailey HA: Human ferrochelatase: Characterization of substrate – iron binding and proton abstracting residues. Biochemistry 40:9821-9827, 2001

Smith AG, Santana MA, Wallace-Cook AD, Roper JM, Labbe-Bois R: Isolation of a cDNA encoding chloroplast ferrochelatase from Arabidopsis thaliana by functional complementation of a yeast mutant. J Biol Chem 269:13405-13413, 1994

Spikes JD: Porphyrins and related compounds as photodynamic sensitizers. Ann NY Acad Sci 244:496-508, 1975

Straka JG, Bloomer JR, Kempner ES: The functional size of ferrochelatase determined *in situ* by radiation inactivation. J Biol Chem 266:24637-24641, 1991

Takeda J, Ohya T, Sato M. Ferrochelatase transition state model: rapid incorporation of copper (II) into nonplanar dodecaphenylporphyrin. Inorg Chem 31:2877–2880, 1992

Taketani S, Inazawa J, Nakahashi Y, Abe T, Tokunaga R: Structure of the human ferrochelatase gene: exon/ intron gene organization and location of the gene to chromosome 18. Eur J Biochem 205:217–222, 1992

Taketani S, Nakahashi Y, Osumi T, Tokunaga R: Molecular cloning, sequencing, and expression of mouse ferrochelatase. J Biol Chem 265:19377–19380, 1990

Taketani S, Tokunaga R: Purification and substrate specificity of bovine liver-ferrochelatase. Eur J Biochem 127:443–447, 1982

Taketani S, Tokunaga R: Rat liver ferrochelatase. Purification, properties, and stimulation by fatty acids. J Biol Chem 256: 12748-12753, 1981

Thunell S, Harper P, Brun A. Porphyrins, porphyrin metabolism and porphyrias. IV. Pathophysiology of erythyropoietic protoporphyria — diagnosis, care and monitoring of the patient. Scand J Clin Lab Invest 60:581-604, 2000

Todd DJ, Hughes AE, Ennis KT, Ward AJ, Burrows D, Nevin NC: Identification of a single base pair deletion (40 del G) in exon 1 of the ferrochelatase gene in patients with erythropoietic protoporphyria. Hum Mol Genet 2:1495-1496, 1993

Todd DJ: Erythropoietic protoporphyria. Br J Dermatol 131:751-766, 1994

Wang X, Piomelli S, Peacocke M, Christiano AM, Poh-Fitzpatrick MB: Erythropoietic protoporphyria: four novel frameshift mutations in the ferrochelatase gene. J Invest Dermatol 109:688-691, 1997

Wang X, Poh-Fitzpatrick M, Carriero D, Ostasiewicz L, Chen T, Taketani S, Piomelli S: A novel mutation in erythropoietic protoporphyria: an aberrant ferrochelatase mRNA caused by exon skipping during RNA splicing. Biochim Biophys Acta 1181:1198-200, 1993

Wang X, Poh-Fitzpatrick M, Chen T, Malavade K, Carriero D, Piomelli S: Systematic screening for RNA with skipped exons--splicing mutations of the ferrochelatase gene. Biochim Biophys Acta 1271:358-362, 1995

Wang X, Poh-Fitzpatrick M, Piomelli S: A novel splicing mutation in the ferrochelatase gene responsible for erythropoietic protoporphyria. Biochim Biophys Acta 1227:25-27, 1994

Wang X, Yang L, Kurtz L, Lichtin A, DeLeo VA, Bloomer J, Poh-Fitzpatrick MB: Haplotype analysis of families with erythropoietic protoporphyria and novel mutations of the ferrochelatase gene. J Invest Dermatol 113:87-92, 1999

Wang X: Molecular characterization of a novel defect occurring de novo associated with erythropoietic protoporphyria. Biochim Biophys Acta 1316:149-152, 1996

Went LN, Klasen EC: Genetic aspects of erythropoietic protoporphyria. Ann Hum Genet 48:105-117, 1984

Whitcombe DM, Carter NP, Albertson DG, Smith SJ, Rhodes DA, Cox T M: Assignment of the human ferrochelatase gene (FECH) and a locus for protoporphyria to chromosome 18q22. Genomics 11:1152-1154, 1991

Wiman A, Floderus Y, Harper P: Novel mutations and phenotypic effect of the splice site modulator IVS3-48C in nine Swedish families with erythropoietic protoporphyria. J Hum Genet 48:70-76, 2003

Wolf U: Identical mutations and phenotypic variation. Hum Genet 100:305-321, 1997

Wu CK, Dailey HA, Rose JP, Burden A, Sellers VM, Wang BC. The 2.0 Å structure of human ferrochelatase, the terminal enzyme of heme biosynthesis. Nature Struct Biol 8:156-160, 2001

Yotsumoto S, Shimada S, Terasaki K, Taketani S, Kobayashi K, Saheki T, Kanzaki T: A novel A(-4)-to-G acceptor splice site mutation leads to three bases insertion in ferrochelatase mRNA in a patient with erythropoietic protoporphyria. J Invest Dermatol 117:159-161, 2001